Economic Geology
Vol. 98, 2003, pp. 1535–1574

Geology of the Bajo de la Alumbrera Porphyry Copper-Gold Deposit, Argentina

John M. Proffett†
P. O. Box 772066, Eagle River, Alaska 99577

Abstract

The Bajo de la Alumbrera porphyry Cu-Au deposit, Argentina, is in the eastern Andes, near the north edge of a region of reverse fault-bound basement uplifts that overlie a low-angle segment of the subduction zone. Alumbrera, now above the transition from steep to flat subduction, formed at ~7 Ma in the Farallón Negro volcanic field, which was active as volcanism was waning regionally above the flattening subduction zone. Reconstruction of volcanic structure suggests that the top of the exposed orebody was emplaced beneath about 2.5 km of andesite and dacite but not directly beneath the vent of a stratovolcano. Production plus remaining resources are 605 million metric (Mt) tons of ore that averages 0.54 percent Cu and 0.64 g/t Au.

The deposit is centered on a closely spaced cluster of small felsic porphyry stocks and dikes, emplaced into andesites during seven phases of intrusion. Dikes of several phases define a radial pattern. Most of the porphyries are very similar to one another, with phenocrysts of plagioclase, hornblende, biotite, and quartz, in a matrix of fine-grained quartz, K-feldspar, and minor plagioclase, biotite, and magnetite. Individual porphyries are distinguished mainly on the basis of intrusive contact relationships.

Highest Cu-Au grades are associated with abundant quartz veins, secondary K-feldspar, ±magnetite, ±biotite, ±anhydrite, in the earliest porphyry (P2), and adjacent andesite. P2-related mineralization is truncated by porphyries of the second phase of ore-related intrusions (Early P3 and Quartz-eye porphyry), which contain similar but generally less intense mineralization and alteration. Porphyries of the next phase (Late P3) truncate mineralization associated with earlier phases and are weakly mineralized with Cu-Au, sparse quartz veins, and secondary biotite. The still later Northwest porphyries truncate most Cu-Au, quartz veins, and potassic alteration, and themselves contain only traces of such mineralization and partially biotitized hornblende. Postmineral porphyries, the youngest, truncate all such mineralization and alteration, and none of their hornblende is biotitized. Los Amarillos porphyry and igneous breccia, along the western periphery of the porphyry cluster, is between P2 and Early P3 in age but shows little relationship to mineralization.

Zones of secondary K-feldspar associated with the earlier porphyries are surrounded by a larger zone of secondary biotite. All significant Cu-Au lies within these potassic zones. The biotite zone is surrounded by epidote-chlorite alteration lacking significant sulfides. Like potassic alteration, epidote-chlorite alteration is also truncated by Postmineral porphyries. Strong feldspar destructive alteration, consisting mostly of veinlet-controlled sericite-quartz-pyrite, is younger than all secondary K-feldspar, biotite, and epidote-chlorite and occurs in a shell in the outer parts of the biotite zone. Weaker feldspar destructive alteration occurs inside and outside this shell. Pyrite veins with sericite-quartz-pyrite alteration cut Postmineral porphyries.

In the earliest secondary K-feldspar assemblage, which is usually barren of Cu sulfides, biotite is altered to magnetite plus K-feldspar. Most Cu sulfides are associated with slightly later K-feldspar-biotite ± magnetite assemblages. Where feldspars and biotite are not overprinted by later feldspar destructive or chloritic alteration, Cu minerals are bornite and chalcopyrite, coexisting with magnetite. Barren as well as Cu sulfide-bearing assemblages are associated with early veinlets, including A-type quartz, which are truncated by the next later porphyry. Deposition of Cu-Au during or between emplacement of closely related porphyries suggests high temperatures and magmatic fluids, and the assemblage bornite-chalcopyrite-magnetite indicates a relatively low sulfidation state, and along with the assemblage K-feldspar-biotite ± magnetite ± anhydrite a relatively high oxidation state. Cu-Au distribution is not related to feldspar destructive zones nor to the interface between sericitic and potassic zones. Much Cu-Au mineralization, however, has been overprinted by late alteration, resulting in partial destruction of feldspars, chloritization of mafics, and sulfidation of bornite-chalcopyrite-magnetite to chalcopyrite-pyrite ± relict magnetite. This probably took place at significantly lower temperature.

A low-grade core zone consists in large part of barren K-feldspar-magnetite alteration and quartz veins in Early P3 porphyry, and in part consists of later barren porphyry, so is mostly younger than the Cu-Au deposited with P2 porphyry.

The youngest features at Alumbrera include small postore normal faults, gypsum veins due to hydration and mobilization of anhydrite, local dissolution of gypsum veins, and locally developed thin zones of near-surface oxidation, leaching, and secondary enrichment.

Introduction

Bajo de la Alumbrera (referred to as "Alumbrera" here for brevity) is a major porphyry Cu-Au deposit, located within the Farallón Negro district, Catamarca Province, northwest Argentina, in the eastern Andes (Figs. 1–4A). Production plus remaining resources total 605 million metric tons (Mt) of ore, with an average grade of 0.54 percent Cu and 0.64 g/t Au (D. Keough and L. Rivera, pers. commun., 2000). Owned by Yacimientos Mineros Agua de Dionisio (YMAD), it has recently been developed by Minera Alumbrera Ltd., a joint venture of MIM Holdings (now Xstrata), Rio Algom and North (whose interests are now held by Wheaton River and Northern Orion), and mining began in 1997. The Farallón Negro district coincides with a large complex of Miocene

†E-mail: proffettak@aol.com

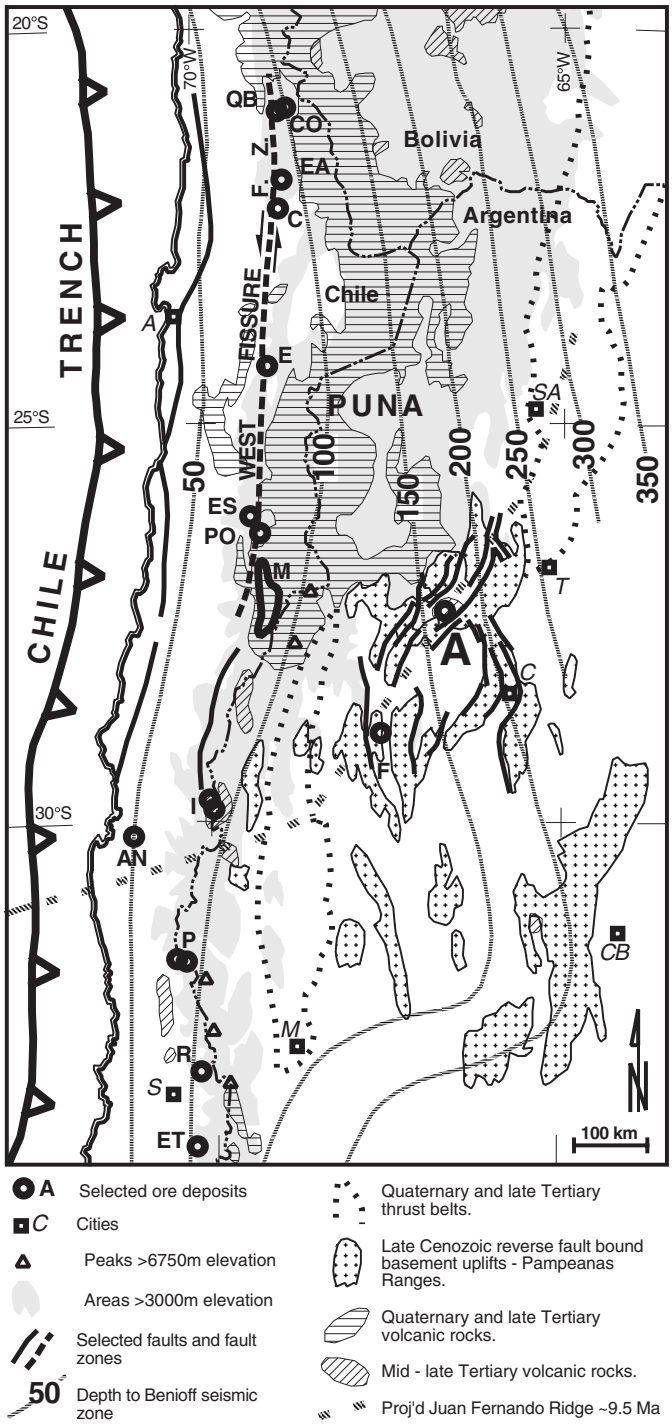

FIG. 1. Map of part of the Andes, showing selected tectonic features and ore deposits. Includes data from Commission for the Geologic Map of the World (1981) and Jordan et al. (1983), with contours to seismic zone from Cahill and Isacks (1992). Projection of Juan Fernando seamount chain at 9.5 Ma interpolated from Cross and Pilger (1982), using ages for sea-floor magnetic anomalies from Haq and Van Eysinga (1998). Ore deposits: A = Alumbrera, AN = Andacollo, C = Chuquicamata, CO = Collahuasi, E = Escondida, EA = El Abra, ES = El Salvador, ET = El Teniente, F = Famatina, I = El Indio/Tambo, M = Maricunga belt, P = Los Pelambres/Pachón, PO = Potrerillos, QB = Quebrada Blanca, R = Río Blanco/Los Bronces. Cities: *A* = Antofagasta, *C* = Catamarca, *CB* = Córdoba, *M* = Mendoza, *SA* = Salta, *S* = Santiago, *T* = Tucumán.

volcanic and intrusive rocks and includes other porphyry-type occurrences, as well as vein deposits (Fig. 2). This paper and accompanying maps (four of the maps are provided in an envelope as a supplement to this issue and will be referred to as Maps 1–4, Proffett, 2003) and sections summarize the results of about 10 mo of field work and an equivalent amount of map compilation and interpretation, supported by limited laboratory work. Field work included detailed surface mapping of the Alumbrera deposit area in 1994 and 1995, before mining began (Fig. 4A), mostly at 1:2000 scale on a topographic base (minor areas at 1:5000 scale on an air photo base), logging of drill core, and limited detailed and reconnaissance mapping in the surrounding district. In most areas the outcrop mapping method was used (see Proffett, 2003, Map 2). In mapping of mineralized areas and drill core, methods were used that allowed several features to be recorded independently, including rock type, several alteration features, quartz veins, quartz vein abundance, secondary magnetite, sulfide veins and disseminations, limonite and Cu oxides after sulfides, and especially contact and timing relationships (Fig. 4B).

Regional Tectonic Setting

The Farallón Negro district and volcanic field is located just east of the south end of the Puna, a plateau that makes up the highest part of the Andes in northwestern Argentina and northeastern Chile (Fig. 1). A dominant structural feature of the eastern Andes south and southeast of the Puna is the Sierras Pampeanas, a region of broad basins and ranges, with the Farallón Negro district located in the northern part (Fig. 1). Most basins and ranges are bound by northeast- or north-south–trending reverse faults (Fig. 2), with Paleozoic basement uplifted up to several kilometers in the ranges. Fault characteristics and earthquake focal mechanisms indicate east-west compression on some faults and northwest-southeast compression on others (Jordan et al., 1983; Allmendinger, 1986; this study). In the Farallón Negro district reverse faulting was younger than most igneous activity, which ceased ~6 Ma (Sasso and Clark, 1998; this study; Fig. 3). Small normal faults at Alumbrera (described below) indicate minor northeast-southwest extension younger than sericitic alteration dated at 6.75 Ma (Sasso and Clark, 1998), and slickensides also indicate minor strike slip on some of these faults. Larger normal faults, one north dipping and one west dipping, have also been mapped during the present study (Fig. 2, the Buenaventura fault and a 73° dipping fault near Durazno). The data demonstrate that variations from reverse to strike-slip to normal faulting have taken place in late Cenozoic time, in what has been dominantly a northwest-southeast to east-west compressional system.

Most of the Sierras Pampeanas coincides with a gently dipping segment of the Benioff zone (Barazangi and Isacks, 1976; Jordan et al., 1983). The change in dip of the Benioff zone at the north end of this segment is gradual (Bevis and Isacks, 1984; Cahill and Isacks, 1985, 1992), and the Farallón Negro district is located above this transition (Fig. 1), where the Benioff zone dips ~18°.

Quaternary and active volcanoes, common above more steeply dipping parts of the Benioff zone, are absent above the gently dipping segment (Fig. 1). Mid-Tertiary volcanics are common above the gently dipping segment in the Western

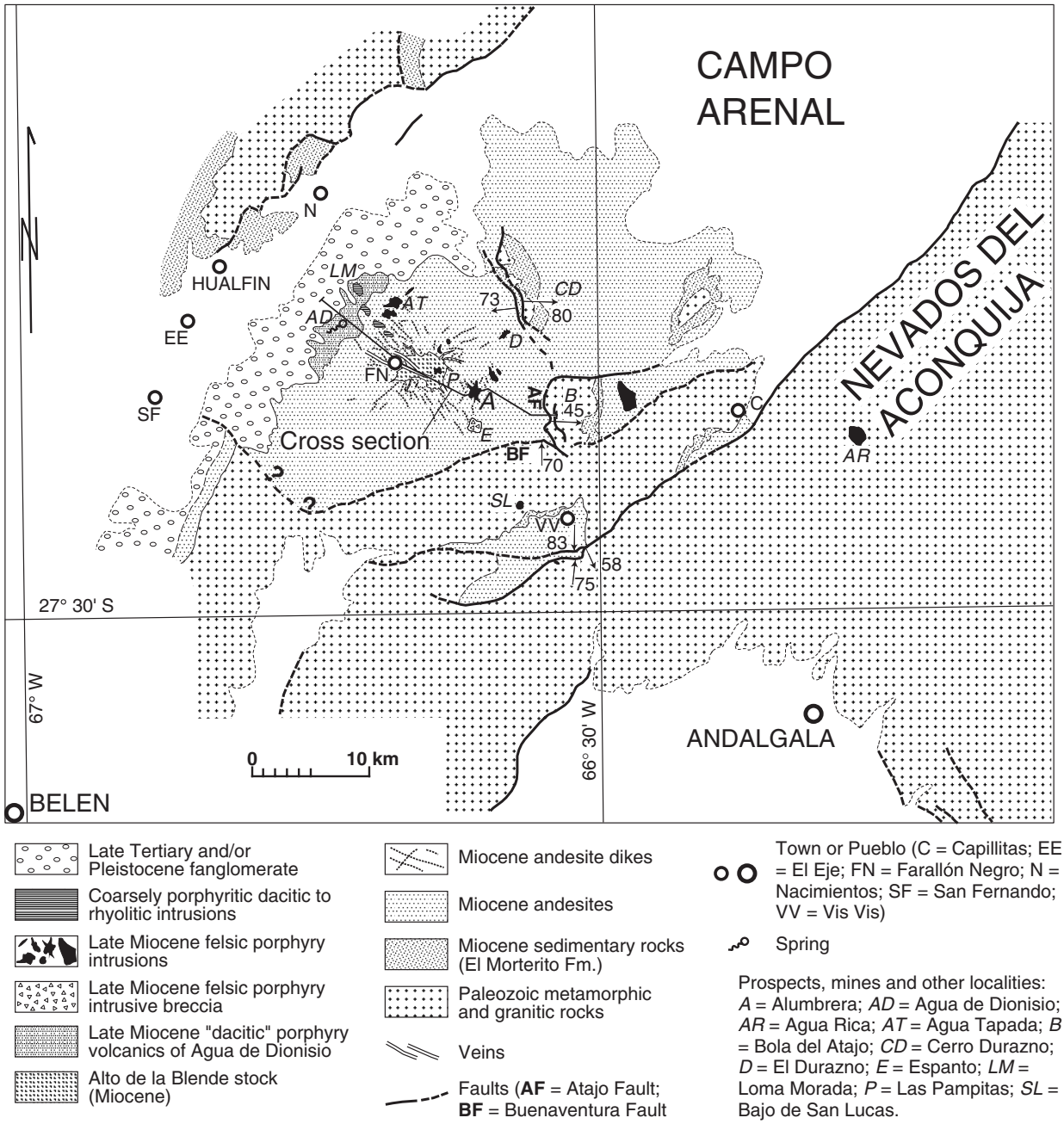

FIG. 2. Generalized geologic map of the Farallón Negro district, Argentina, showing location of Alumbrera and district cross section. From González Bonorino (1947), Llambías (1970, 1972), and from air photo and satellite image interpretation, and reconnaissance mapping by the author.

Andes but starting in the Miocene volcanism began to spread eastward (Caelles et al., 1971), thought to have been caused by flattening of Benioff zone (Kay et al., 1988), and resulted in isolated igneous centers in the eastern Andes, including the Farallón Negro volcanic field.

A possible cause of the Benioff zone flattening was suggested by Pilger (1981), who postulated that a possible northeast extension of the Juan Fernández Ridge (a seamount chain) was subducted and a relatively buoyant crust along this ridge caused the flattening. Interestingly, according to reconstructions by Cross and Pilger (1982), the postulated subducted ridge would have been beneath the Farallón Negro district ~9 to 10 Ma (Fig. 1), just before the main andesitic phase of volcanism, dated at ~7.5 to 8.5 Ma by Sasso and Clark (1998). The dip of the Benioff zone at the time of Farallón Negro volcanism and mineralization is speculative. If it has continued to flatten through late Cenozoic, as Kay et al. (1988) suggest for the southern part of the low angle segment, it may have dipped more steeply, but if Pilger's (1981) model is correct, it may have dipped more gently beneath Farallón Negro at the time the ridge was being subducted.

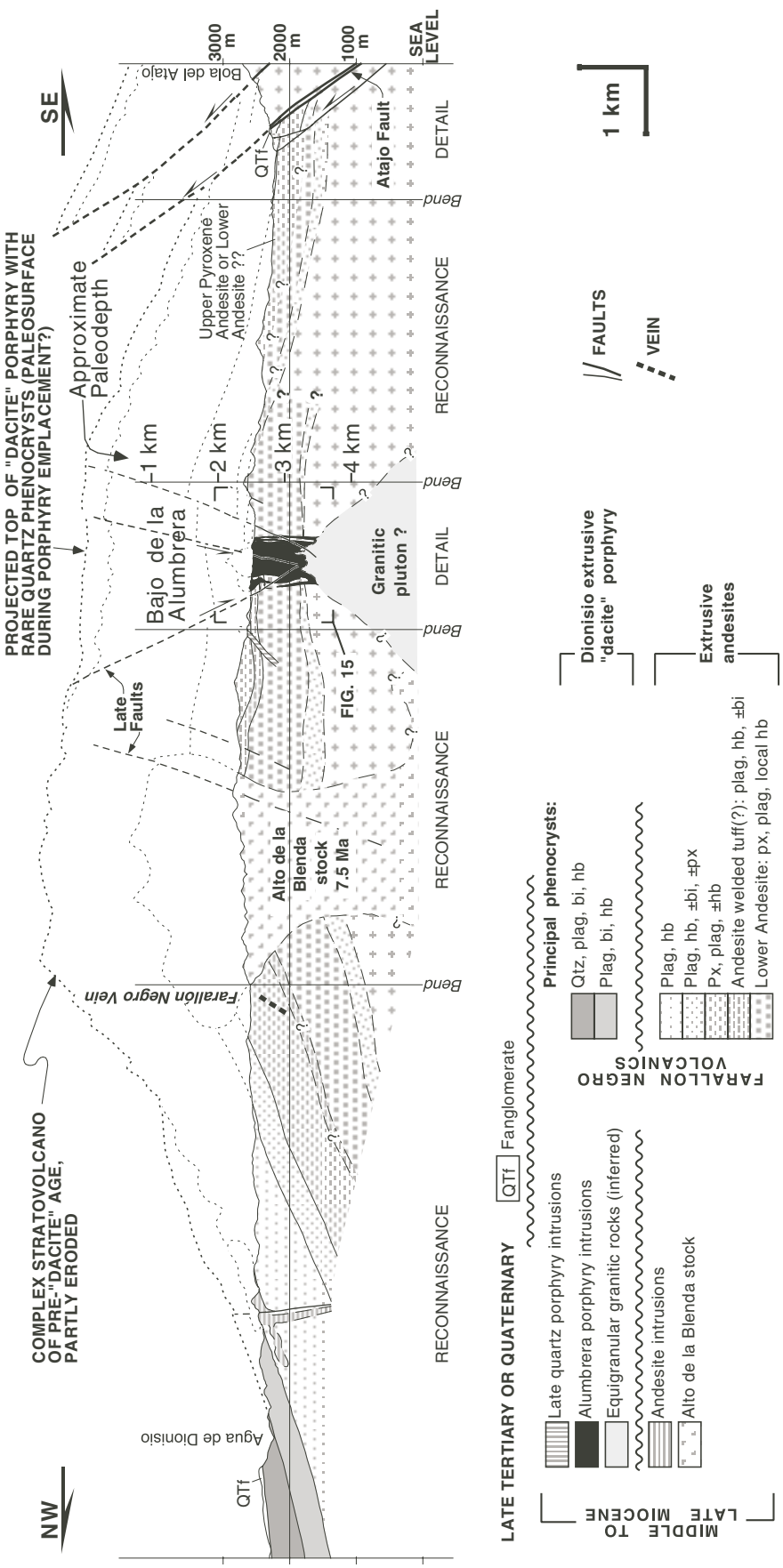

FIG. 3. Geologic cross section through the Farallón Negro district, showing the setting of the Alumbrera porphyry copper deposit. Parts labeled "detail" are interpreted from detailed mapping and core logging and parts labeled "reconnaissance" are interpreted mainly from reconnaissance mapping and air photo interpretation, with some information from Llambías (1972 and unpub. map, Yacimientos Mineros Agua de Dionisio). Predacite cone is based on interpretation of andesite stratigraphy and profiles of typical stratovolcanoes from Williams and McBirney (1979). "Dacite" is used as a field term. Abbreviations as in Tables 1 and 2.

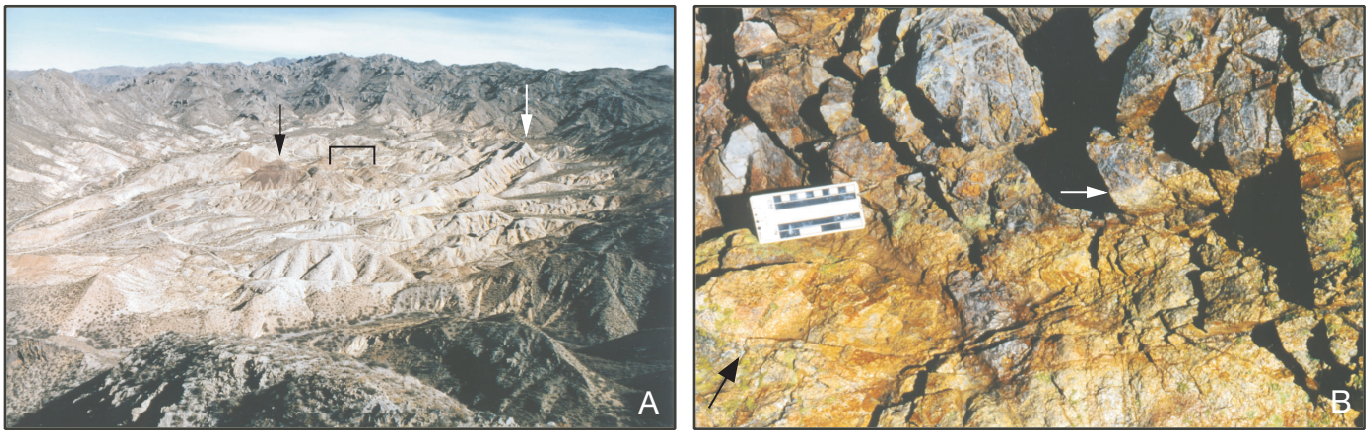

FIG. 4. A. View of Bajo de la Alumbrera, looking south, before mining. The hill beneath black arrow is Colorado Norte, underlain by high-grade P2; beneath white arrow is Los Amarillos underlain by strong sericitic alteration and abundant pyrite. Brackets indicate low-grade core zone. Figure 6 crosses view just behind these points but looking in opposite direction. B. Contact between P2 (above) and Early P3. Note abundant quartz veins in P2, most of which are truncated at contact (such as right of white arrow). Note sparse veins in Early P3 (black arrow). Divisions at top of scale are cm. West bank of Arroyo Alumbrera, 75 m west of Colorado Sur. North to right.

Several late Cenozoic Andean porphyry copper deposits (Pachón, Pelambres, Río Blanco, El Teniente) are scattered near the south margin of the gently dipping segment of the Benioff zone (Fig. 1; see also Skewes and Stern, 1994), in a broadly similar space-time setting to Alumbrera. Such relationships may also be present in the western United States, where similarities have been noted between Laramide (earliest Tertiary) uplifts of the central Rocky Mountains and the Sierras Pampeanas (Barazangi and Isacks, 1976; Jordan et al., 1983). It is speculated that the Benioff zone beneath the Laramide uplifts was also unusually flat (Jordan et al., 1983), also thought to have been caused by subduction of buoyant oceanic crust (Engebretson et al., 1985). Some of the largest porphyry copper deposits in the western United States are of Laramide age and are located near the north (Butte) and south edges (most Arizona-New Mexico deposits) of the Laramide uplifts. Alumbrera is therefore in a similar tectonic setting to these deposits. This suggests that the space-time location along magmatic arcs for Alumbrera and for certain other porphyry copper deposits may be somehow linked to the occurrence of gently dipping segments of the Benioff zones and/or to the subduction of unusually buoyant oceanic crust, such as seamount chains and oceanic plateaus.

Geologic Setting of the Farallón Negro District

Basement rocks of the Farallón Negro district (Figs. 2–3) are granitic and metasedimentary (González Bonorino, 1947) and are of early Paleozoic age (Caelles et al., 1971; McBride et al., 1976). These rocks are overlain, above a major unconformity, by a sequence of red to gray sandstones, siltstones, and pebble conglomerates of Miocene age (El Morterito Formation), up to several tens of meters thick (González Bonorino, 1947; Llambías, 1970, unpub. map). A few volcanic clasts occur near the top of this unit, and it is overlain by the Farallón Negro Volcanic Group, a thick pile of mainly andesites and dacites (González Bonorino, 1947; Llambías, 1970, 1972; Proffett et al., 1998; Sasso and Clark, 1998).

Farallón Negro Volcanics and related intrusions

The Farallón Negro Volcanics consist of a thick pile of andesites that are overlain by extrusive porphyritic dacite near Agua de Dionisio, along the western edge of the district (Figs. 2–3; "andesite" and "dacite" are used here as field terms). Andesitic intrusions occur in many areas of andesitic volcanic rocks and between Alumbrera and Farallón Negro the andesites are intruded by the Alto de la Blenda stock, a fine-grained rock of approximate quartz monzodiorite composition (Figs. 2–3). Numerous andesitic dikes cut the andesitic volcanics and some cut the Alto de la Blenda stock, but very few cut the extrusive Dionisio dacites. Small intrusive complexes of felsic porphyry, younger than the andesites, the Alto de la Blenda stock, and the andesitic dikes occur throughout the Farallón Negro Volcanic field. These are commonly associated with mineralization, including that at Alumbrera (Figs. 2–3). These porphyries are similar petrographically and in age to the extrusive Dionisio dacites, to which they are probably related. Local intrusions and domes of coarsely porphyritic dacite and of rhyolite are the youngest rocks of the complex (Fig. 2).

Andesitic volcanic rocks: Around the edges of Bajo de la Alumbrera (Figs. 5A, 6; Proffett, 2003, Map 1) about 670 m of andesite are exposed (1,150 m with deep drilling exposures included). These are subdivided stratigraphically based principally on identity, abundance, size, and mode of occurrence of phenocrysts, as summarized in Figure 5A. Most of these andesites are monolithologic breccias and tuff breccias, in which matrix and fragments are similar with regard to phenocrysts, though not necessarily with regard to color. Some clastic units are very well lithified and appear to be welded. Less common are lava flows, heterolithologic breccias, volcanic conglomerates, and volcanic sandstones.

Near Río Vis Vis, 6 km southeast of Alumbrera, ~370 m of andesitic volcanic rocks are exposed (Fig. 5B). The lower 85 m here resembles, and may correlate with, the Lower Andesite and/or the Upper Pyroxene Andesite at Alumbrera.

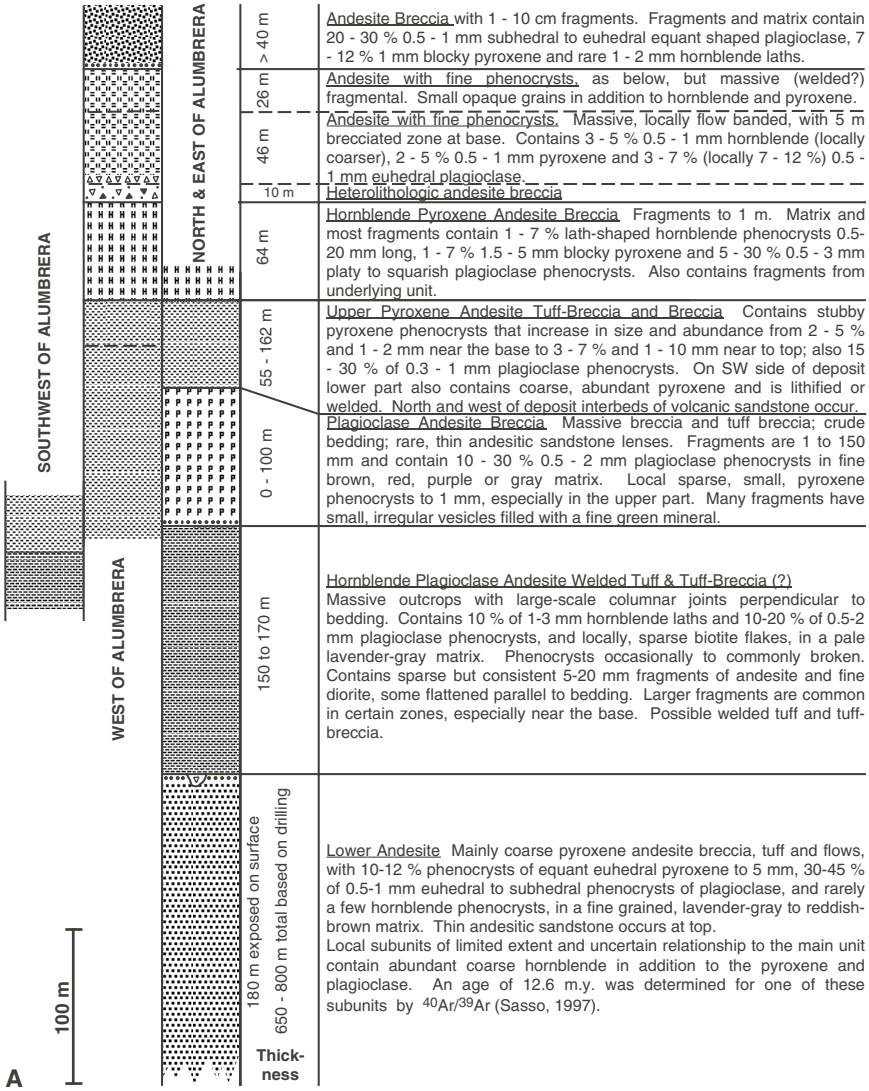

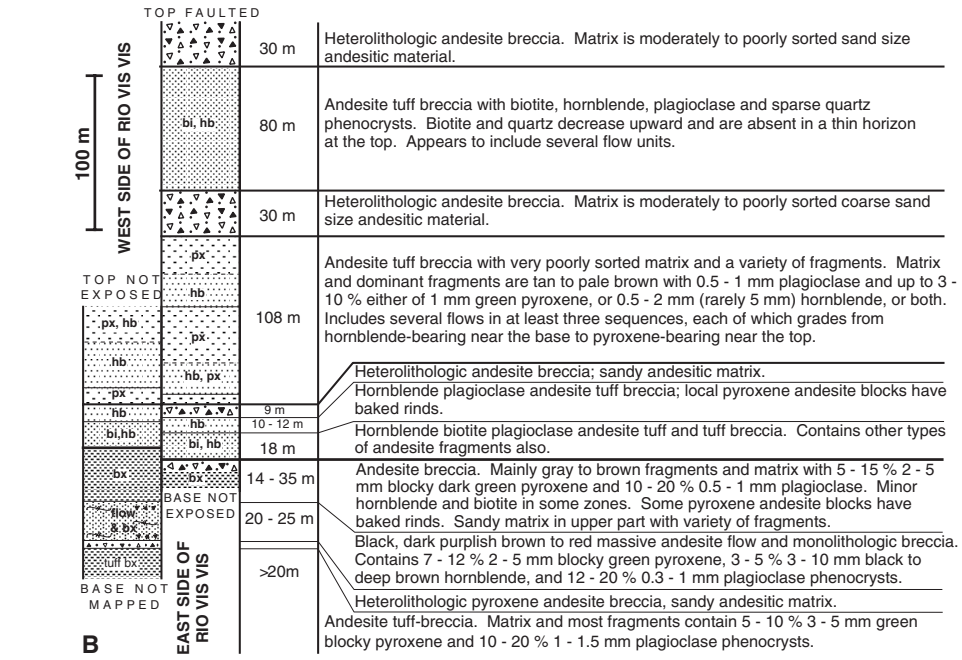

FIG. 5. Stratigraphy of late Tertiary andesite. A. Near Bajo de la Alumbrera. B. Río Vis Vis area, 6 km southeast of Alumbrera.

Figure 6
FOLDOUT

The upper part of the section consists of nearly 300 m of well-lithified tuff breccias containing plagioclase, hornblende, biotite, and fine-grained pyroxene phenocrysts (Fig. 5B). These do not resemble units exposed near Alumbrera but are similar to rocks from higher in the section, exposed near Farallón Negro (Fig. 3).

Drilling indicates that the base of the volcanic section at Río Vis Vis lies at shallow depth, and that the entire 1,150 m of section at Alumbrera is represented by no more than ~300 m of section at Río Vis Vis. Many Alumbrera units (Fig. 5A) are missing at Río Vis Vis, where flow units are generally thinner than at Alumbrera, and a higher proportion of volcanics have been reworked by sedimentary processes. The volcanic section near Río Vis Vis appears to be more distal in characteristics than that near Alumbrera.

In contrast, volcanic rocks exposed near the Alto de la Blenda stock 2 to 3 km west of Alumbrera (Fig. 3) appear to be more proximal. Rocks here that appear to correlate with the Hornblende Plagioclase Welded Tuff (?) unit are quite thick, include strongly lithified (welded?) zones, and abundant large fragments similar in composition to the tuff, and are associated with massive and flow-banded rocks of similar composition that may be intrusions, flows, or domes.

About 2.4 km of andesitic volcanic rocks are exposed west of the Alto de la Blenda stock (Figs. 2–3). The lowest part of this section resembles the uppermost part of the section at Alumbrera (Fig. 5A). Above this are ~300 m of tuffs and tuff breccias with hornblende, biotite, and plagioclase that resemble the upper part of the Río Vis Vis section (Fig. 5B), with which they may correlate (Fig. 3). Above these is ~1,000 m of breccias, flows, and tuffs containing moderate amounts of medium-grained hornblende and fine- to medium-grained plagioclase, with rare biotite and/or pyroxene. A few interbeds of volcanic sediments are also present.

An $^{40}Ar/^{39}Ar$ age of 12.56 ± 0.36 Ma (middle Miocene) has been determined on hornblende that appears to be from a subunit of the Lower Andesite (see Fig. 5A) and several K-Ar and $^{40}Ar/^{39}Ar$ ages of 8.1 to 8.6 Ma (late Miocene) have been determined from other parts of the andesite section (Caelles et al., 1971; Sasso, 1997; Sasso and Clark, 1998).

Alto de la Blenda stock: The Alto de La Blenda stock, about 4 km in diameter (Llambías, 1972), intrudes at least the lower half of the andesitic section (Figs. 2–3). Some of the andesitic dikes that intrude andesitic volcanic rocks cut the stock, and others are cut by the stock. Felsic porphyries, some mineralized, as at Bajo Las Pampitas (Fig. 2), cut the stock. The age of the stock is thus similar to or slightly younger than the upper part of the andesitic volcanics. An $^{40}Ar/^{39}Ar$ age of 7.50 ± 0.20 Ma has been determined on hornblende from the stock (Sasso, 1997).

Rocks of the stock are very fine grained and contain hornblende, biotite, magnetite, pyroxene, plagioclase, minor quartz, and in most phases, very fine grained K-feldspar. The proportions of these minerals suggest a quartz monzodiorite to locally diorite or monzonite composition. The stock is similar in composition to some of the andesites that it intrudes. Dikes of rock similar to the stock extend from the stock for hundreds of meters into the andesite.

Andesite dikes and other andesite intrusions: A variety of andesite dikes cut andesitic volcanics, and some cut the Alto de La Blenda stock. Andesite dikes of several types and orientations are cut by the Alumbrera felsic porphyries, and no porphyries have been observed to be cut by andesite dikes.

At Alumbrera, dikes have a variety of orientations, including steeply dipping with west-northwest, northwest, north-northwest, north-south, north-northeast, and northeast strikes, as well as gently to moderately dipping orientations (Fig. 6; Proffett, 2003, Map 1). Near Farallón Negro, east-west– and west-northwest–trending steep orientations are common. Many of the dikes shown in maps by Llambías (1972) appear to define a radial pattern centered near the Alto de la Blenda stock (Fig. 2). Andesite dikes are less common near the western and northern edges of the district (Llambías, 1972) and in the Río Vis Vis area. Various types of dikes are characterized by different phenocryst assemblages, which may include plagioclase, pyroxene, hornblende, and biotite in various combinations, grain sizes, and textures.

Large irregular bodies of intrusive andesite occur in several parts of the volcanic complex. They include sills as well as steep bodies, have a variety of phenocryst assemblages, and may be of various ages. According to Llambías (1972), some, mapped as La Chilca Andesites, lie near the outer part of the andesite exposures along a ring, which he interpreted as a possible caldera fracture. The present study has found no evidence for caldera collapse in the upper part of the volcanic section, but further work is needed in this regard, especially in the lower part of the section.

Dacitic volcanics of Agua de Dionisio: In the Agua de Dionisio area the andesites are overlain, conformably or possibly disconformably, by a section of porphyritic dacite breccias and tuffs at least 800 m thick (Figs. 2–3; "dacite" used as a field term; may include quartz latite and/or rhyolite).

The lower part is porphyritic dacite with few or no quartz phenocrysts (Table 1) and is well exposed in quebradas (ravines) southeast of Agua de Dionisio. Most common are monolithologic breccias, and some units include +10-m blocks of flow-banded dacite. Flow-banded intrusions or domes also occur.

The upper part of the section is porphyritic dacite with quartz phenocrysts (Table 1). Most rocks are monolithologic breccias and tuffs with fragments and matrix of similar composition and of similar (Fig. 7A) or variable color. Breccia blocks up to 1 m in size are common. The section is crudely bedded with 10-cm– to 5-m–thick beds. Some tuff breccias and tuffs appear to be welded. Some have broken phenocrysts and may have been deposited as thin ignimbrites. This upper part of the section includes both biotite hornblende dacite and biotite dacite (Table 1).

Despite the abundance of andesite dikes and other intrusions in underlying andesites, the extrusive porphyritic dacite has not been observed to be intruded by andesite dikes or other intrusions, except for rare, thin, dark, hornblende-biotite–bearing sills and dikes near the base of the section. Fragments of andesite similar to that in a nearby dike and sill complex that cuts andesitic volcanic rocks occur in basal porphyritic dacite southeast of Agua de Dionisio. Therefore Dionisio extrusive porphyritic dacites are apparently younger than andesitic dikes and therefore probably also younger than the Alto de la Blenda stock. The Dionisio extrusive dacites have similar age relationships to the small felsic porphyry in-

TABLE 1. Descriptions of Alumbrera Rock Units and "Dacites" of Agua de Dionisio

Unit	Plagioclase Percent	Plagioclase Size (mm)	Plagioclase Description	Quartz Percent	Quartz Size (mm)	Quartz Shape	Biotite Percent	Biotite Size (mm)	Hornblende Percent	Hornblende Size (mm)	Minor minerals	Matrix
Lower Dionisio dacitic volcanics	10–25	0.5–5	Euh-subh; An55–85	None to very rare			2–7	0.5–3 diam flakes	5–15	0.5–2 laths	prim mgt(?), ap, sph(?)	Aphanitic (devitrified glassy); pale tan, gray or purplish; plag microlites
Upper Dionisio dacitic (bi–hb) volcanics	15–30	0.5–5	Subh-euh; An50–75	0.5–1	1–5	Rdd, resorbed	3–7	0.5–3 diam flakes and books	4–7	1–3 laths	prim mgt, ap, sph, px, zirc	Glassy or devitrified; pale gray, tan or pinkish; plag microlites
Upper Dionisio dacitic (bi) volcanics	5–30	0.5–5	Subh-euh; An48–60	0.5–1	0.5–5	Rdd, resorbed	5–10	0.5–3.5 diam flakes and books	none		sph, ap, prim mgt	Devitrified glassy; white, pale gray, tan or pinkish; plag microlites
Northeast porphyry	10–20	2–6	Subh	Very rare			2–4	2–3 (rarely 5) diam, thin books	2–5	1–4 laths (usually alt'd)	prim mgt	Very fine grained, pale greenish to tan
P2	10–25 (rarely to 30%)	0.5–5	Subh; An45–56+	Sparse	2–6	Rdd, resorbed	1–4	1–2 diam × 1–3 thk	1–3	Alt'd to irreg. clots sec bi	ap, zirc, sph, prim(?) mgt	Pink, polygonal 0.02–0.08 mm Kf ≥ qtz, ±minor bi and/or mgt.
Los Amarillos porphyry	5–20? obscured by alteration	1–3	Anh, subh, rarely euh	0–3	0.5–5	Rare euh, some rdd, resorbed, many broken	0–?	local 1–2 mm flakes, local fine clots	0–?	Obscured by alteration	obscured by alteration	Aphanitic to very fine to coarser grained (0.2–0.4 mm) qtz and alt'd feldspar
Early P3	15–40 (usually 25–35)	0.5–6 (usually 1–5)	Euh-subh; An35–62+	0.2–0.5 (rarely 1–5)	1–4 (locally 2–7)	Rdd, resorbed to slightly irreg	1–6	0.5–2 diam × 1–3 thk	2–5	Alt'd to clots and laths of sec bi	sph (alt'd to lx), ap, prim mgt, zirc	Polygonal 0.015–0.12 mm Kf > qtz, (ab), ±bi, ±mgt; unalt'd: fine gray; Kf alt'd: coarse, pink
Quartz–eye porphyry	15–40 (usually 25–35)	0.5–6 (usually 1–5)	Euh-subh	2–5	2–7	Irreg to rdd, resorbed	1–6	0.5–2 diam × 1–3 thk	2–5	Alt'd to sec bi clots and laths	sph (alt'd to lx), ap, zirc, prim mgt	Polygonal, 0.015–0.12 mm Kf > qtz, minor ab, ±bi, ±mgt
Late P3 (North porphyry)	20–40	0.5–5	Subh-euh	±1	0.5–6	Rdd, resorbed	2–5	1–3 diam × 1–3 thk	2–5	bi'd laths	prim mgt, ap, sph (alt'd to lx), zirc	Very fine, pale gray
Late P3 (central)	10–35	0.5–6	Subh-euh; An28–74	0.2–1	1–5	Squarish, w/ rdd corners	2–5	0.5–3 diam × 0.3–2 thk (local 10 × 5)	1–4	0.5–3 irreg clots and 5 long laths	0.5–2 mm prim mgt, ap, sph, zirc?	Very fine to aphanitic pale gray; Kf > qtz >> very fine plag; minor bi and/or hb
Late P3 (Campamento)	25–35	2–5	Subh-euh	<0.5	1–4 (locally to 8)	Subh-anhl, rdd, resorbed	2–7	1–3.5 diam × 1–3.5 thk	3–5	1–3 laths and irreg clots; locally bi'd	local Kf phenos, prim mgt, ap, zirc, sph?	Aphanitic, white to pale green; Kf > qtz >> fine plag
Northwest (NW dikes)	10–20	1–5	Subh-euh	≤0.5	2–7	Rdd, resorbed, irreg.	3–7	1–3 diam × 1–3 thk	2–5	1–5 long laths (not bi'd)	sparse fine mgt, (sph?, ap?, zirc?)	Aphanitic, pale green
Northwest (in main stock, pale)	20–30	0.5–5	Subh–anhl	Rare	1–2	Rdd, resorbed	2–5	0.5–2	2–5	Laths to 3 long (part bi'd)		Pale gray to greenish gray; has minor mgt
Northwest (in main stock, dark)	15–25	0.5–5	Subh–anhl	Rare	1–2	Rdd, resorbed	2–5	0.5–2	3–7	Laths to 3 long (part bi'd)	fine mgt (in matrix),(sph?, ap?, zirc?)	Similar to pale phase but more fine plag (<0.5mm) in matrix
Postmineral porphyry	10–15 (locally higher)	1–8		0.5–2	Up to 5		2–3	1–2	10– 15	1–3 long laths (not bi'd)	dissem. mgt (sph?, ap?, zirc?)	Very fine, gray

From visual estimates in outcrop, drill core, sawed slabs, and thin sections, checked by computer measurements of selected areas on sawed slabs

Abbreviations: ab = albite; alt'd = altered; anhl = anhedral; ap = apatite; bi = biotite; bi'd = biotitized; Descrip = Description; diam = diameter; dissem = disseminated; euh = euhedral; hb = hornblende; irreg = irregular; Kf = K-feldspar; lx = leucoxene; mgt = magnetite; phenos = phenocrysts; plag = plagioclase; prim = primary; px = pyroxene; qtz = quartz; rdd = rounded; sec = secondary; sph = sphene; subh = subhedral; thk = thick; zirc = zircon

Plagioclase An estimated optically, 5 to 25 measurements each; higher An zones in P2 and Early P3 not measurable due to alteration

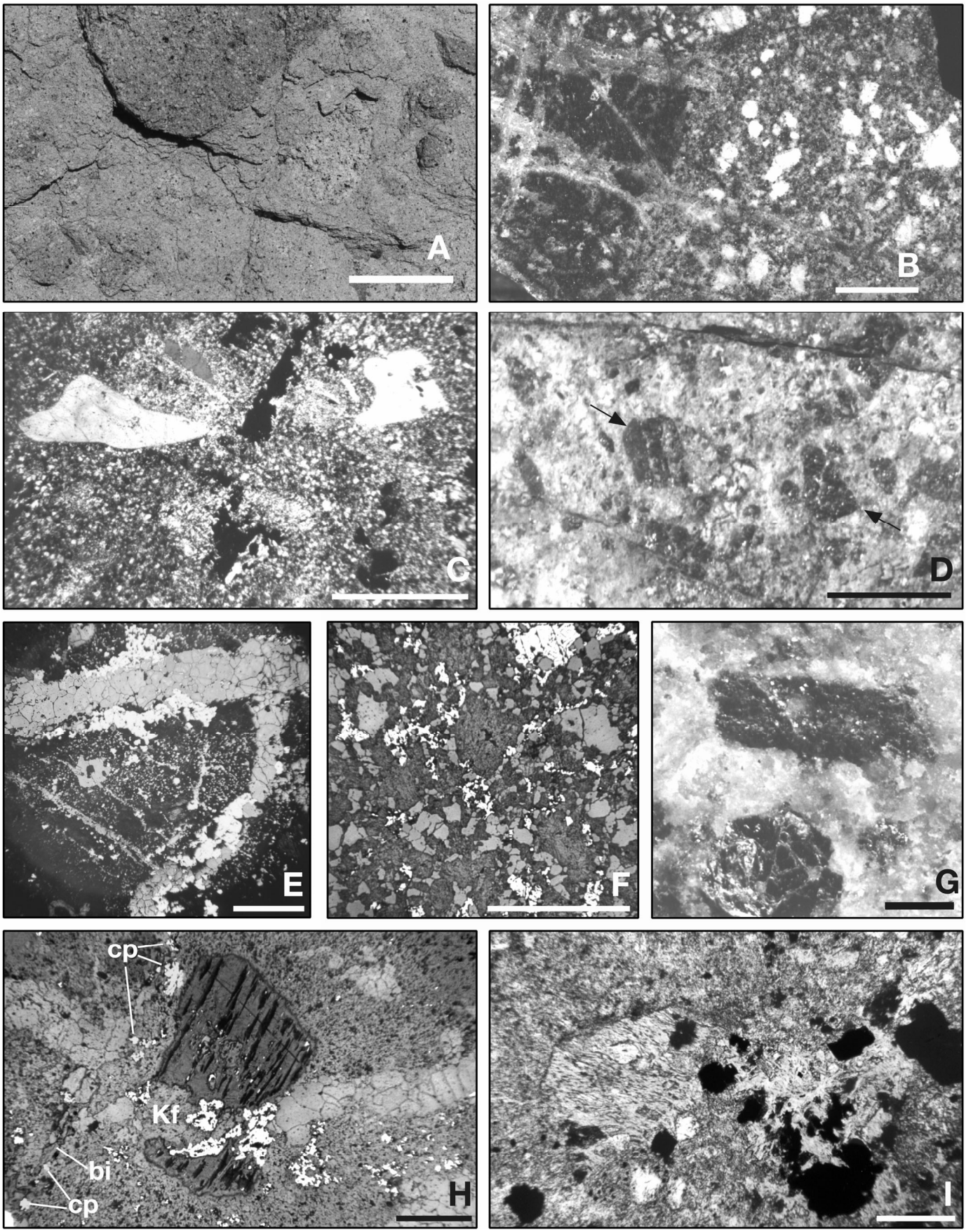
A
B
C
D
E
F
G
cp
Kf
bi
cp
H
I

trusions of the district (discussed below), to which they are also petrographically very similar, and they are interpreted here as volcanic equivalents of some of these intrusions. Because some of the felsic porphyry intrusions are mineralized, the volcanic equivalent Dionisio dacites are important in estimating mineralization emplacement depths.

Biotite from volcanic rocks near the west edge of the complex, apparently the lower part of the Dionisio dacite, has yielded an $^{40}Ar/^{39}Ar$ age of 7.49 ± 0.09 Ma (Sasso, 1997) or late Miocene.

Felsic porphyry intrusions: Felsic porphyries occur in several small clusters throughout the Farallón Negro district, many related to mineralization (Figs. 2–3). Those at Alumbrera (Fig. 6; Proffett, 2003, Maps 1–2) are described below. Small stocks of similar porphyry associated with porphyry copper-type occurrences are scattered along a poorly defined northwest trend at Bajo Las Pampitas, Bajo de Agua Tapada, and Bajo de San Lucas (Fig. 2); the latter two have $^{40}Ar/^{39}Ar$ ages of about 7.4 Ma on biotite (Sasso, 1997). Bajo del Espanto, 2 km south of Alumbrera (Fig. 2), is a steep-walled pipe, 1 km in diameter, of tuff breccia containing abundant fragments of felsic porphyry and of andesitic and basement fragments. Later felsic porphyry dikes cut the pipe. This complex was probably a vent for some of the extrusive porphyritic dacites.

Coarsely porphyritic dacite and rhyolite intrusions: Small intrusions of flow-banded coarse-grained porphyry occur along a northwest trend in the northwest part of the district (Fig. 2; Macho Muerto rhyodacites of Llambías, 1972). The largest of these, at Loma Morada, dated at 6.14 ± 0.05 Ma (Sasso, 1997), intrudes and deforms the Dionisio extrusive dacite. They contain abundant large plagioclase phenocrysts, scattered large sanidine and quartz phenocrysts, hornblende laths, and abundant biotite in a slightly pumiceous pale gray matrix. These, along with a few other small bodies of rhyolite or dacite (Llambías, 1972; Sasso, 1997), represent the youngest igneous activity in the district.

Overall structure and history of the volcanic complex: In general, the Farallón Negro volcanic complex evolved from early mafic andesites (and basalts) to later more felsic rocks.

Although the Farallón Negro volcanics are now bordered in many places by Paleozoic basement, very few basement fragments occur in the volcanic rocks. Basement fragments in the Bajo del Espanto intrusive breccia and in smaller intrusive breccia dikes indicate that the rare basement fragments observed in volcanic rocks were probably derived from the walls of magma chambers or conduits. No evidence has been observed for sedimentary debris of basement origin in the volcanics, suggesting that there were not areas of uplifted basement within or adjacent to the volcanic complex during volcanism and that the volcanic field was high relative to its surroundings.

No evidence was found during this study for a west-northwest–trending extensional basin, proposed to have helped localize the Farallón Negro igneous complex (Sasso and Clark, 1998). In fact, the thin character of the immediately underlying El Morterito Formation (Fig. 3), compared to thicker sections to the east and west (González Bonorino, 1947; Allmendinger, 1986), argue against such a basin.

Sillitoe (1973, Fig. 6) interpreted dips in the andesites to indicate that Alumbrera was emplaced directly beneath the peak of an andesitic stratovolcano. It is clear from mapping however that the andesites have been deformed by later structural events and in many places do not dip away from Alumbrera (Fig. 6; Proffett, 2003, Map 1). The lack of abundant large andesitic intrusions and the dominance of breccias and tuffs over flows at Alumbrera support the interpretation that Alumbrera was not an important center of andesitic volcanism (Proffett, 1999). Local vents for Lower Andesite are suggested by associated intrusions northeast of Alumbrera. As concluded by Llambías (1972), a likely center for most andesitic volcanism is 3 to 5 km west of Alumbrera, as suggested by the presence of the Alto de la Blenda stock and other intrusions, by the center of a crude radial pattern shown by

FIG. 7. A. Extrusive porphyritic dacite breccia of Agua de Dionisio. Pale gray subangular blocks and lapilli in a matrix of similar material. Located in quebrada 800 m WNW of top of Loma Morada. Scale = 10 cm. B. P2 with A quartz veins and magnetite-K-feldspar alteration on left truncated at contact of Early P3 on right. Note that some A quartz-magnetite veins with K-feldspar halos cut both porphyries. From low-grade core zone. Scale = 1 cm. Sawed drill core, hole 51-52.2, 211.3 m, 0.03 percent Cu, 0.06 ppm Au. C. Thin section of Los Amarillos porphyry with complete feldspar destructive alteration, crossed nicols. Note quartz phenocryst splinters, some partly resorbed. Bright mottled patches are sericitized plagioclase sites; black below center is pyrite; sericite replacing biotite occurs in lower right side of the pyrite. Gypsum occurs in some of the other dark areas. Matrix replaced by fine-grained quartz, sericite, and rutile. Scale = 1 mm. From quebrada 135 m NNE of Los Amarillos. D. Abundant quartz vein fragments (dark, arrows point to two larger ones) in outcrop of Quartz-eye porphyry (160 m SW of Colorado Sur). Note that some fragments are angular and some are rounded. Scale = 1 cm. E. Three generations of quartz-magnetite A veins in Early P3 (reflected light). The thick one displaces the one at right, which in turn displaces the thin ones. Bright mineral is magnetite, medium gray is quartz. Fine magnetite is associated with the thin veins and coarse magnetite is irregularly distributed along the margins of the thicker ones. Cu sulfides are associated with none of the veins. Scale = 1 mm. Drill hole 49-60, 361.0 m, 0.7 percent Cu, 0.8 ppm Au. F. Early P3 from low-grade core zone altered to K1 mosaic (reflected light). Bright mineral is magnetite (with minor titanohematite or ferrian ilmenite), medium gray is quartz and dark areas are K-feldspar. No biotite, Cu sulfides or chlorite remain. Scale = 1 mm. Drill hole 48-54, 390.0 m, 0.05 percent Cu, 0.0 ppm Au. G. Hornblende phenocrysts in North porphyry altered to fine-grained shreddy secondary biotite (top). Primary biotite book (bottom). Scale = 1 mm. Broken surface, 166 m NNW of Colorado Norte. H. Biotite book in P2 cut by a K1 assemblage A vein, which is in turn displaced by a K3 assemblage vein at left (reflected light). Note K-feldspar (Kf) in earlier vein with magnetite (white) where it cuts the biotite. Chalcopyrite (pale gray) and biotite (bi) occur in later vein. Scale = 0.5 mm. Drill hole 49-60, 186.0 m, 0.9 percent Cu, 1.5 ppm Au. I. Two chloritized mafic phenocrysts in Lower Andesite tuff-breccia (plane-polarized light). The left one is replaced by parallel chlorite flakes and was probably an unbiotitized pyroxene and the right one consists of randomly oriented shreddy chlorite and was probably formerly a biotitized mafic mineral. From outer part of secondary biotite zone. Scale = 0.2 mm. Arroyo Ron, 460 m S47W of primary crusher.

andesite dikes (Fig. 2; Llambías, 1972), and by the more proximal characteristics of the volcanic rocks. On the other hand, andesites at Alumbrera appear to be more near source than those to the southeast, such as at Río Vis Vis, which may have been on the outer flank of the complex. A former complex andesitic stratovolcano with multiple vents, broadly centered above the Alto de la Blenda stock (Fig. 3), may have been partly eroded before eruption of the Dionisio extrusive dacites. Felsic porphyry intrusive centers, some of which may have vented to feed the extrusive dacites, and some of which are mineralized, are distinctly younger than the andesites and in general did not share the same vents as the andesites.

District structure

Small normal faults mapped near Alumbrera (described below) indicate minor east-northeast–west-southwest extension that took place after porphyry copper mineralization, that is, since 6 or 7 Ma. Gentle folds or warps in the Farallón Negro Volcanics at Alumbrera (described later) may in part be due to emplacement of porphyries and in part related to faulting.

Major faults occur in the eastern and southern part of the complex, especially along contacts between the volcanic rocks and older rocks (Fig. 2).

Major moderately dipping reverse faults (Atajo fault system) form the boundary between the Farallón Negro Volcanics and the Paleozoic basement at Bola del Atajo (Figs. 2–3). There is no evidence that the faults in any way influenced deposition of the andesites or the underlying Miocene sandstone, so they were apparently active after eruption of the andesites at 7.5 to 13 Ma. The faults are overlain unconformably by Pliocene or Pleistocene alluvium on terraces 70 to 100 m above present streams. This alluvium was probably deposited in fans along the Bola del Atajo range front, due to uplift along the Atajo fault system. Minor structures in the fault gouge and bends in fault planes suggest displacement approximately in an east-west direction. Therefore, there appears to be evidence of major east-west compression here within the same time interval (but not necessarily exactly the same time) as minor east-northeast–west-southwest extension at Alumbrera.

The southern boundary of the Farallón Negro Volcanics in this area is the Buenaventura fault (Fig. 2). This fault dips steeply north, so apparent displacement is normal; replacement of wall rocks with silica and sulfides has occurred locally along it.

North of Durazno, Farallón Negro andesites are faulted down to the west against Miocene sandstones along a west-dipping fault of apparent normal displacement (Fig. 2). The fault is intruded by an andesite dike, so it may have been active during part of the volcanic activity. It suggests minor east-west extension but could instead be strike slip or of volcanotectonic origin. It may be related to an apparent eastside-up displacement of the lower part of the volcanic section 2.5 km east of Alumbrera (Fig. 3). A few hundred meters east of the normal fault north of Durazno, Paleozoic granite is faulted up to the east against Miocene sandstone along a steeply east-dipping reverse fault (Fig. 2), suggesting east-west compression. This fault may be related to the Atajo fault system.

Two km south of Vis Vis, a major range front fault separates the Farallón Negro Volcanics to the northwest from uplifted Paleozoic granitic and metamorphic rocks in the range to the southeast (Fig. 2). This fault dips steeply southeast in most exposures examined. Alluvial fan deposits along the range front appear to be affected by the fault, suggesting a Pliocene or Quaternary age for faulting. This fault can be traced in air photos through the mountains to the northeast, where it is the range front fault of the Sierra Nevados de Aconquija. This and other faults parallel to it in the region suggest compressive deformation in a northwest-southeast direction.

Little evidence has been observed for influence of these district-scale and regional structures on deposition of volcanic units or emplacement of intrusions. Dike and veinlet orientations at Alumbrera and elsewhere in the district define crude radial patterns, suggesting relationship to local intrusive events, with local preference for northwest or northeast dike orientations. Evidence for emplacement of dikes of any age along fault planes is only rarely observed (e.g., Proffett, 2003, Map 1).

Faults at Bajo de la Alumbrera

Faults that cut the Alumbrera deposit include steeply dipping westside-down normal faults in the eastern and central part and moderately northeast dipping normal faults in the southwestern part (Proffett et al, 1998). Rare, steep, eastside-down faults and east-northeast–trending, southside-down faults are also present but have insignificant displacement.

The larger faults typically consist of one or more strands of strongly sheared fault clay and sheared breccia, one to several tens of centimeters thick, within a zone of altered and broken rock up to a few meters thick. Gypsum veins are common along many faults.

Age of faulting: All faults displace porphyries about the same amounts as extrusive andesite units, indicating that displacement was younger than the porphyries (Fig. 6; Proffett, 2003, Maps 1–2). The zone of intense sericitic alteration, dated at 6.75 ± 0.09 Ma (Sasso and Clark, 1998), is also displaced, but there are narrow zones of late-phase sericitic and argillic alteration and late veins along most faults (Fig. 8; Proffett, 2003, Map 3). Therefore the faults were active before circulation of the latest hydrothermal fluids had ceased. Direct age relationships between northeast- and west-dipping normal faults have not yet been observed, but late alteration appears to be less intense along northeast-dipping faults, so they may be a little younger.

No evidence has been found for significant faulting before or during emplacement of porphyries or the main stages of mineralization. Continuity of volcanic units shows that porphyries were not emplaced along faults (Proffett, 2003, Map 1).

Westside-down normal faults: The largest westside-down normal fault is the Gypsum fault (Proffett, 2003, Maps 1–2). It dips 45° west-southwest to about 90° (Fig. 6). Several small splays split from the footwall side and trend southeast. Volcanic and porphyry units are displaced across the Gypsum fault 125 to 150 m down to the west. Displaced units do not indicate much strike-slip component, but horizontal slickensides on some fault exposures (P. Forrestal, pers. commun., 1997) suggest minor late strike slip. In some exposures foliation in fault clay dips to the west at a lower angle than the fault itself. The foliation is thought to have formed at high

Figure 8
FOLDOUT

angle to the shortening direction, consistent with westside-down dip-slip displacement.

Several other westside-down normal faults, with up to 80-m displacement, occur east and west of the Gypsum fault or merge with it (Fig. 6; Proffett, 2003, Maps 1–2).

Northeast-dipping normal faults: The largest northeast-dipping normal fault is Steve's fault, in the southwest part of the deposit (Proffett, 2003, Map 1). It dips 45° to 50° northeast near the surface and steepens to about 55° to 60° at depth and northward. It displaces the porphyry stock, alteration and mineralization ~200 m, hanging wall northeasterly relative to footwall (Fig. 6). Faults subparallel to Steve's fault to the northeast and southwest (Proffett, 2003, Map 1) have normal displacements of a few meters or tens of meters.

Relationship between faulting and tilting: Gentle tilting, as recorded in andesites, could explain the unusual dips of some fault planes. For example, the 56-50 fault dips vertically to steeply east in the central part of the stock, and parts of Steve's fault dip only 45° to 55° northeast. These dips could have resulted from local, gentle, westward tilting, as observed for andesite units near these faults (Fig. 6; Proffett, 2003, Map 1), of an originally steeply west-southwest dipping 56-50 fault and an originally steeply northeast dipping Steve's fault—more typical attitudes for normal faults.

Depth of emplacement of the Alumbrera deposit

The Alumbrera porphyries and other felsic porphyry intrusive centers are similar petrographically and in age to the Dionisio extrusive dacites, and some are probably intrusive equivalents. Most of these porphyry intrusions have sparse quartz phenocrysts and are younger than otherwise similar porphyry intrusions that lack quartz phenocrysts (e.g., the Northeast porphyry at Alumbrera, described below). In this regard they resemble units in the upper part of the Dionisio dacite section, which have similar amounts of quartz phenocrysts and which overlie otherwise similar porphyritic volcanic rocks that lack quartz phenocrysts (Table 1). The ore-related porphyries at Alumbrera are older than other, more quartz-rich, porphyry intrusions exposed west and northwest of Alumbrera (Fig. 6) and so were apparently emplaced relatively early in the period of quartz-bearing porphyry activity. They may therefore correlate most closely with the lower part of the quartz-bearing dacite porphyry volcanic section. This is not to imply that the Alumbrera porphyries themselves vented but rather that some of the group of similar, probably comagmatic, felsic porphyry centers (e.g., Espanto) vented to feed the Dionisio extrusive dacites.

The surface at the time of ore-related porphyry intrusion is therefore tentatively interpreted to have been near the transition from extrusive dacites without quartz phenocrysts to those with quartz phenocrysts (Fig. 3), although it could have been above or below this by a few tens or hundreds of meters. This contact projects about 2.5 to 2.8 km above the pre-mine surface at Alumbrera (Fig. 3; Proffett, 1999) or 3.2 to 3.5 km above drill penetrations ~650 m deeper, which is the approximate lower limit of 0.5 percent Cu ore as interpreted in Figure 6. Assuming average rock densities of about 2.4 g/cm^3 for the upper kilometer of volcanic rocks and 2.65 g/cm^3 below this, these depths would correspond to lithostatic pressures of 0.6 to 0.7 kbars for the pre-mine surface at Alumbrera and 0.8 to 0.9 kbars for the interpreted bottom of 0.5 percent Cu (Proffett et al, 1998). Hydrostatic pressure would have been 0.25 to 0.28 kbars for the pre-mine surface and 0.31 to 0.34 kbars for the interpreted bottom of 0.5 percent Cu.

Alumbrera Porphyries

The porphyries at Alumbrera occur in a closely spaced cluster of small bodies emplaced during at least seven phases of intrusion (Fig. 6, Table 1; Proffett et al., 1998; Proffett, 1999, 2003, Maps 1–2). At the center are irregular stocks, surrounded by dikes that define a crude radial pattern, with a weak preference for north-northwest orientations. This pattern was in part recognized by Bassi and Rochefort (1980) and Stults (1985). The radial pattern can best be explained by local causes, but the preferred north-northwest orientation could be due to either local or regional tectonic causes. Exposed contacts and drill hole data indicate that most porphyry intrusions dip steeply (Fig. 6; Proffett, 2003, Maps 1–2). All porphyries are felsic; contemporaneous mafic or intermediate intrusions were not observed during this study.

Nearby porphyries that do not appear to be part of the Alumbrera system include a north-northwest–trending dike of uncertain age in the northeast part of Map 1 (Proffett, 2003, colored as Northwest porphyry) and some quartz-eye–rich bodies in the west and northwest parts of Map 1 (Proffett, 2003). One of the quartz-eye–rich bodies cuts epidote-chlorite–altered andesite in the outer part of the Alumbrera alteration pattern but is itself little altered (Proffett, 2003, Map 3). This, and the lack of spatial relationship to alteration, suggests it is younger than the Alumbrera system. These porphyries will not be discussed further here.

With the possible exception of Northeast porphyry, a minor dike, no porphyry older than P2 has been found within the Alumbrera cluster; "P1," used previously (see Guilbert, 1995, for a summary), was found to be invalid as a rock unit and has been abandoned. Most porphyries of the cluster are closely related to mineralization in space and time (Figs. 6, 8, 9–10; Proffett, 2003, Maps 1–4) and are similar to one another in that they all contain phenocrysts of plagioclase, hornblende, biotite, and quartz, in a quartz-feldspar matrix (Table 1, Figs. 11 A-F, 12A-B). They are distinguished and mapped mainly on the basis of intrusive contact relationships (Figs. 4B, 7B, 11B, F; Proffett et al., 1998; Proffett, 1999, 2003, Map 2); separate units were generally established only where consistent relationships could be mapped over multiple outcrops and/or drill holes. Within some units, notably Early P3 and some Northwest porphyry bodies, intraporphyry contacts can occasionally be found but cannot be mapped consistently within areas of significant size. Only Northeast porphyry and Los Amarillos porphyry show no obvious relationship to mineralization patterns (Figs. 6, 13; Proffett, 2003, Map 1).

The oldest of the ore-related porphyries, P2, is the most strongly mineralized; each subsequent porphyry is mineralized less intensely, and the youngest, Postmineral porphyry, is essentially unmineralized (Proffett, 1999). Cooling ages of 6.8 to 7.1 Ma have been determined by $^{40}Ar/^{39}Ar$ on biotite from the Alumbrera porphyries (Sasso and Clark, 1998).

"Dacite" has been used as a field term for Alumbrera porphyries, because they generally lack K-feldspar phenocrysts, but the presence of K-feldspar in the matrix and as local, rare

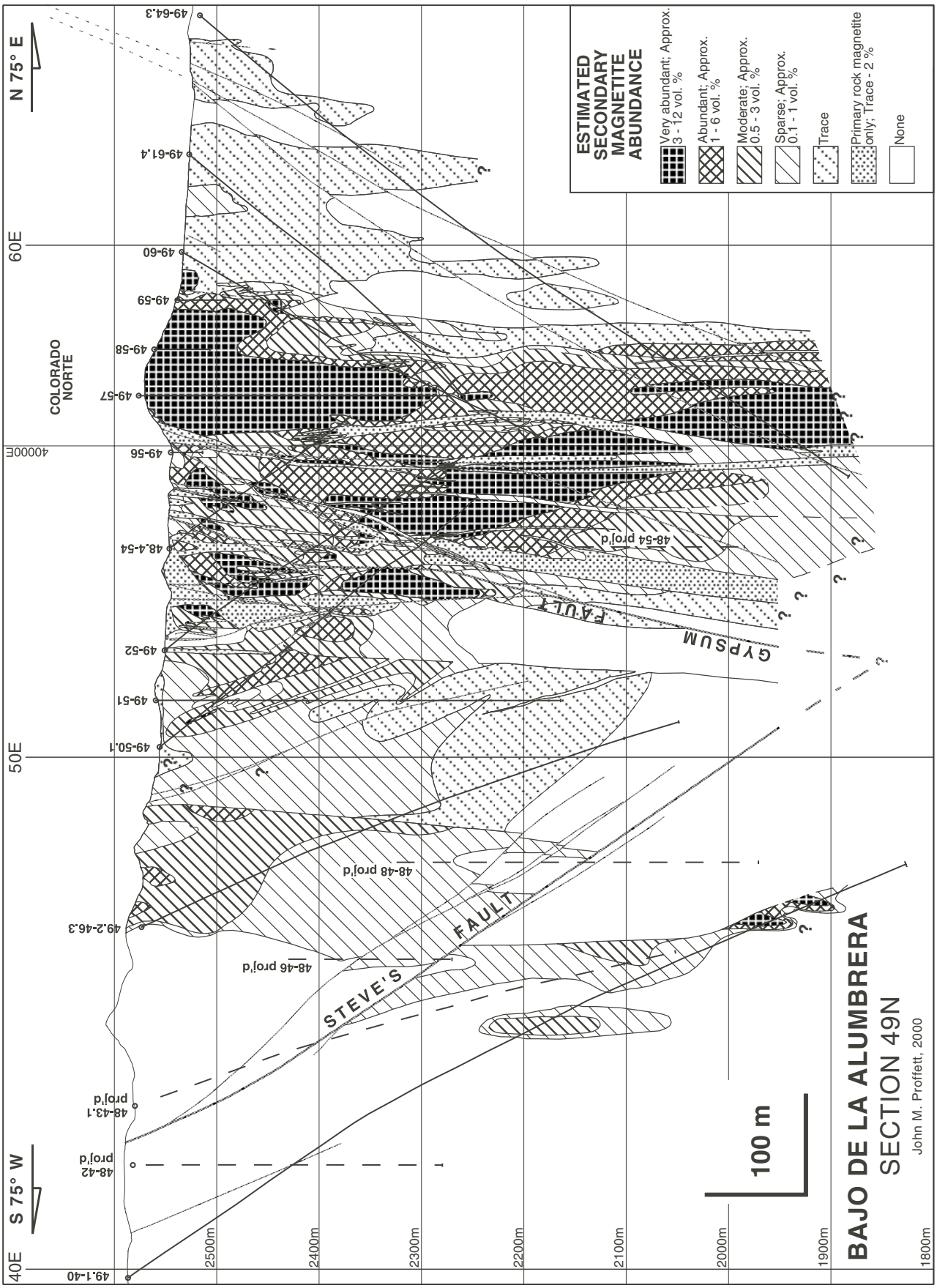

FIG. 9. Cross section 49N, showing rough estimates of secondary magnetite abundance, as interpreted from surface mapping and relogging of drill core, and calibrated with magnetic susceptibility measurements made every meter on selected drill holes by the Minera Alumbrera staff (pers. commun.). Some information for drill holes 49.1-40 and 49-64.3 from logs by Steve Brown and Javier Madrid (pers. commun.).

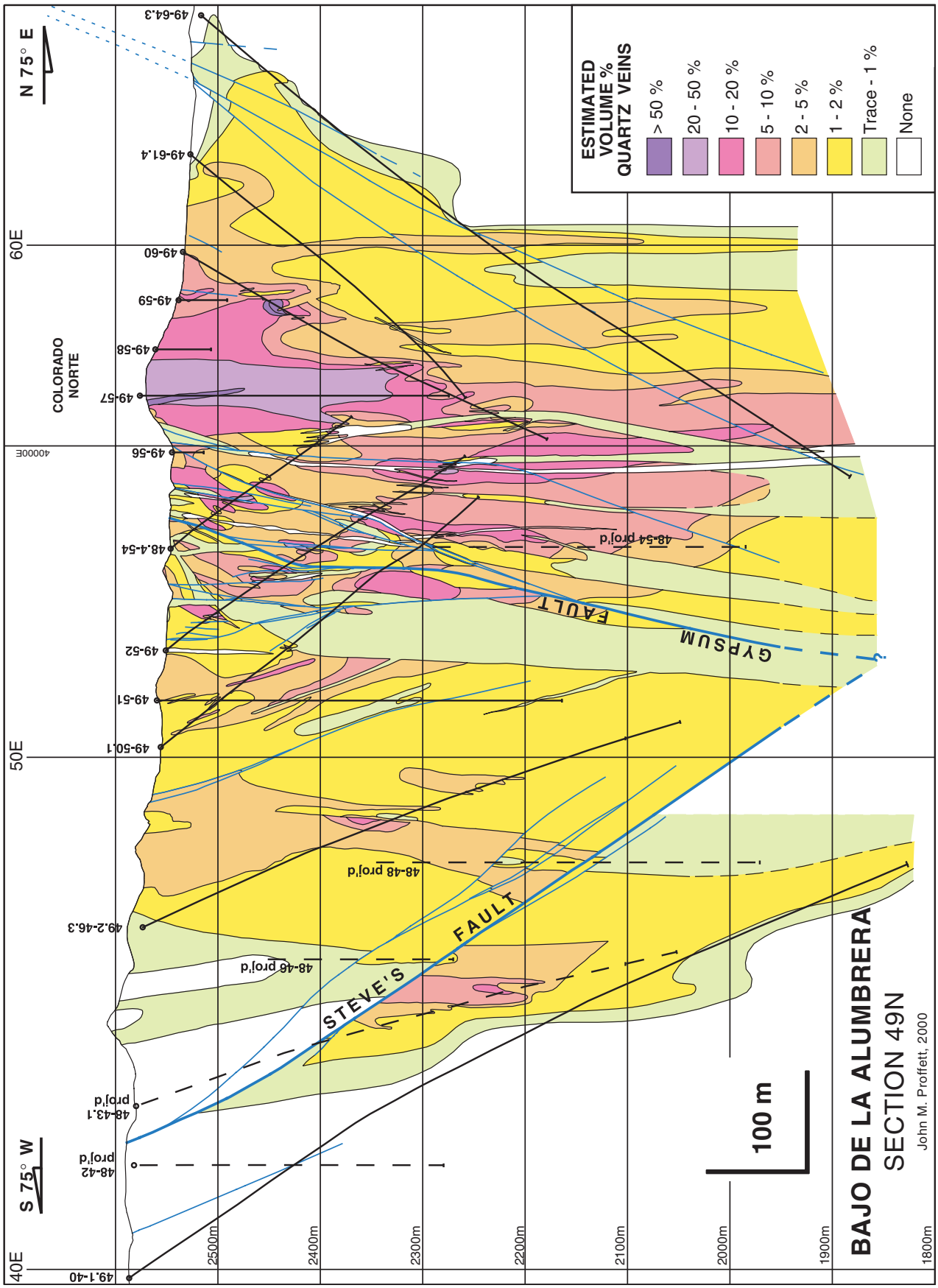

FIG. 10. Cross section 49N, showing estimated quartz vein abundances as interpreted from surface mapping and relogging of drill core. Some information for drill holes 49.1-40 and 49-64.3 from logs by Steve Brown and Javier Madrid (pers. commun.).

phenocrysts suggests more potassic compositions. Evaluation of chemical analyses is difficult, especially for earlier porphyries, because of alteration overprint. Of many available analyses, only one, sample BLA48 of Ulrich (1999), which is from the dike of Late P3 near Arroyo los Celestes in the south part of Map 1 (Proffett, 2003), can be confidently considered to be essentially unaltered. Ulrich's (1999) analysis, along with modal estimates of other examples of unaltered Late P3 (Table 1), indicates compositions in the IUGS granite field but very near the boundaries of the granodiorite, quartz monzonite, and quartz monzodiorite fields. Modal phenocryst proportions in P2 and Early P3 are similar to those in Late P3, suggesting similar compositions, but these, as well as parts of Late P3, have undergone at least weak potassic alteration, including possible matrix recrystallization, making K_2O and CaO values especially difficult to evaluate.

Inclusions of other rocks are common in Los Amarillos porphyry and igneous breccia and are occasionally present in other porphyries, especially near contacts. These consist of older porphyries and quartz veins, andesitic volcanic rocks, Paleozoic granite, and metamorphic rocks from the basement, and rocks similar to those of the Alto de la Blenda stock and its related dikes.

Pre-Alumbrera (Northeast) porphyry

A steeply west-dipping, 5- to 20-m-wide porphyry dike trends north-northeast from northeast of Colorado Norte (Table 1, Proffett, 2003, Map 1). Relationships between this porphyry and others are not exposed, but it shows no apparent relationship to the alteration-mineralization pattern, and in the area of 78100N, 40170E it is mineralized and cut by quartz veins to a degree similar to andesite country rock. Similar porphyry east of Colorado Sur is apparently cut by a dike of Early P3. It most likely predates the ore-related porphyries.

P2 porphyry

The main body of P2 (also known as "Colorado Norte porphyry") occupies the northeast part of the main stock. The west contact with Early P3 is irregular, and west of this P2 occurs as isolated patches surrounded by Early P3 and other porphyries (Fig. 6; Proffett, 2003, Map 1). P2 intrudes andesite but has not been observed to truncate quartz veins in any rock nor have quartz vein fragments been observed in it. Veins and other mineralization in P2 have been observed to be cut by Early P3 (Figs. 4B, 7B), Quartz-eye porphyry, and all younger porphyries (Proffett, 2003, Map 2).

P2 is everywhere more strongly mineralized with quartz (±magnetite) veins, potassic alteration, and Cu-Au than adjacent later porphyries (Figs. 4B, 6, 7B, 8-11B, 13; Proffett, 2003, Maps 1, 3-4), and original rock minerals and texture are commonly partly destroyed. Even low-grade P2 patches in the low-grade core zone are higher in grade than surrounding Early P3 (Fig. 6). Mineralized fractures and veinlets of various types, described below, are typically spaced a few millimeters to a few centimeters apart in P2 and immediately surrounding andesite.

Los Amarillos porphyry and igneous breccia

Los Amarillos porphyry occurs in an irregular, crescent-shaped body that partly surrounds the west part of the main porphyry stock (Proffett, 2003, Map 1). Most of it is overprinted by strong sericitic alteration, and original composition and textures are obscure (Table 1). It was previously mapped in part as "pre-Main Stage porphyry" (Stults, 1985), but it is probably younger than P2.

Los Amarillos porphyry is cut by Northwest porphyry dikes, and by small bodies of quartz-veined porphyry, probably Early P3. It contains abundant andesite fragments, quartz vein fragments, and fragments of intensely quartz-veined rock. Because all known quartz veins are younger than P2, these fragments suggest that Los Amarillos porphyry is younger than P2. If older than P2, the fragments indicate a still older phase of quartz veining, for which no other evidence has been found.

The northwest contact of Los Amarillos porphyry with andesite dips easterly (Proffett, 2003, Map 1), and drill holes below its outcrop area encounter mostly andesite (Fig. 6), indicating a downward-narrowing body. Just north of Los Amarillos, and also 250 m south-southeast, Los Amarillos porphyry appears to grade into a coarser grained porphyry, tentatively shown in Map 1 (Proffett, 2003) as Early P3, but alteration makes it difficult to determine if these are different porphyries or variations of the same.

Quartz phenocrysts are irregular in size, shape, and abundance and many are broken; some are sharp-edged splinters (Fig. 7C). Most, including many of the splinters, are partly resorbed and rounded. Locally the matrix is sufficiently coarse that the rock is fine-grained equigranular. Many parts of this unit resemble igneous breccia described below and may also be igneous breccia.

Rock included in the Los Amarillos porphyry map unit, but which is clearly igneous breccia, is exposed along the west margin of the Early P3 stock (Fig. 6; Proffett, 2003, Maps 1–2, 77800N-77980N, 39615E). It intrudes andesite to the west and is intruded by Early P3 to the east. Drill hole 48-48 indicates that the breccia contacts are steep and that it persists to at least 300-m depth (Fig. 6).

The matrix of igneous breccia consists mainly of 0.3- to 1-mm quartz and feldspar, but due to alteration, the proportion of K-feldspar to plagioclase is undetermined. Angular to rounded quartz vein fragments, millimeters to centimeters in size, are common. Fragments of porphyry, probably P2, and andesite up to a few tens of centimeters in size also occur; many of these contain quartz-magnetite and quartz veins that are truncated by the breccia matrix. Other quartz-magnetite and quartz veins cut the breccia matrix; these veins are more abundant than in adjacent Early P3, and some appear to be truncated at the Early P3 contact. Though igneous breccia is overprinted by sericitic alteration, textural evidence for relict potassic alteration is preserved; that in fragments is truncated by breccia matrix, and that in the matrix is truncated by adjacent Early P3.

Early P3 porphyry

Early P3 constitutes the largest part of the main porphyry stock and a few small surrounding radial dikes. It truncates quartz veins in P2 (Figs. 4B, 7B) and andesite and contains fragments of these rocks and of mineralized quartz veins (Fig. 11B). Quartz veins and other mineralization that cut Early P3 are cut by Late P3 (Fig. 11F-G), Northwest, and Postmineral

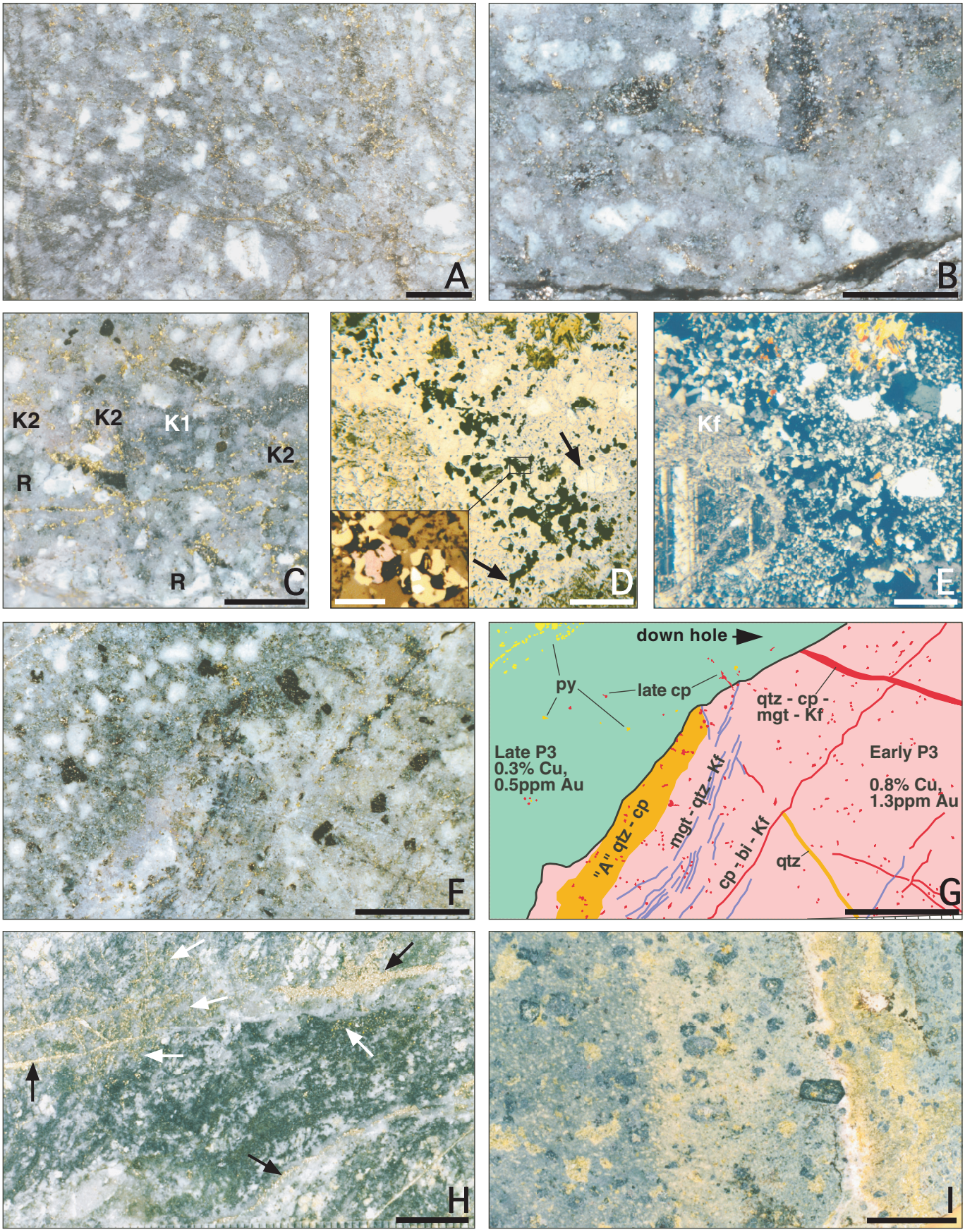
A
B
K2
K2
K1
K2
R
R
C
D
Kf
E
F
down hole
py
late cp
qtz - cp - mgt - Kf
Late P3
0.3% Cu,
0.5ppm Au
Early P3
0.8% Cu,
1.3ppm Au
"A" qtz - cp
mgt - qtz - Kf
cp - bi - Kf
qtz
G
H
I

porphyries. Within Early P3 there is more than one phase, but it has not been possible to separate them consistently.

Early P3 generally has moderate Cu and Au grades, except in the low-grade core of the deposit (Fig. 6). Quartz vein abundance and potassic alteration intensity in Early P3 varies from low to very high, and though generally weaker than in P2, the intensity of this mineralization cannot be used to distinguish these porphyries with certainty. Contact relationships must be used. For example, in drill hole 49-52 below the gypsum fault in the low-grade core zone (Fig. 6), the abundance of quartz veins and potassic alteration in Early P3 is high, but this interval can be identified as Early P3 because of the presence within it of patches and fragments of P2 that have even more abundant veins, many of which are truncated at the Early P3 contacts. Near the bottom of drill hole 49-50.1, 40 m west of this location, porphyry with mineralization of similar intensity contains only rare quartz vein fragments, and no other contact relationships with P2, so is identified only tentatively as Early P3. Early P3 on the surface west of Colorado Norte has similar alteration and vein intensity to small patches of P2 nearby, but truncates veins in these patches, so is mapped as Early P3. Mineralized fractures and veinlets are typically spaced about one to a few centimeters apart in Early P3 but locally are more closely spaced.

As expected in a large body with multiple subphases, Early P3 varies somewhat in composition and texture (Table 1).

Quartz-eye porphyry

This unit occurs in the southeast part of the main stock. It truncates quartz veins in adjacent P2 and in fragments of P2; P2 fragments, along with quartz vein fragments (Fig. 7D), are common in Quartz-eye porphyry near the P2 contact. Quartz-eye porphyry truncates large quartz veins in andesite 250 m south of Colorado Sur, and is itself cut by similar quartz veins (Proffett, 2003, Map 2). Quartz veins in Quartz-eye porphyry are truncated by weakly quartz-veined Late P3. Along contacts between Quartz-eye porphyry and Early P3 exposed on the surface, age relationships are uncertain, but where porphyries that resemble these two units occur in a nearby drill hole, the one that resembles Quartz-eye porphyry cuts the one that resembles Early P3. Quartz-eye porphyry is therefore tentatively considered to be younger than Early P3.

Quartz-eye porphyry resembles Early P3, except that it contains more abundant quartz phenocrysts (Table 1). It forms pale surface outcrops due to weak sericitic (and argillic?) alteration. The matrix is generally pale pink but is locally darker due to fine-grained biotite.

Quartz-eye porphyry is generally moderately to strongly quartz veined, with weak to moderate potassic alteration, but contains fewer quartz veins and less potassic alteration than P2. It contains moderate Cu and Au grades. Because of the similar characteristics and age relationships, Quartz-eye porphyry may be a quartz-eye–rich phase of Early P3. Quartz vein fragments, as well as quartz phenocrysts are commonly resorbed and rounded, and many quartz eyes could be partly digested quartz vein fragments (Fig. 7D).

Late P3 porphyries

Several porphyries that are consistently younger than Early P3 (Fig. 11F-G) and Quartz-eye porphyry are divided into two groups, Late P3 and Northwest porphyries. Age relationships between individual bodies of these late porphyries are rare, and there may be some overlap in age between the two groups.

Late P3 includes North porphyry, Campamento porphyry, and small bodies near the center and to the southwest of the main stock (Table 1, Proffett, 2003, Map 1). They truncate quartz veins and potassic alteration in Early P3 and older rocks (Fig. 11F-G; Proffett, 2003, Map 2) and are intruded by small bodies of Northwest porphyry (Proffett, 2003, Map 2). Late P3 contains sparse quartz veins and is generally weakly to very weakly mineralized with Cu and Au. Mineralized fractures

FIG. 11. A. P2 with plagioclase mostly replaced by K-feldspar along quartz-magnetite-chalcopyrite A vein on right. Shreddy biotite greenish (weakly chloritized). Scale = 5 mm. Sawn drill core, hole 49-60, 329.3 m, 1.0 percent Cu, 1.1 ppm Au. B. Early P3, with P2 fragment (upper center and right) that has a quartz-magnetite-chalcopyrite A vein and K-feldspar alteration truncated by the Early P3. Open veinlet (bottom) may have had gypsum or anhydrite. Note chalcopyrite is more abundant in the fragment. Scale = 5 mm. Sawn drill core, hole 49-51, 164.9 m, 1.2 percent Cu, 2.2 ppm Au. C. P2 with plagioclase partly altered to K-feldspar near patch with secondary magnetite (K1) and near patches with chalcopyrite, ±magnetite, ±biotite (K2). Original texture, with nearly fresh plagioclase, preserved only in rare patches (R). Late alteration overprint is very weak. Scale = 5 mm. Sawn drill core, hole 49-60, 207.7 m, 1.0 percent Cu, 1.6 ppm Au. D. Thin section, plane-polarized light, of Early P3 with a diffuse A vein (upper left to lower right) of quartz, K-feldspar, magnetite, titanohematite or ferrian ilmenite, biotite, bornite, and chalcopyrite (K2). Plagioclase altered to K-feldspar along vein. This vein displaces a thin magnetite-quartz vein that trends from lower center to right center (arrows) and which also has a K-feldspar halo where it cuts plagioclase phenocrysts, out of view (K1). Biotite and remaining plagioclase nearly fresh. Scale is 0.5 mm. Inset shows bornite (pinkish), magnetite (bright brownish), and titanohematite or ferrian ilmenite (white, below and right of bornite) of vein in reflected light and cavities (black areas), which may have been anhydrite. Inset scale, 0.05 mm. Drill hole 49-60, 361 m, 0.7 percent Cu, 0.8 ppm Au. E. Same area as D, cross nicols, which shows quartz-K-feldspar of the vein, biotite (yellow and orange), and K-feldspar replacing plagioclase phenocryst (Kf). The four quartz grains just below biotite, upper right, are part of a vein fragment. F and G. Veins and Cu mineralization in Early P3 truncated by Late P3, as explained in G. Weak sericitic alteration of plagioclase and chloritization of mafics overprints both porphyries. Note more chalcopyrite in Early P3 but minor amounts in Late P3 near contact and crossing contact. Note barren pyrite vein farther from contact in Late P3. Scale = 1 cm. Sawn drill core, hole 49-51, 132 m. H. Typical ore in P2 that has been overprinted by moderate feldspar destructive alteration and chloritization. Pyrite (black arrows) occurs in veinlets and chalcopyrite (white arrows) is mostly disseminated. Magnetite that is part of early assemblage near center is partly destroyed in halo of pyrite veins. Scale = 1 cm. Sawn drill core, hole 51-52.2, 370 m, 2.0 percent Cu, 1.8 ppm Au. I. Lower andesite altered to epidote-chlorite. Pyroxene phenocrysts are altered to actinolite, chlorite, and minor epidote, matrix contains chlorite, epidote, and albite. Note minor white quartz along epidote-rich vein, which is rare in this alteration zone. West side of Arroyo Alumbrera 230 m S 25° W of primary crusher.

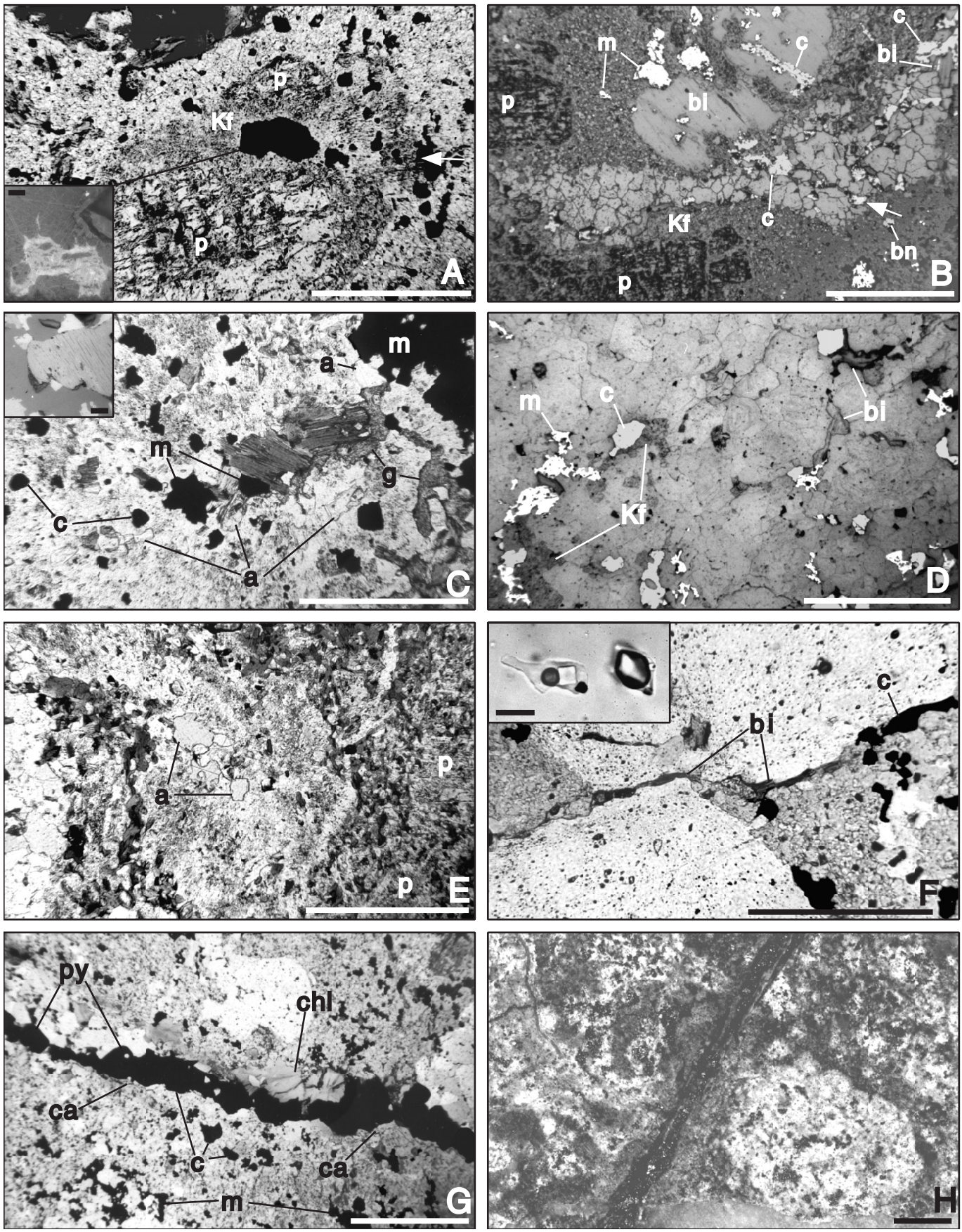
p
Kf
p
A
m
c
bl
p
bl
c
Kf
c
bn
p
B
m
a
m
g
c
a
C
m
c
bl
Kf
D
a
p
p
E
c
bl
F
py
chl
ca
c
ca
m
G
H

and veinlets are typically spaced a few to tens of centimeters apart in Late P3. Potassic alteration is only locally developed and, where present, involves only biotitized hornblende (Fig. 7G) and little or no secondary K-feldspar. A thin dike of North porphyry at the north end of the body is altered to epidote-chlorite (78730N, 40050E).

Northwest porphyries

Northwest of the main stock are several north-northwest–trending porphyry dikes, some of which continue beyond the limit of mapping (Proffett, 2003, Map 1). These cut all andesite dikes and Los Amarillos porphyry. Several small, late porphyry stocks and irregular dikes cut the north part of the main porphyry stock (Proffett, 2003, Maps 1 and 2) and truncate veinlets in P2, Early P3, and Late P3. One of these (77980N, 39750E) can be followed from the main stock northwestward through Los Amarillos porphyry, where it splits and becomes two of the north-northwest–trending dikes. Thus the dikes to the northwest have been correlated with the late porphyries in the main stock. The late porphyry bodies in the main stock are mineralized with very sparse Cu sulfides and quartz veinlets and partly biotitized hornblende. The dikes to the northwest cut epidote-chlorite–altered andesite and are themselves moderately altered to epidote-chlorite.

Some bodies of Northwest porphyry (such as at 78050N, 39935E; Proffett, 2003, Map 2), contain two porphyry phases, a pale gray and a darker gray phase (Table 1).

Postmineral porphyries

Thin, discontinuous, north-northwest–trending dikes of Postmineral porphyry occur in the northwest part of the main stock and farther to the northwest. They cut all other porphyries as well as all potassic and epidote-chlorite alteration and carry essentially no Cu sulfides. Hornblende in these porphyries is usually not biotitized, even where the porphyries cut potassic alteration. In areas of intense sericitic alteration, they are less altered than the rocks they intrude but are overprinted by some sericitic alteration.

Coarse matrix porphyry

Deep drilling reveals coarse matrix porphyry (S. Brown, pers. commun., 2000) near the center of the porphyry complex about 650 m below the pre-mine surface (Fig. 6, drill hole 49-64.3). It is similar to Early and Late P3, except that quartz and feldspar of the matrix is mostly 0.1 to 0.2 mm, with a few irregular grains up to 1 mm.

Alteration and Mineralization

As has been noted previously (e.g., Stults, 1985; Guilbert, 1995), Bajo de la Alumbrera exhibits a nearly symmetrical pattern of alteration zoning (Fig. 4A). This pattern may be the result of relatively uniform host rocks and lack of significant tilting. This symmetry is well expressed in the distribution of generalized alteration types (potassic, epidote-chlorite, feldspar destructive; Proffett, 2003, Map 3), but distribution of alteration, Cu-Au mineralization, quartz veins, and secondary magnetite within the ore-related potassic zone is controlled by intrusions of the central porphyry cluster (Proffett, 1999) and is less symmetrical (Figs. 6, 8–10, 13; Proffett, 2003, Maps 1, 3–4).

As at El Salvador, Chile (Gustafson and Hunt, 1975), alteration-mineralization is grouped into Early, Transitional age,

FIG. 12. Abbreviations as in Tables 1 and 2, except a = anhydrite, c = chalcopyrite, ca = calcite, g = gypsum, m = magnetite, and p = plagioclase. A. Very thin A vein or seam (white arrow), which here can be traced only as a disconnected string of biotite, magnetite, and sulfide grains (black) and as a K-feldspar (Kf) alteration halo where the vein cuts the plagioclase phenocryst. There is very little trace of vein where it projects through matrix. Dark area, upper left, is a biotite book. Scale, 0.5 mm. Inset shows detail (reflected light) of part of the large opaque grain, which is bornite (darker gray background) with chalcocite or digenite exsolution texture (pale gray area in lower half), and a tiny Au grain (white, upper right). Inset scale, 10 μm. Early P3, drill hole 49-60, 361 m, 0.7 percent Cu, 0.8 ppm Au. B. Typical A quartz vein, with irregular walls, cutting P2 (reflected light). Note K-feldspar halo (Kf) where vein cuts plagioclase phenocryst. Chalcopyrite (pale gray) occurs mostly in A vein, with minor amounts along cleavage of biotite book. White mineral is magnetite. Note secondary biotite in A vein with quartz and chalcopyrite (upper right). Seam, upper left to lower right (white arrow), has secondary K-feldspar where it cuts the upper plagioclase, and it also cuts the biotite book and the A vein. Scale, 1 mm. Drill hole 49-60, 324.8 m, 1 percent Cu, 1.2 ppm Au. C. K2 assemblage pervasively developed in andesite near P2 contact (plane light). Light-colored background is mostly K-feldspar, with biotite to right of center, and anhydrite, chalcopyrite-(bornite), and magnetite with titanohematite or ferrian ilmenite. Note irregular veins of gypsum apparently forming from anhydrite. Scale, 0.5 mm. Inset is from large magnetite grain in upper right. It shows, in reflected light, typical magnetite (darker gray) and several hematite grains (lightest gray). The large, medium gray grain, center and right, is tentatively identified (optically) as titanohematite or ferrian ilmenite, and the dark gray lines inclined toward the lower right within this grain appear to be ilmenite exsolution lamellae. Inset scale, 10 μm. Drill hole 49-61.4, 261 m, 1.3 percent Cu, 1.6 ppm Au. D. K2 assemblage mosaic in P2 (reflected light). Note growth zones in the quartz (medium gray) just above center. Field of view is about 80 percent quartz. Scale, 1 mm. Drill hole 49-60, 257.6 m, 1 percent Cu, 2.3 ppm Au. E. Biotitized andesite (right) with a halo of K-feldspar (light), anhydrite, and biotite (medium-dark gray) along an A quartz vein (left edge). Sparse fine-grained chalcopyrite (black). Plane light, scale 0.5 mm. Drill hole 49-61.4, 252.8 m, 0.4 percent Cu, 0.6 ppm Au. F. Quartz eye in P2, rich in fluid inclusions, is displaced along a biotite-chalcopyrite (K3) vein (plane light). Where the vein cuts plagioclase (out of view) there is a K-feldspar halo. Note ~20- to 50-μm halo along vein in which inclusions are mostly absent. Scale, 0.5 mm. Inset shows examples of fluid inclusions in the quartz; saline inclusion (left) has salt crystal, vapor bubble, and rounded triangular opaque; vapor-rich inclusion has a small anhydrite (?) crystal (lower right corner), a small salt crystal, and a very small opaque with the salt. Scale = 10 μm. Drill hole 49-60, 208 m, 1 percent Cu, 1.6 ppm Au. G. Late chalcopyrite-pyrite vein in P2 (plane light), with chlorite and calcite. Note that vein truncates A quartz vein at right edge. Much of the disseminated opaque is magnetite, which is less abundant near the late vein. Scale, 1 mm. Drill hole 49-60, 235.2 m, 1.3 percent Cu, 3 ppm Au. H. Intense feldspar destructive alteration in andesite tuff-breccia. Lighter shades are mostly sericite-quartz-pyrite. Darker shades, including inner halo of pyrite vein, are quartz-pyrite-sericite with kaolinite and possibly minor pyrophyllite. Scale = 1 cm. Sawn drill core, hole 37-46, 25 m, <0.01 percent Cu, 0.007 ppm Au.

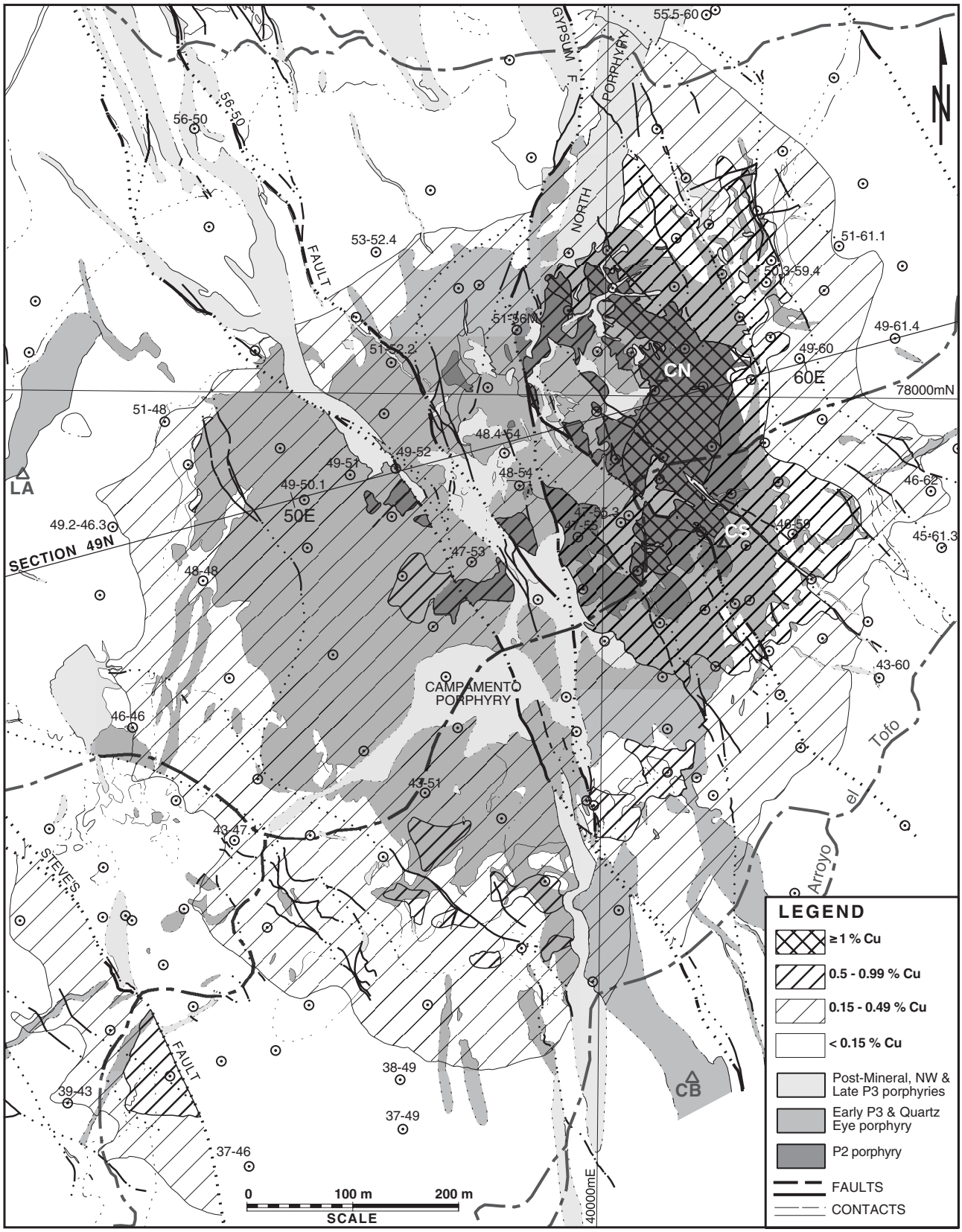

FIG. 13. Distribution of Cu grade at the surface, Bajo de la Alumbrera, before supergene leaching and enrichment, interpreted from near-surface drill hole assays and surface mapping of sulfides, limonite, and Cu oxides. Au distribution closely reflects Cu distribution, with Au (ppm)/Cu (%) varying from ~0.8 to ~1.6. Drill holes also shown, with numbers for selected holes referred to in text or other figures. CN = Colorado Norte, CS = Colorado Sur, LA = Los Amarillos, CB = Cerro Blanco.

and Late. Early includes mainly potassic features, for which individual porphyries serve as time lines and show, by cross-cutting relationships, that these features were repeated during and/or following each of the earlier porphyry intrusions (Fig. 14). Transitional features followed the three main mineralized porphyries (P2, Early P3, and Quartz-eye porphyry) and lack evidence of multiple repeats after each porphyry. Epidote-chlorite, which surrounds biotitized andesite of the outer part of the potassic zone (Fig. 8; Proffett, 2003, Map 3), is Transitional and possibly Early but is older than the youngest porphyry (Proffett, 1999). Late, which constitutes mostly pyritic, feldspar destructive alteration, is mainly younger than the youngest porphyry and is most strongly developed in a ring that coincides largely with outer parts of the secondary biotite zone (Fig. 8; Proffett, 1999, 2003, Map 3).

Cu sulfides and Au are closely associated in space and time with potassic assemblages, but epidote-chlorite lacks significant sulfides. Much potassic and epidote-chlorite alteration has been overprinted by late, weak to intense, feldspar destructive alteration and chloritization (Fig. 8).

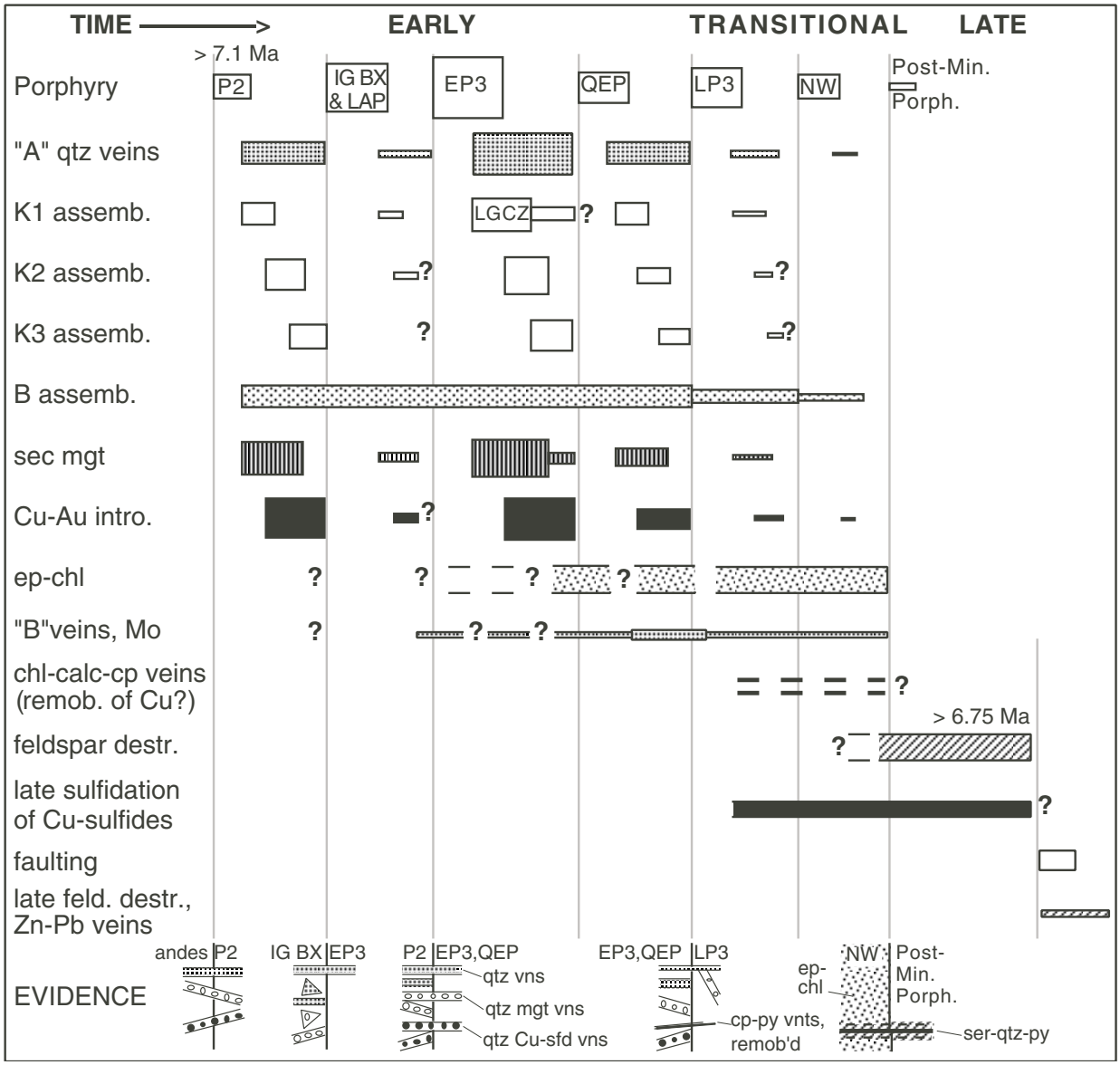

FIG. 14. Timing of intrusive, alteration and mineralization events at Alumbrera, with porphyries and late faulting serving as time lines. Time axis is not necessarily to scale. For example, all intrusive events could have taken place in a relatively short time, and feldspar destructive alteration could have occupied a much longer time interval. Absolute ages shown are $^{40}Ar/^{39}Ar$ ages (Sasso and Clark, 1998) and should be considered as minimum. Width of bars is roughly proportional to intensity or volume of event. Examples of types of evidence observed to determine relative ages are shown diagrammatically at bottom, where the vertical lines represent contacts between the rock units indicated, and types of veins or alteration, distinguished by patterns (as labeled on some of the diagrams), are shown truncated by the contact or crossing the contact. Triangles represent vein fragments, with same patterns as for veins. Abbreviations as in Table 1 and 2, and as follows: assemb. = assemblage, destr. = destructive, feld. = feldspar, intro = introduction, LGCZ = low-grade core zone, min. = mineral, porph. = porphyry, remob. = remobilization, remob'd = remobilized, sfd = sulfide, vns = veins, vnts = veinlets.

Low-sulfidation Cu-Fe-S-O assemblages associated with potassic alteration were sulfidized during the late overprint (Proffett, 1999).

Potassic alteration-mineralization

Because of the late alteration and sulfidation overprint (discussed below), it was necessary to give careful attention during mapping and core logging to distinguish between primary potassic alteration-mineralization features and the effects of the late overprint. Relict textural features (e.g., Fig 7I) were commonly used to trace early alteration zones through later alteration overprint (Fig. 8; Proffett, 2003, Map 3). However, descriptions of potassic assemblages (Table 2) rely heavily on observations of outcrops, core intervals, and petrographic specimens selected to be as free as possible from overprint by late veinlets and their alteration halos.

The most widespread potassic alteration feature is replacement of mafic sites by secondary biotite. Secondary K-feldspar, secondary magnetite, and quartz veins are abundant in the immediate vicinity of the porphyry cluster. The maps and sections show that the distribution of secondary K-feldspar, secondary magnetite, and abundant quartz veins coincide closely, but not exactly, with each other (compare Figs. 6, 8–10; Proffett, 2003, Maps 1, 3–4), and these are commonly associated with each other in potassic alteration assemblages. Quartz veins and other early veins are an essential part of potassic alteration, which in many cases occurs as halos along the veins. However, quartz veins can occur with or without K-feldspar halos and with or without secondary magnetite. Likewise, secondary magnetite, though commonly disseminated with secondary K-feldspar or in veins with K-feldspar halos, can also occur in veinlets where secondary K-

TABLE 2. Description and Age Relationships for Early Alteration-Mineralization Assemblages

Unit	Essential minerals	Description	Occurrence and age relationships
K1	Kf-mgt-qtz; little or no sulfides	Qtz-mgt A veins w/ halos in which plag is alt'd to Kf; Bi books alt'd to Kf + mgt along some veins and in patches; where most intense, mosaics of Kf-mgt-qtz without bi or chl occur and bi books may be completely replaced; not studied in sulfate zone, so presence or absence of anh unknown; along late veins high in the system earlier sec bi is alt'd to Kf + mgt	Many veins in P2 are truncated by Early P3, and most in P2 and Early P3 are truncated by Late P3; a few K1 veins occur in Late P3, and most are cut by Northwest porphyry; rare K1 veins in Northwest porphyry Within each porphyry K1 veins are cut by K2 and later veins; late K1 veins also cut previously bi'd andesite and Early P3, w/ weak cp (B assemblage), high in the system
K2	Kf-mgt-bi-qtz-cp(or cp-bn or bn-cc)	A veins of qtz-mgt-Cu sulfide-bi-±Kf, w/ halos in which plag is alt'd to Kf; Bi and Kf stable adjacent to veins and may occur as part of veins; where most intense, mosaics of 0.05-0.4 mm qtz-Kf-mgt-bi-Cu sulfide occur; Anh may be present in sulfate zone, especially in andesite	Some veins in P2 appear to be cut by Early P3; most in P2 and Early P3 are cut by Late P3; rare in Late P3 and unknown in Northwest porphyry; at a given locality K2 veins cut K1 veins and are cut by K3 and younger veins
K3	Bi-Kf-qtz-cp	Small A veins of bi-qtz-cp w/ halos in which plag is alt'd to Kf; also occurs as irregular patches w/ abund sec bi; Anh may be present, especially in andesite; may be closely related to B assemblage described below	Most abundant in P2 and common in Early P3 and andesite; some K3 veins in P2 appear to be truncated by Early P3; most in P2 and Early P3 are truncated by Late P3; K3 veins cut K1 and K2 veins and are cut by feldspar destructive alteration veins
Kc	Kf-mgt-chl-qtz	Qtz, sec Kf and mgt occur w/ chl in A veins and their halos, even where bi in adjacent rock is not chl'd (therefore chl not likely a late overprint)	Not often recognized due to late overprint; occurs in Early P3 and andesite; Kc observed cutting B assemblage and cut by a qtz-mgt vein
B	Sec bi	In porphyries: hb alt'd to bi, Ti oxides, ±qtz, ±sulfides, ±mgt, ±anh; in andesite: hb and px alt'd to bi, Ti oxides, ±anh, ±sulfides, ±qtz, ±mgt; matrix alt'd to bi, plag, Ti oxides, ±sec Kf, ±anh, ±ap; ±qtz, ±mgt; generally associated with cp, may contain minor prim or sec mgt	All mafics in P2, Early P3, Quartz-eye porphyry and surrounding andesite are biotized (or alt'd to other potassic assemblages); in Late P3 most but not all hb is bi'd; in Northwest porphyry hb is partly bi'd; in Postmineral porphyry hb is not bi'd, even where bi'd in surrounding rocks
EC	Ep-chl-ab-±mgt-±act; little or no sulfides	Mafics alt'd to act and/or chl and/or ep, mgt and rutile; plag alt'd to ab or olig, (±ep), (±ser), (±calc); matrix pale green, with fine-grained chl, ab- or olig- altered plag, ep, rutile, mgt, ±calc; andesitic fragments may be alt'd mostly to ep; sec mgt locally abundant, locally absent; vein qtz rare, minor amounts occur in ep veinlets	Strong EC overprints Northwest porphyry and Late P3; Postmineral porphyry truncates EC in older rocks but is not EC altered; Py D veins with feldspar destructive alteration halos cut irreg fractures that control EC and cut Post mineral porphyry, indicating EC is a distinctly older event than feldspar destructive alteration; secondary bi is chl'd where EC and B overlap (Fig. 7I)

Abbreviations: act = actinolite; anh = anhydrite; bn = bornite; calc = calcite; cc = chalcocite or digenite; chl = chlorite; chl'd =chloritized; cp = chalcopyrite; ep = epidote; olig = oligoclase; px = pyroxene; py = pyrite; ser = sericite; other abbreviations as in Table 1; minerals in parentheses () are minor phases; ± means mineral may or may not be present

feldspar halos are discontinuous or apparently absent. Early veins provide timing relationships between alteration assemblages, so will be described first, followed by the principal potassic assemblages (B, K1, K2, K3, and Kc, Table 2).

Early veins: It has been found convenient to classify early veins according to the scheme of Gustafson and Hunt (1975, Table 2), recognizing that there are certain variations in vein characteristics between deposits. The earliest types are A veins. The smallest of these are only seams, traceable as strings of small magnetite, biotite, or Cu sulfide grains where they cut porphyry matrix and as K-feldspar halos where they cut phenocrysts (Fig. 12A-B; also Gustafson and Hunt, 1975, fig. 16). Quartz texture and vein structure are the main basis for vein classification; most A veins consist dominantly of equant, anhedral to polygonal, equigranular quartz. Grain size varies from similar to that of porphyry matrix (0.02–0.1 mm), to more typically 0.1 to 0.3 mm, and rarely 0.5 mm (Figs. 7B, E, H, 11D-E, 12B). Other minerals sometimes present in Alumbrera A veins, including magnetite, K-feldspar, chalcopyrite, bornite, biotite, and anhydrite, in various combinations, are generally similar in grain size and shape to the quartz. A veins with quartz only may cut, or be cut by, those that also have magnetite and/or Cu sulfides. Many of the earliest A veins have little or no internal structure; Cu sulfides, magnetite or K-feldspar, if present, are evenly disseminated through the vein. Other A veins, especially later ones, have weak internal structure, such as banding defined by layers of differing grain size or by layers of differing abundance of magnetite, K-feldspar, or Cu sulfides. Some A veins, especially earlier ones, may vary in thickness, may be continuous over only short distances, and may be randomly oriented. Vein walls may be irregular, even appearing to grade into porphyry matrix, or may be smooth (Figs. 7B, E, H, 11D-E, 12B). Later A veins may occur in parallel sets, though at Alumbrera these are usually continuous over distances of only one to a few tens of meters. Geometric relationships (Fig. 7E, H) suggest that many A veins fill space opened along fractures, but this is often difficult to confirm, and some may partly replace the rock.

B veins generally cut A veins and are characterized by coarser quartz, which commonly occurs in imperfect prismatic grains elongated at a high angle to vein walls, and which may exhibit some crystal faces. Crystals commonly grow from each wall, terminating at a center line, but more complex veins may have multiple bands. B veins are more continuous than A veins and have a greater tendency to occur in parallel sets. Some B veins are associated in space and time with A veins and earlier porphyries, but many cut late porphyries that truncate most early mineralization and will be discussed under Transitional mineralization. Most A and B veins are steep but a few are nearly horizontal (Proffett, 2003, Map 2).

Most A veins in P2 and Early P3 vary in thickness from less than 0.2 mm to about 2 cm. Veins of similar thickness cut Quartz-eye porphyry, but in addition, veins up to a few tens of centimeters thick and continuous over several meters are associated with this unit. These consist of pale gray to pale pinkish gray quartz with chalcopyrite (±pyrite) and/or molybdenite and may contain A- or B-type quartz, or both. Many have been refractured as pyritic D veins (see below). Most occur in parallel sets and most cut the thinner types of A veins. A few continue into adjacent P2 or andesite, and a few, in andesite, are early and are truncated by Quartz-eye porphyry. Similar veins occur north of Colorado Norte, where they cut andesite and Early P3 but are cut by Late P3 (Proffett, 2003, Map 2). Some gently dipping examples in Quartz-eye porphyry end abruptly at contacts with older rocks.

Quartz vein abundance as estimated during mapping (A and B types grouped) is shown in Map 4 (Proffett, 2003) and in Figure 10. Most are A veins, especially in areas of highest abundance. Quartz veins, especially A veins, are most abundant in P2 and in immediately adjacent andesite. Early P3 and Quartz-eye porphyry truncate many veins in P2 and have in general fewer quartz veins (Figs. 4B, 7B, 11B; Proffett, 2003, Map 2), although the most strongly veined parts of these porphyries may have more veins than least veined parts of P2 (Figs. 6, 10; Proffett, 2003, Maps 1, 4). Each later porphyry truncates veins in earlier porphyries and has fewer veins. Most B veins are younger than the earlier three porphyries and many also cut Late P3. Estimates of the total amount of vein quartz associated with each porphyry are shown in Table 3.

The outer edge of significant Cu mineralization on the surface coincides closely with the outer edge of 1 percent quartz veins, and zones of higher grade Cu coincide with higher quartz vein abundance (Fig. 13; Proffett, 2003, Map 4). The ratio of estimated total vein quartz to Cu associated with each porphyry increases with each younger porphyry (Table 3). Essentially all quartz veins lie within the potassic zones, and only the outer fringe of the biotite zone lacks significant quartz veins.

An unusual veinlike occurrence, found along the P2 contact with andesite (Fig. 8, DH 49-60, 97–110 m), consists of coarse-grained (~1 cm) quartz (commonly with crystal faces), magnetite, and chalcopyrite. Similar veins have been found that also contain coarse-grained biotite.

Secondary biotite assemblage: Fine-grained, randomly oriented, shreddy biotite replacing mafic minerals (mainly hornblende and pyroxene) occurs in clusters that reflect shapes of former phenocrysts (Fig. 7G) or, where strongly developed, in irregular clusters. Primary biotite phenocrysts (books) are rarely replaced. Where plagioclase is altered to K-feldspar along A veins, such as where B assemblage grades into K3 in biotitized andesites, anhydrite is especially common (Fig. 12E).

The zone in which secondary biotite is the principal early alteration mineral (Table 2, B assemblage) is about 1.7 × 1 km in size at the surface (Proffett, 2003, Map 3) and includes or surrounds all Cu-Au mineralization and all zones of secondary K-feldspar alteration. It is the dominant type of potassic alteration in less-fractured parts of P2, Early P3, and Quartz-eye porphyry, and in a large volume of surrounding andesites. There is a narrow zone of partly biotitized mafic minerals just outside the outer boundary of complete biotitization (Proffett, 2003, Map 3). Hornblende in Late P3 is completely biotitized in most of the potassic zone, but complete biotitization does not extend as far out as it does in andesite. Hornblende in Northwest porphyries is only partly biotitized throughout the potassic zone (Proffett, 2003, Map 3).

Secondary K-feldspar assemblages: Secondary K-feldspar may replace matrix minerals, plagioclase and biotite phenocrysts.

TABLE 3. Rough Estimates of Rock Volume and Tons of Cu and Vein Quartz Associated with Each Mineral-Related Porphyry

Unit (porphyry)	Volume of porphyry	Associated Cu (t)	Associated vein quartz (t)	Ratio quartz vein/Cu
P2	0.03 km^3	1.3×10^6	10.4×10^6	8
Early P3	0.2 km^3	1.9×10^6	22.7×10^6	11.9
Quartz-eye	0.05 km^3	0.7×10^6	10.4×10^6	14.9
Late P3	0.08 km^3	0.08×10^6	1.5×10^6	18.8
Northwest	0.03 km^3	Insignificant	Insignificant	-
Postmineral	0.006 km^3	None	None	-
Total	0.39 km^3	4.0×10^6	45×10^6	11.2

Based on Figures 6, 10, and 13, in this paper, and Proffett (2003, Maps 1, 4), and on limited drill hole information off 49N section and on rock-mineralization age relationships; includes amounts assumed to have been eroded and to lie below limit of drilling, assuming geometry of Figure 15I; these assumed amounts are about 30 to 40% for rock volumes, 10 to 30% for quartz vein, and 15 to 20% for Cu; rock volume includes veins

It generally coexists with secondary magnetite, secondary biotite or both, along with quartz ± anhydrite (Table 2). Copper sulfides are an integral part of most secondary K-feldspar assemblages that also contain secondary biotite. Secondary biotite in K-feldspar assemblages can occur in veinlets, as well as replacing mafic minerals. Where K-feldspar partially replaces plagioclase, remaining plagioclase adjacent to the K-feldspar is generally sodic. Along secondary K-feldspar vein halos this sodic plagioclase may represent an outer halo, and in some cases sodic plagioclase may occur adjacent to early veinlets without intervening K-feldspar.

Secondary K-feldspar occurs mainly in the central cluster of porphyry stocks and in immediately adjacent andesite. For purposes of mapping and core logging, it has been classified as weak, moderate, and strong (Fig. 8; Proffett, 2003, Map 3), each of which may include one or more of the assemblages K1, K2, K3, or Kc (Table 2), as halos along different A veins or in patches. "Weak" consists of pinkish patches of 0.03- to 0.3-mm K-feldspar and quartz in porphyry or andesite matrix, or of K-feldspar in thin, widely spaced vein halos. Fine-grained biotite and/or secondary magnetite may be disseminated in porphyry or andesite matrix. All areas of weak secondary K-feldspar have more than 1 percent quartz veins and most coincide approximately with the 2 to 5 percent quartz vein zone (Proffett, 2003, Maps 3-4). The outer limit of significant Cu-Au coincides with the outer limit of the zone in which patches of weak secondary K-feldspar alternate with secondary biotite assemblage (Proffett, 2003, Map 3).

In areas mapped as "moderate" and "strong" secondary K-feldspar, plagioclase phenocrysts as well as matrix feldspars are partly to completely replaced by K-feldspar. Such phenocrysts lose their euhedral or subhedral shape and with the strongest alteration only a few small relicts of plagioclase remain (Fig. 11A, C). This alteration commonly occurs as halos along various types of A veins and is most strongly developed where vein density is high (Proffett, 2003, Maps 3-4).

The most intensely developed zones of assemblages K1, K2, and K3, the highest Cu-Au grades, and the most abundant quartz veins are hosted by P2, the oldest ore-related porphyry, or by adjacent andesite. Much of this mineralization is truncated by Early P3 and Quartz-eye porphyry, which themselves are less strongly mineralized with the same assemblages, quartz veins, and Cu-Au ore. Most of this alteration and mineralization is in turn truncated by the next porphyry, Late P3. These relationships indicate that secondary K-feldspar assemblages, and associated quartz veins and Cu-Au mineralization, formed during emplacement of the earlier porphyries. Secondary K-feldspar is intermixed with, and grades out into, the secondary biotite assemblage, with lower Cu-Au grades. Intense secondary K-feldspar, with magnetite and abundant quartz veins, also occurs with low Cu-Au grades in a low-grade core, developed mainly in Early P3 (Figs. 6, 8–10).

K1, which is associated with little or no sulfides (Table 2), generally occurs as the earliest veins and patches in higher grade copper zones (Figs. 7E, H, 11D-E), although a few K1 seams and veinlets cut Cu-bearing A veins (Fig. 12B). K1 is also the principal assemblage in the K-feldspar-altered part of the low-grade core (Fig. 7B, F). Age relationships (Table 2, Figs. 7B, 11F-G) indicate that K1 was deposited during or between emplacement of the porphyries. Multiple generations of quartz-magnetite A veins (Fig. 7E) as well as disseminated magnetite may be associated with K1, and a large portion of the abundant magnetite in the Alumbrera deposit (Fig. 9) is part of this early assemblage. Rock between K1 halos generally has secondary biotite in hornblende sites. In the low-grade core this biotitized rock, as well as the veins and halos, lack associated sulfides. Zones of late K1 veinlets overprint B assemblage with low to moderate Cu grade in Early P3 and andesite high in the deposit. Cu sulfides appear to be removed from these K1 halos, so apparently this higher level K1 is younger, rather than older than Cu sulfides, and occurs above, rather than within or below, Cu-Au ore.

Much secondary magnetite associated with K1 is very fine grained (<0.1 mm) compared to slightly later magnetite associated with Cu sulfides. Where magnetite + K-feldspar has formed by partial alteration of biotite, these three minerals are generally found in contact (Fig. 7H), and where chlorite is present, its distribution suggests it formed by later alteration of the biotite, rather than directly as part

of the alteration of biotite to magnetite plus K-feldspar. Some, but not all, secondary magnetite in K1 occurs in contact with grains of a second, nonisotropic opaque mineral, tentatively identified optically as titanohematite or ferrian ilmenite.

Where not overprinted by later alteration, much of the Cu at Alumbrera is associated with K2 assemblage (Table 2) in small A veins and patches (Figs. 11A, C-E, 12A, C). K2 is most abundant in P2 and is common in Early P3 and Quartz-eye porphyry. In these, K2 is truncated by Late P3 (Fig. 11F-G), and although relationships are widely obscured by late overprint, some K2 veins in P2 are truncated by Early P3 (Fig. 11B).

Potassic alteration in andesites generally contains more biotite and less K-feldspar than that in adjacent porphyries, probably because of higher initial Mg and Fe in the andesites. However adjacent to some zones where K2 assemblage occurs in porphyries, K2 also occurs in andesite in irregular intergrown patterns and along A veins (e.g., DH49-61.4, 260–262.3 m, Figs. 6, 12C).

Rock between K2 vein halos and patches is generally altered to B assemblage with Cu sulfides and minor magnetite. However, Cu sulfides are significantly more abundant in the K2 assemblage (Fig. 11A). K2 mosaics occur in higher grade zones in P2 (Fig. 12D).

Secondary magnetite associated with K2 is commonly intergrown with polygonal to irregular equant grains of one or more nonisotropic opaque phases, which are always less abundant than the magnetite (Fig. 12C, inset). These phases are tentatively identified (optically) as titanohematite and/or ferrian ilmenite, as in K1.

Where not overprinted by later alteration, significant amounts of Cu occur as fine-grained chalcopyrite in K3 assemblage (Table 2), especially in P2, but also in Early P3 and andesite (Figs. 7H, 12B, E). K3 in these rocks is truncated by Late P3, and many biotite-bearing veinlets in P2 have also been observed to be truncated by Early P3.

Rock adjacent to K3 vein halos and patches is generally altered to B assemblage (Fig. 12E), which contains less chalcopyrite than the adjacent K3.

Kc assemblage (Table 2) is difficult to study due to the abundant chloritic overprint (see below). The chlorite apparently formed from Mg and Al released during alteration of biotite to K-feldspar plus magnetite.

Magnetite: Most secondary magnetite occurs within zones of secondary K-feldspar (compare Figs. 8 and 9). Magnetite that is part of K1 and K2 assemblages tends to be fine-grained (<0.2 mm), and occurs in monomineralic veins, in quartz-magnetite A veins and seams (Figs. 7E, 11D), and disseminated with K-feldspar and quartz in porphyry matrix and in secondary mosaics (Figs. 7F, 12C-D). Some secondary magnetite is younger and coarser grained (0.2–1 mm); this cuts most (but not all) A quartz veins and veins with K1, K2, and K3 assemblages. This younger magnetite occurs in irregular patches and discontinuous veins and in more continuous veins in parallel sets. Coarse-grained magnetite is often irregularly distributed along one or both margins of early A veins (Fig. 7E), where it appears to be late relative to the quartz. However, at least part of this late, coarse-grained magnetite in P2 and Early P3 is truncated at contacts with Late P3. Coarse-grained magnetite constitutes a few percent to half or more of the secondary magnetite in Cu-Au zones as well as the barren core. It is not certain whether late, coarse-grained magnetite originated through new introduction of iron or from remobilization of earlier magnetite.

Plagioclase may occur in direct contact with late, coarse-grained magnetite or there may be a K-feldspar alteration halo between these minerals. Some such K-feldspar halos are where coarse-grained magnetite follows earlier veins. Both coarse- and fine-grained magnetite are partly to completely destroyed in halos of late pyritic veins, including D veins, and those with calcite and chlorite (Figs. 11H, 12G, discussed below).

Late overprint of potassic assemblages: Where potassic assemblages have not been overprinted by later alteration, biotite and remaining plagioclase are fresh (Figs. 11A-E, 12A-C). However, in much (more than half) of the deposit potassic assemblages have been overprinted in halos of late pyritic veinlets or in pervasive zones where halos of close-spaced pyritic veinlets overlap (Figs. 11H, 12G). Here biotite is partly or completely chloritized and relicts of plagioclase that had not previously been altered to K-feldspar are partly altered to sericite, calcite, chlorite, or clay. Magnetite may be partly altered to hematite along microfractures and grain margins. Where late alteration is intense, all feldspars and mafic minerals are sericitized and magnetite is destroyed, leaving only relict textures and A quartz veins as evidence of the former presence of potassic assemblages. This alteration, and pyritic veins that control it, are distinctly later events, because they cut and overprint Late P3 and Northwest porphyries, which themselves truncate most potassic alteration (Fig. 11F-G).

Minor calcite also may be present in early veinlets and replacing various minerals in potassic alteration that otherwise show little evidence of late overprinting, and it is not certain whether this calcite is the result of weak late overprinting or is locally a minor part of potassic alteration.

Sulfide assemblages with early alteration and late overprint: Although the most common sulfide assemblage at Alumbrera is chalcopyrite-pyrite, in relict patches of potassic assemblages where late alteration overprint is insignificant (biotite and remaining plagioclase are mainly fresh), sulfides are mostly fine grained chalcopyrite and/or bornite in A veins and as disseminations (Figs. 11C-E, 12B-C; Proffett, 1999). Rarely isolated grains of bornite with chalcocite or digenite exsolution lamellae occur (Fig. 12A). Actual phases present at depositional temperatures may have included intermediate solid solution or bornite solid solution. These sulfides were deposited at conditions where magnetite, titanohematite and/or ferrian ilmenite, K-feldspar, biotite, quartz, and anhydrite were stable. Pyrite does not appear to have been a part of these assemblages and has not been seen in contact with bornite or digenite. Even in outer fringes of the secondary biotite zone, in relict patches that lack late overprint, the minor amounts of Cu present are in Cu sulfides with little or no pyrite.

Within the large volume of potassic alteration that has been overprinted (chloritized biotite, partly sericitized, calcite altered, and clay-altered plagioclase) chalcopyrite is the dominant sulfide and pyrite is common. Pyrite occurs mainly in late veins which cut all A veins (Fig. 12G). Chalcopyrite also

occurs in these veins, and disseminated in their halos, but bornite has not been observed. Part of the earlier magnetite is destroyed, apparently sulfidized, near such veins (Fig. 11H). It appears that early, low-sulfidation Cu-Fe-S-O assemblages were sulfidized to a higher sulfidation, pyrite-chalcopyrite assemblage during late alteration overprint (Proffett, 1999).

Space-time distribution of Cu-Au mineralization: At the deposit scale (Figs. 6, 8–10, 13; Proffett, 2003, Maps 3–4), zones of highest grade Cu-Au ore generally occur with strongest development of K2 and K3 assemblages and greatest abundance of A quartz veins in P2 and within K2, K3, and B assemblages in adjacent andesite. High- and moderate-grade Cu-Au ore also occurs with these assemblages in and adjacent to Early P3, especially in the west and south parts of the deposit (Figs. 6, 8) and in Quartz-eye porphyry. The close association of more abundant Cu sulfides with stronger K2 and K3 assemblages is clear on a more detailed scale also (Figs. 11A, C-E, 12B, D). Low Cu-Au coincides with zones where K1 assemblage is dominant, in the low-grade core of Early P3 and above better grade Cu-Au in and around the upper parts of Early P3 (Figs 6, 8–9).

Where late alteration overprint is weak, a large proportion of the Cu sulfides present occurs in A veins (Figs. 7H, 11A-B, D-F, 12B), and in some cases this relationship survives late overprint. Alteration and A veins associated with Cu-Au ore in P2 are truncated by Early P3 (Fig. 11B) and those in Early P3 are truncated by Late P3 (Fig. 11F-G). This and the abrupt change of Cu-Au grades at these contacts, with the earlier, but otherwise similar porphyries being higher grade (Fig. 6), indicate that mineralization associated with each porphyry took place before emplacement of the next later porphyry. This interpretation is consistent with observations in certain other deposits (Gustafson and Hunt, 1975; Proffett, 1979; Clode et al., 1999). The total amounts of Cu estimated to be related to each porphyry are given in Table 3.

Grade breaks often occur at porphyry contacts, even where late alteration overprints both porphyries (Fig. 11F-G). Zones of overprinted ore commonly have similar patterns of Cu and Au grades, relict A quartz veins, relict magnetite, and relict potassic minerals to those in adjacent nonoverprinted zones. Cu-Au grades do not correlate well with the distribution of late alteration-sulfidation overprint (Figs. 6, 8), except in local zones to be described below under "Transitional age alteration and mineralization."

Throughout the deposit, Au is closely associated spatially with Cu, and bulk Cu/Au ratios do not vary greatly between different host rocks, alteration assemblages, or sulfide assemblages. Where free gold has been observed (N.J.W. Croxford, unpub. repts., 1994, 1995; this study), most occurs in ore that has been overprinted by late alteration. This gold occurs most commonly as 5- to 10-μm or larger grains within, and especially at the margins of, chalcopyrite grains but also with nearby late alteration minerals. Erratic gold values, including some very low values as well as rare visible gold, are found only in a few thin (meter-scale) very late pyritic vein zones and their feldspar destructive halos. Little free gold has been observed where late overprint is weak, although a 2.5-μm grain was observed in a rare occurrence of bornite with chalcocite exsolution lamellae (Fig. 12A). These observations suggest that at least part of the gold in nonoverprinted ore may be submicroscopic in the early Cu sulfides (see also Simon et al., 2000) and that some of this may have been liberated to form coarser grains during later overprint. The overprint did not cause significant remobilization on a deposit scale but only locally and in very late veins (see also Gammons and Williams-Jones, 1997).

Low-grade core: A low-grade core zone (Guilbert, 1995) southwest of Colorado Norte was found to consist of four distinct entities (Fig. 6): (1) small patches of P2, (2) a large mass of Early P3, (3) intrusions of Late P3, and (4) small bodies of Northwest porphyry (Proffett, 1999).

The P2 patches appear to be remnants surrounded by Early P3. They are well mineralized with A veins and secondary K-feldspar assemblages and have Cu-Au grades that are low to moderate but higher than in adjacent Early P3. The Cu is mainly in late veinlets that cut A veins and K-feldspar alteration.

Early P3 comprises most of the low-grade core (Fig. 6). It is moderately to intensely mineralized with abundant quartz veins and K1 alteration but sparse sulfides (Figs. 8–10). Where chalcopyrite is present, it occurs mostly in late veinlets.

A steep body of Late P3 in the west part of the low-grade core (Fig. 6) has secondary biotite but low Cu and Au grades. A similar porphyry, possibly a faulted part of the same body, occurs in the footwall of Steve's fault in drill hole 48-48 (Fig. 6). Several small bodies of Northwest porphyry occur in the low-grade core on the surface (Proffett, 2003, Map 1) and appear to dip steeply (Fig. 6). In these bodies hornblende is partly biotitized, but there is little other alteration or mineralization.

Fluid inclusions in potassic alteration-mineralization: A difficulty in the study of fluid inclusions at Alumbrera, where multiple stages of mineralization overprint each other, is identifying which stage the inclusions represent (see also Roedder, 1971). Also, it has been suggested that A-type quartz veins may have been deposited originally as amorphous silica and that their equant, anhedral quartz formed by recrystallization, such that inclusions may not represent conditions of vein formation (cf. Fournier, 1985, 1999). For the present study inclusions were only examined petrographically, and the following descriptions are limited to examples from potassic alteration zones as free as possible from late overprint and where potential problems related to A vein origin are minimal.

In DH 49-60, 208.0 m, A-type quartz veins associated with K2 assemblage and adjacent quartz phenocrysts in P2 contain similar fluid inclusions of saline and vapor-rich types (Fig. 12F). Where a later A vein with K3 assemblage displaces the quartz phenocryst, there is a 0.02-to 0.05-mm-wide halo which has been swept free of most fluid inclusions (Fig. 12F). The inclusions, whether primary or secondary, are therefore older than K3 assemblage and apparently formed here in approximately the same time interval as K2 assemblage. The saline inclusions have a small vapor bubble and at least one large cubic isotropic salt crystal (Fig. 12F, inset). Some also have a smaller salt crystal and/or a high-relief, high-birefringence, translucent crystal (anhydrite?). Most have a red hexagonal hematite grain and a small equant

opaque grain. The opaque is usually brassy, appears to have a tetragonal shape, and is probably chalcopyrite. The vapor-rich inclusions contain a large vapor bubble and a small amount of liquid (Fig. 12F, inset). Many have a very small, equant, apparently tetragonal, opaque grain, and some have what appears to be a small salt crystal and/or an anhydrite grain (Fig. 12F, inset). Those without salt crystals apparently formed from low-salinity vapor, but those with salt crystals are of high salinity and possibly formed by trapping a vapor-brine mixture.

Fluid inclusions in K2 mosaic quartz (Fig. 12D) occur in a pattern of hexagonal growth zones in the quartz and appear to be a primary part of the assemblage. They include saline and vapor-rich inclusions as described above but also a few that appear to be liquid rich, with a small bubble and no solids except for a very small opaque grain.

Coexisting saline and vapor-rich fluid inclusions similar to those described above are also found in chalcopyrite-bearing A veins with K3 assemblage in biotitized andesite that is free from evidence of late overprinting.

Assuming that the small, brassy, tetragonal-appearing opaques are chalcopyrite, rough estimates based on relative sizes of the inclusions and the opaque grains and on proportion of liquid (Mavrogenes et al., 1992) suggest concentrations of 0.1 to 1 wt percent Cu in fluids for the saline inclusions. Rough estimates of salinity made in a similar way (cf. Roedder, 1981), assuming the larger isotropic cubic crystals are NaCl and the liquid is H_2O solution, suggest concentrations of ~40 to 70 wt percent NaCl. Cu analyses and salinity estimates for some Alumbrera saline inclusions (Heinrich et al., 1999, table 1) fall mostly within these ranges, although specific alteration assemblages of the analyzed inclusions are not known. Other major components of the fluids would be Fe, S, and probably Ca and K.

That the small opaques in vapor-rich inclusions may be chalcopyrite is also supported by microanalysis of inclusions from Alumbrera, which indicates 0.03 to 0.3 wt percent Cu in vapor-rich inclusions that coexist with brine inclusions in a possible boiling relationship (Heinrich et al., 1999, table 1) and up to 3 wt percent Cu in certain other vapor-rich inclusions (Ulrich et al., 1999). Specific alteration assemblages of these inclusions are also uncertain.

A few saline and vapor-rich fluid inclusions were found in pervasive K1 mosaic quartz of the low-grade core deep in Early P3 (DH 48-54 390.0 m). The saline inclusions have a small vapor bubble, at least one salt crystal, and a very small brownish translucent grain, but opaque grains are very small or absent, suggesting fluids here carried less Cu and Fe. A few liquid-rich inclusions are also present, with a small vapor bubble and a very small opaque grain. However, biotite here is partly chloritized, so the inclusions could have been modified by later overprint. Higher in the low-grade core (DH 49-52, 337 m) saline and vapor-rich inclusions in a boiling assemblage contain about 0.3 and 0.03 wt percent Cu, respectively, and 9 and 0.07 wt percent Fe, respectively (Heinrich et al., 1999, table 1, sample BLA-A). Inclusions associated with early barren K1 assemblage in high-grade Cu ore have yet to be studied but might help determine if this assemblage is barren because the fluids lacked Cu or because conditions were not right for Cu deposition.

Epidote-chlorite

Epidote-chlorite alteration (Table 2, Fig. 11I) occurs in a large ring that surrounds and overlaps with the secondary biotite zone (Proffett, 2003, Map 3). The outer transition to near-fresh andesite crosses steep topography with little change in trend, suggesting a steep dip (Fig. 8; Proffett, 2003, Map 3). The essential features of epidote-chlorite are replacement of mafic minerals by chlorite, actinolite, or epidote, replacement of plagioclase by oligoclase or albite, ± epidote, a general lack of sulfides (except where overprinted by later pyrite veins), and a lack of sulfates (Table 2, Fig. 11I). This type of alteration is sometimes referred to as "propylitic" (e.g., Gustafson and Hunt, 1975), but this term was not used here to avoid confusion with late chloritic alteration associated with weak feldspar destruction and pyritization, which has also been referred to as "propylitic" (e.g., Lowell and Guilbert, 1970).

Age relationships (Table 2) constrain both epidote-chlorite and potassic alteration as older than Postmineral porphyry and feldspar destructive alteration (Proffett, 1999). However, most potassic alteration preceded Late P3, and only weak secondary biotite followed Northwest porphyries (Table 2). Because strong epidote-chlorite overprints Northwest porphyries, this alteration must have still been active when secondary biotite alteration was ending and after secondary K-feldspar alteration had ceased. This is also indicated by the presence of chloritized biotite where epidote-chlorite overlaps the secondary biotite zone (Fig. 7I). Epidote-chlorite generally lacks significant quartz veins.

Transitional age alteration and mineralization

B veins: Although some B-type quartz veins (Gustafson and Hunt, 1975) occur with A veins and earlier porphyries, as described above, many cut late porphyries that truncate most early mineralization and are of transitional age (Fig. 14). B veins are described above under "Early veins" but later B veins are generally more continuous and thicker (up to several cm) than earlier ones. Some have feldspar destructive alteration halos, but care must be used in interpreting these halos because some are due to later pyritic D veins along refractured B veins. Chalcopyrite and/or pyrite commonly occur along B vein centerlines. East of Colorado Sur, magnetite occurs in some B veins; molybdenite is associated with many, especially in outer zones. Anhydrite may also occur in B veins where it has not been dissolved.

B veins are present throughout the zone of quartz veins (Proffett, 2003, Map 4) but are more common in outer zones. There they occur in a radial set centered ~150 m southwest of Colorado Norte. B veins constitute a high proportion of the few quartz veins that cut Late P3 and Northwest porphyries, but many are truncated by these porphyries.

Anhydrite veins: Some anhydrite veinlets are of Transitional age. In the molybdenite zone anhydrite veins commonly contain molybdenite. At depth, on the west side of the deposit, chalcopyrite occurs along anhydrite veins with alteration halos in which secondary biotite is chloritized. Still deeper are older anhydrite-magnetite veins with fresh biotite.

Molybdenite distribution: Molybdenite is not abundant at Alumbrera. It is distributed mainly in a ring that coincides

with the outer part of the copper zone, where age relationships with porphyries and other veins are sparse. Molybdenite occurs in banded quartz veins (B veins), in anhydrite veins, and along fractures. Most molybdenite-bearing veins cut Early P3 where this rock occurs in the molybdenite zone, but below Steve's fault (DH 46-46, ~775 m) a quartz-molybdenite vein fragment occurs in Early P3 that is cut by other, later quartz-molybdenite veins.

Transitional(?) or late(?) chalcopyrite (±pyrite) veins: In some areas, part of the Cu occurs in chalcopyrite (±pyrite) veins with weak or indistinct halos of chloritized biotite and partial alteration of plagioclase to sericite or calcite. These veins may also contain chlorite, calcite, anhydrite, quartz, and hematite, which are usually subordinate to the sulfides. The chalcopyrite (±pyrite) veins cut all A veins and potassic alteration (Fig. 12G) and most magnetite-bearing veins. They are abundant where late alteration-sulfidation overprints early, Cu-bearing, secondary K-feldspar zones. These chalcopyrite-rich veins may cut adjacent late porphyries (such as Late P3) but typically penetrate them only millimeters or centimeters, and changes in grade occur essentially at the porphyry contacts (Fig. 11F-G shows a very small example, labeled "late cp"). This is strong evidence that these chalcopyrite (±pyrite) veins are the result of late remobilization of Cu. In late porphyries farther from contacts, such late veins carry mainly pyrite (Fig. 11F-G, upper left). The small amount of Cu-Au mineralization present in the low grade core occurs mostly in thin chalcopyrite (±pyrite) veins of this type that cut K1 alteration and A veins. In a few areas of Early P3 with B assemblage, late chalcopyrite (±pyrite) veins with chloritic halos appear to significantly augment Cu-Au grade. It is not certain if these veins introduced new Cu and Au or only remobilized some from nearby early high-grade zones. It is also uncertain whether these veins are a weakly developed part of late feldspar destructive alteration, are of Transitional age, or both.

Late mineralization: Feldspar destructive alteration and pyrite

Pervasive feldspar destructive alteration (Table 4; Figs. 7C, 12H), with abundant pyrite (2–10 vol %) ± anhydrite, occurs in a shell that overprints the outer parts of the secondary biotite zone (Proffett, 1999) and locally the inner edge of the epidote-chlorite zone (Fig. 8; Proffett, 2003, Map 3). In many places secondary biotite is found outside the shell, between the shell and the epidote-chlorite zone (Proffett, 2003, Map 3). This shell is 350 to 400 m wide in the downdropped block between the Gypsum fault and Steve's fault and 200 to 300 m wide to the east and west. It narrows downward, and its inner edge dips moderately outward (Fig. 8).

The shell of pervasive feldspar destructive alteration includes abundant D veins (Gustafson and Hunt, 1975), which are pyritic veins with sericite-quartz-pyrite halos in which rock texture is partly destroyed (Fig. 12H). In many parts of the zone these halos overlap and where they do not, between the halos, alteration occurs in which feldspars and mafics are almost completely destroyed, but in which texture is well preserved (Fig. 12H). Limited petrographic work suggests that sericite is the dominant alteration product of feldspars and mafic minerals in the alteration where texture is preserved, as well as in the halos where texture is destroyed. This work suggests that intermediate argillic alteration (Meyer and Hemley,

TABLE 4. Descriptions and Age Relationships for Feldspar Destructive Alteration

Unit	Essential minerals	Description	Occurrence and age relationships
Feldspar destructive alteration, strong	Ser-qtz-py-(rutile)-±anh	Ser-qtz-py-±rutile-±anh replaces rock in cm-scale halos along mm-scale py-(qtz)-(±anh) veins (D veins); where intense, adjacent halos overlap; kaolinite or dickite (and pyrophyllite?) may occur in inner halos; Plag sites alt'd to ser, ±qtz; mafic sites alt'd to ser, qtz, py, rutile; sph alt'd to rutile ±qtz; Fe-Ti oxides alt'd to rutile; sec mgt alt'd to py and/or specular hematite; fine-grained silica resulting from alteration of feldspars to sericite contributes to partial destruction of texture	D veins cut all potassic and epidote-chlorite assemblages and related veins and are cut by gypsum veins; D veins cut Postmineral porphyry but adjacent rock may be more strongly feldspar destructive alteration alt'd; main feldspar destructive alteration zone displaced by late faults (Gypsum fault, Steve's fault, etc.); late-phase feldspar destructive alteration occurs as halos along late faults
Feldspar destructive alteration, weak to moderate	Ser, chl, lx, calc, clay minerals, py	Occurs as outer halos of D veins or between D vein halos; plag sites partly altered to ser and/or calcite and/or clay, including swelling clay; mafic sites altered to chl and lx; texture generally preserved	Same age relationships as strong feldspar destructive alteration; occurs both inside and outside the shell of strong feldspar destructive alteration
Feldspar destructive alteration, green alteration	Ser, chl, lx, calc, py	Occurs as halos of py-cp veins or between D vein halos where these cut potassic alteration; plag sites partly altered to chl, ser and calc; mafic sites altered to chl, calc, lx, ±py; Kf fresh or partly alt'd; texture generally preserved; veins contain py, calc, chl, ±qtz, and where they cut Cu ore, cp occurs in veins and halos; locally mgt partly alt'd to hematite, along microfractures, grain edges, or fine chl veinlets	Similar age relationships to strong feldspar destructive alteration; occurs inside the shell of strong feldspar destructive alteration; where veins w/ green alteration cross from higher grade Cu zones into lower grade zones, such as in Late P3 or Northwest porphyries, they contain cp and py in the higher grade zones but mainly py in the lower grade zones

Abbreviations as in Tables 1 and 2; minerals in parentheses () are minor phases; ± means mineral may or may not be present; kaolinite or dickite in inner D vein halos and sericite identified optically; swelling clay identified megascopically in weak feldspar destructive alteration

1967) may also be present where texture is preserved and minor advanced argillic alteration (Meyer and Hemley, 1967) may be present where texture is destroyed. Because microscopic and X-ray analysis at Alumbrera is limited, no attempt has been made to subdivide these in maps and sections.

Less intense feldspar destructive alteration occurs in discontinuous zones both outside and inside the shell of pervasive feldspar destruction (Proffett, 1999) and inside the shell it overprints many parts of the ore zone (Figs. 11H, 12G). Strong feldspar destruction here is restricted to D vein halos. Between the halos, late alteration involves chloritization of mafic minerals and partial alteration of plagioclase to sericite, chlorite, calcite, and clays. This constitutes the weak to moderate feldspar destructive alteration and green alteration (Fig. 11H) of Table 4, which together coincide more or less with the areas shown in Figure 8 as "mafics partly chloritized" and "mafics mostly chloritized." This alteration includes 1 to 2 vol percent pyrite.

D veins form a radial pattern around Alumbrera, centered southwest of Colorado Norte (Proffett, 2003, Map 4). A less-developed, conical concentric pattern also occurs, with veins dipping moderately inward toward the same center.

Neither D veins nor any other pyritic veins have been observed to be truncated by any porphyries. Where a Northwest porphyry dike crosses the zone of strong sericitic alteration in the northwest part of the deposit (Proffett, 2003, Maps 1, 3), this alteration appears to be as strongly developed in the porphyry as in adjacent older rocks, except for some slightly less-altered patches near the center of the dike. Feldspar destructive alteration and D veins also cut Postmineral porphyry dikes, but within the feldspar destructive zone this porphyry is generally less pervasively altered than adjacent older rocks. Less intense alteration in these late porphyries may be due to less fracturing than in wall rocks and/or possible higher temperatures in cores of these late dikes, at the time that feldspar destructive alteration was taking place. Alternatively, in the case of Postmineral porphyry, the dikes may have been emplaced after some feldspar destructive alteration had taken place but before it ended. An $^{40}Ar/^{39}Ar$ age of 6.75 ± 0.09 Ma has been reported for sericite from the strong feldspar destructive zone (Sasso and Clark, 1998).

Sulfidation and remobilization of Cu with late alteration: As discussed above, the chalcopyrite-pyrite assemblage that constitutes most of the ore at Alumbrera (Fig. 11H) is associated with late veins and alteration and apparently resulted from late sulfidation of lower sulfidation assemblages originally deposited with potassic alteration. Some of these veins may be of transitional age (see above) but some have sericitic halos (Fig. 12H) and appear to be part of the late-stage event. Cu-Au grade patterns in most places are little affected by this late overprint but are instead related to A veins, early potassic alteration, and porphyry contacts. Where late veins and their halos cut Cu-Au ore they carry chalcopyrite and pyrite, but where they cut low-grade or barren late porphyry they carry mostly only pyrite. Where they cut contacts between ore and younger porphyries, small amounts of chalcopyrite may occur along them for a short distance into the younger porphyry, but Cu-Au grades in the younger porphyry are in every case significantly lower, with the change in grade taking place over a distance of a few millimeters at the contact. Cu and Au were apparently remobilized over only short distances during late alteration.

Pb and Zn with feldspar destructive alteration: A few veins with sphalerite and galena occur near the outer edge of the zone of strong feldspar destructive alteration (Proffett, 2003, Maps 3-4). Where alteration is pervasive, only pyrite occurs, but where it is less pervasive, sphalerite and galena locally occur.

Latest stage feldspar destructive alteration and veins: Latest stage feldspar destructive alteration occurs along faults that displace the main zone of feldspar destructive alteration. Late-stage veins, with sphalerite, galena, carbonate, and euhedral quartz, and with textures indicative of open space filling, occur along parts of these faults. Brecciated and replaced fault gouge occurs in some veins. Pyrite, chalcopyrite, rare molybdenite and rare coarse-grained free gold have also been observed.

Gypsum and anhydrite

Gypsum occurs at Alumbrera in thin (1–10 mm) veinlets that cut D veins. It has been dissolved in the thin leached capping but is present at the surface where gullies have eroded through this capping. From about 60- to 200-m depth, gypsum has been dissolved from most of the deposit, leaving open fractures. Below this, zones with gypsum alternate with zones in which gypsum has been dissolved. Where gypsum is present, anhydrite is also common, and both are more common in andesite than in porphyries, especially late porphyries. Anhydrite is a part of several primary assemblages and apparently formed when Ca released from the breakdown of plagioclase and hornblende was fixed by combination with sulfate. Gypsum formed by hydration of anhydrite (Gustafson and Hunt, 1975) and apparently expanded out into fractures due to the large volume increase involved in the hydration (Fig. 12C). Still later, gypsum was dissolved in certain zones by ground waters (Gustafson and Hunt, 1975).

Supergene mineralization

Supergene oxidation, leaching, and secondary enrichment of sulfides are less important at Alumbrera than at many other porphyry copper deposits. In most of the deposit, oxidation and leaching have occurred only in the upper few meters, and prior to mining, unoxidized sulfides were exposed in gullies. Oxidation and leaching in many cases are restricted to zones where gypsum has been dissolved; elsewhere gypsum apparently sealed the rock from supergene waters. In the few areas where supergene effects occur at depth, it appears to be due to deep dissolution of gypsum near faults.

Constraints on Processes and Conditions of Ore Genesis

Constraints on genetic interpretations for the Alumbrera deposit provided by field observation, mapping, core logging, and limited supporting laboratory work are considered below, and a sequence of events considered likely to have formed the deposit, in light of these observations, is illustrated in Figure 15.

Porphyry emplacement, potassic alteration, and Cu-Au mineralization

Porphyries, volcanism, and possible magma chamber: The mineralized porphyry complex at Alumbrera was emplaced

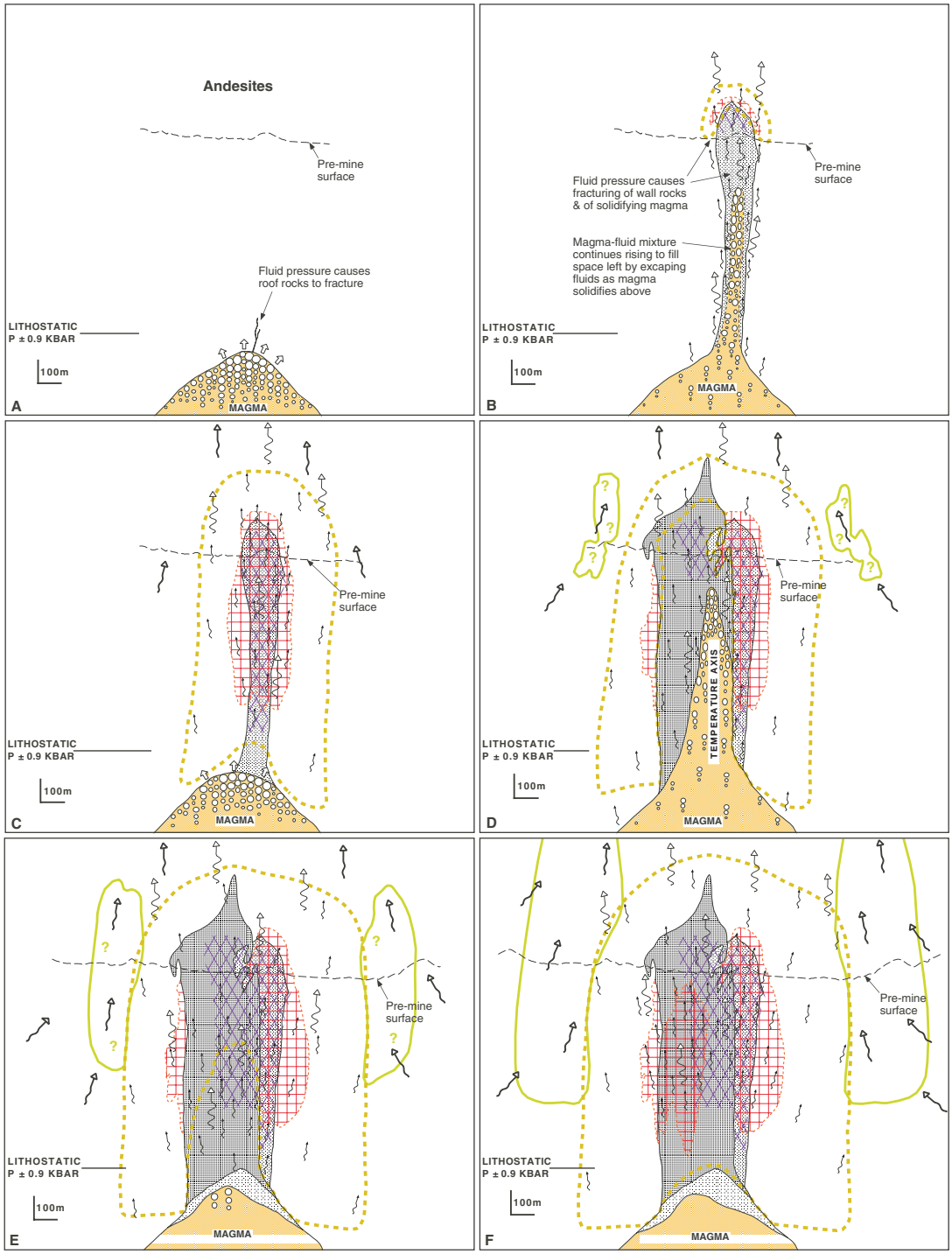

FIG. 15. Emplacement history of Alumbrera orebody, based on section 49N (Figs. 6, 8–10) looking NNW. A. Magma chamber below Alumbrera; exsolving fluids accumulate in upper part. B. Emplacement of P2 and related fluids. Deposition of barren K1 in porphyry and of Cu with K2, K3, or B in cooler andesite. These zones retreat downward as porphyry cools. Sulfur-bearing vapor, which separates from magma and from rising brine, may rise to levels above present exposures. C. P2 cools farther; adjacent andesite is now at temperature similar to porphyry, and fluids are depositing K2 (and K3?) assemblages in both, creating an orebody. Barren K1 may still be forming deep. Surrounding ground water begins to heat and rise. New fluids accumulate in the cupola. D. Emplacement of Early P3 and related fluids. Fluids move up into hot, newly crystallized porphyry, depositing barren K1. Low-grade biotite zone continues to expand. Possible beginning of epidote-chlorite alteration, caused by heating ground water. E. Maximum flux of magmatic fluids is deep in core of Early P3 where temperature is high; barren K1 deposited. Possible remobilization of Cu in adjacent P2. Probable continued expansion of secondary biotite zone, with lower grade Cu in andesite. Ground waters moving inward to replace rising, heated ground waters near porphyry become heated, causing epidote-chlorite alteration. F. Maximum fluid flux rises to slightly cooler parts of Early P3 and deposits moderate to high grades with K2, K3, and B assemblage. Preexisting grades in adjacent P2 and andesite

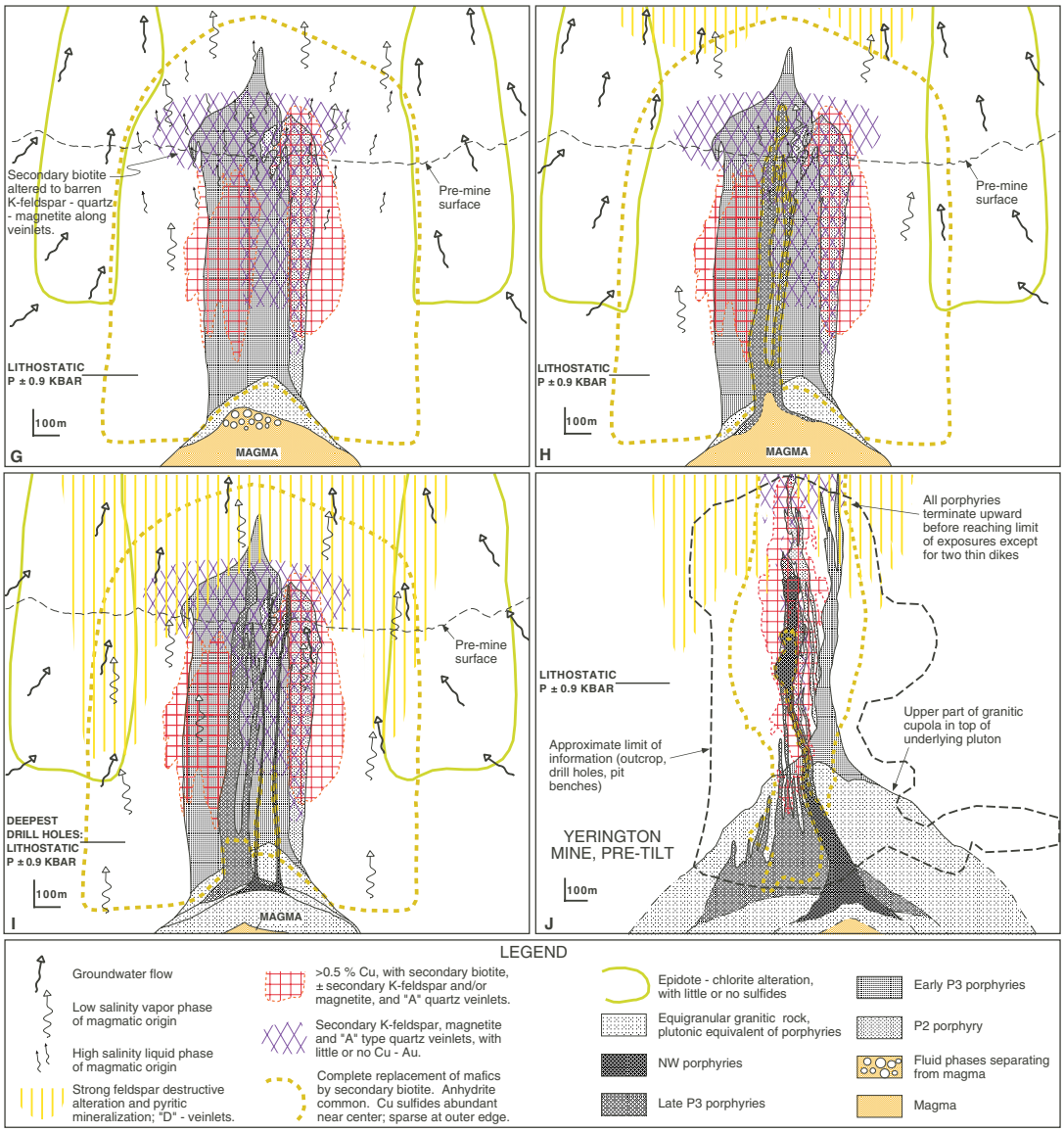

FIG. 15. *(Cont.)*

enhanced. Barren K1 still deposited in hottest parts along temperature axis. G. Maximum fluid flux, now depleted in Cu, rises to higher levels, causing barren K1 alteration of previously biotitized andesite and porphyry. Small amounts of new magmatic fluids, depleted in copper, accumulate in cupola. H. Late P3 emplaced; minor flux of fluids depleted in Cu results in barren K1 alteration in higher temperature areas and in minor low-grade secondary biotite alteration, in and near the Late P3. Secondary biotite zone has ceased to expand; its outer edge is overprinted by epidote-chlorite caused by inward-moving, heating ground waters. Feldspar destructive alteration may have taken place at higher levels, caused by sulfur-bearing, magmatic, low-salinity fluid, probably mixed with rising heated ground water. I. NW porphyry emplaced, with very minor fluids depleted in Cu; partial biotitization of hornblende. Feldspar destructive alteration and sulfidation of earlier deposited copper assemblages retreats to lower levels, caused at least in part by magmatic fluids, which exsolved at late stages from deep in the underlying magma chamber. J. Cross section through the Yerington mine, Nevada, at a stage similar to that of I., for comparison (Proffett, 1979; Proffett and Dilles, 1984; Dilles and Proffett, 1995; unpub. data by M. T. Einaudi and by Proffett). Note scale is smaller than in A-I.

into an earlier stratovolcanic complex, but there is no evidence that the Alumbrera porphyries themselves vented, and there is no evidence for a preexisting vent at Alumbrera. The major porphyries breach the pre-mine surface but are shown in Figure 15 as terminating upward above this because of similarities of Alumbrera to the Yerington mine (Fig. 15J), where mapping shows that ore-related porphyries terminate upward (Proffett, 1979).

Ore-related porphyries are steep, narrow, dike- and pipelike bodies that consist entirely of porphyry and do not constitute the carapace of a larger granitic body as depicted in certain porphyry copper models (e.g., Burnham, 1979, 1997; Gammons and Williams-Jones, 1997).

The sequence of similar felsic porphyries, emplaced closely together in space and time, implies the existence of a magma chamber similar in composition to the porphyries below. A possible model for such a magma chamber is provided by the Yerington mine (Fig. 15J), where tilted exposures reveal that a pluton underlies a mineralized porphyry complex similar to Alumbrera (Proffett, 1979; Proffett and Dilles, 1984; Carten, 1986; Dilles and Proffett, 1995). The bottom of this pluton lies at least 4 to 5 km below its top. Coarse matrix porphyry drilled ~650 m below the pre-mine surface at Alumbrera is similar to porphyries near the top of the pluton at Yerington and suggests the top of such a pluton at Alumbrera may lie near this elevation (Figs. 3, 15). Fragments similar to Alumbrera porphyries, except for equigranular texture, found in breccia dikes 2.5 km south of Alumbrera, also suggest a pluton below. If these fragments are from part of a sub-Alumbrera magma chamber, they suggest a chamber diameter of at least ~5 km. Porphyry phenocrysts, which presumably crystalized, at least in part, in the magma chamber before porphyry emplacement do not include magmatic epidote or other high-pressure phases and are compatible with a magma chamber at shallow crustal levels.

Relationship of mineralization to porphyries: The close space-time association of quartz veins, secondary magnetite, secondary K-feldspar, secondary biotite, anhydrite (where not hydrated to gypsum or dissolved), and Cu-Au mineralization with individual porphyries of a closely related sequence, and truncations of veins, potassic alteration and grade zones by the next younger porphyry, indicate that the volatile fluids that caused mineralization were genetically related to magmatic activity and most likely were exsolved from the magma (cf. Gustafson and Hunt, 1975).

No veins have been observed to be truncated by P2, the oldest porphyry. Therefore significant amounts of volatile fluids apparently did not flow ahead of the porphyry magma as it was being emplaced. This supports either volatile exsolution, accumulation, and emplacement during and/or after porphyry emplacement; or else if volatile fluids exsolved and accumulated in the magma chamber before porphyry emplacement, they were apparently emplaced as an integral part of the magma (e.g., as a bubble suspension or foam; Williams and McBirney, 1979; Cashman and Mangan, 1994). This distribution of quartz veins, secondary magnetite, secondary K-feldspar, and Cu-Au mineralization, in and immediately around individual porphyry intrusions, supports the second interpretation, illustrated in Figure 15. This distribution could also support the first interpretation but some manner of focusing volatile fluids along the already-emplaced porphyry from a much broader region in an underlying magma chamber would be required. One possibility is that pressure release due to porphyry emplacement caused volatile saturation and exsolution from a large part of the magma chamber, which in turn caused stresses and increased strain rate, resulting in temporary brittle behavior and a system of temporary fractures within the magma (Fournier, 1999). The results of Davidson and Kamenetsky (2001) suggest the possibility that a volatile-rich melt phase, immiscible with the principal felsic melt, could also have been involved. With either model, vein truncations at porphyry contacts indicate that mineralization associated with each porphyry occurred before emplacement of the next porphyry.

Quartz veins, secondary magnetite, secondary K-feldspar, secondary biotite, anhydrite, and Cu-Au mineralization are most intensely developed with the earliest ore-related porphyry (P2) and are less strongly developed with each subsequent porphyry. This suggests derivation of magma and volatile fluids for each porphyry mineralization stage from a magma chamber source that was being depleted in volatiles due to losses during each porphyry stage. It does not support a model in which fresh, volatile-rich magma is added to the chamber during each porphyry mineralization stage. The percent phenocrysts appears to increase with younger porphyries (Table 1), which also supports derivation of the porphyries from a single crystallizing magma chamber, rather than from fresh magma for each porphyry. Increase in vein quartz/Cu with younger porphyries (Table 3) also supports derivation of the porphyries from a single crystallizing magma chamber in which the ratio of volatiles was evolving.

Pressure, temperature, and f_{O2}: Based on volcanic reconstruction (Fig. 3), lithostatic pressure through the vertical range of the orebody during porphyry emplacement and early mineralization is estimated at 0.6 to 0.9 kbars, consistent with the presence of saline and vapor-rich fluid inclusions (Sourirajan and Kennedy, 1962). This implies pressures of ~1 kbar and greater for any magma chamber that may have existed below the porphyries and H_2O solubilities in felsic magma of ~3.8 wt percent and greater (Silver et al., 1990; Moore et al., 1998). Lithostatic pressure drop for magma emplaced from the chamber to the level of the orebody would have been ~0.1 to 0.3 kbars, and drops to hydrostatic pressures would have been ~0.4 to 0.7 kbars.

Alumbrera porphyries are similar in composition to synthetic "granodiorite" used in experiments by Naney (1983) on melt-crystal equilibrium. At the 2-kbar pressure of these experiments, lack of pyroxene and presence of biotite and hornblende as nonresorbed crystals would suggest a temperature of ~740° to 790°C for the magma just before porphyry emplacement. Because pressures suggested for a chamber below Alumbrera are mostly lower than 2 kbars, this phenocryst assemblage provides only an approximate temperature and an approximate upper temperature limit for magmatic volatile fluids.

Close space-time association of early mineralization with porphyry emplacement suggests near-magmatic mineralization temperatures (Proffett, 1999), but quantitative temperature measurements were not part of this study. Heinrich et al. (1999, Table 1) list temperatures derived from fluid inclusions

of 400° to 700°C, but it is not yet possible to relate specific measurements to mineralization stages discussed here.

The presence of magnetite, quartz, and sphene in Alumbrera porphyries indicates f_{O2} in the magma between the nickel-nickel oxide (NNO) and magnetite-hematite buffers just before porphyry emplacement or 10^{-15} to 10^{-11} at 750°C (Wones, 1989).

K1 stage: In K1, the earliest mineral assemblage generally associated with each porphyry, igneous biotite may be replaced by K-feldspar and magnetite, with Mg from the phlogopite component apparently either removed from the system or fixed in more magnesian biotite. Experiments (Wones and Eugster, 1965) show that for given biotite compositions, biotite breakdown is not very sensitive to temperature but is favored by increased f_{O2} and is slightly favored by a decrease in pressure. Therefore K1 alteration could be due to a pressure decrease between the magma chamber and the fracture system and/or an increase in f_{O2} to a value above that of the magma chamber. Loss of H_2 (Carmichael et al., 1974; Gustafson and Hunt, 1975) could have contributed to an f_{O2} increase. Mineralizing fluids were not yet saturated in Cu sulfides at the K1 stage, either because of high temperatures, high f_{O2}, low Cu or S concentrations, or a combination of these.

Copper in volatile fluids: Saline fluid inclusions in K2 assemblage contain chalcopyrite crystals of sizes that indicate a few 1,000 ppm Cu in the fluid. Experiments reported by Hemley and Hunt (1992) indicate Cu solubility of only a few 100 ppm at 500°C and 1 kbar, in 6 *m* KCl brines (just below the estimated range of salinities of K2 fluid inclusions) buffered by magnetite, chalcopyrite, bornite, biotite, and K-feldspar—buffers appropriate for K2 assemblage. If Alumbrera magmatic brines were carrying a few 1,000 ppm Cu, the lower experimental solubility at 500°C suggests that deposition of most of the Cu in these brines should have taken place at temperatures higher than this.

Significant amounts of Cu in some vapor-rich fluid inclusions, although generally less than in coexisting saline inclusions (Heinrich et al., 1999, table 1), raises the question of whether Cu and Au were transported mainly by brine, vapor, or both. In experiments, Cu partitions strongly into brine rather than vapor at high f_{O2} in the absence of sulfur (Williams et al., 1995), but at lower f_{O2} (NNO), with f_{S2} buffered by pyrrhotite and intermediate solid solution (Frank et al., 1998), significant Cu also partitions into the vapor. The K2 mineral assemblage suggests conditions intermediate between these experiments. Deposition of Cu sulfides with K2 assemblage seems more in accord with deposition from brine, because K2 is actually a high Fe assemblage, with abundant magnetite, and Fe is thought to partition strongly into brine because of its strong tendency to complex with Cl (Whitney et al., 1985; Burnham, 1997). The common hematite daughter crystals in saline inclusions with K2 supports this conclusion. If the Cu in K2 had been in the vapor, it might be expected to have been carried ahead of the denser brine that carried the Fe, and we should see Cu mineralization with low Fe cut by later magnetite. Instead we see abundant magnetite deposited ahead of, and accompanying Cu, and where late magnetite occurs it shows little systematic relationship to early Cu. Other Cu, such as that with the lower Fe K3 assemblage or B assemblage, may possibly have been carried by vapor.

Required quantities of volatile fluids and magma: The quantity of volatile fluids necessary to transport the Cu associated with each porphyry phase depends on whether the Cu was carried by brine, vapor, or both. Rough calculations have been made for brine-only and brine plus vapor (Table 5) required to transport the Cu associated with P2 and for the total Cu in the entire deposit (Table 3). The calculations assume Cu concentrations and salinities for brine and vapor suggested by fluid inclusions (see above and Heinrich et al., 1999) and experimental work (Sourirajan and Kennedy, 1962; Bodnar et al., 1985; Chou, 1987). For brine and vapor exsolving simultaneously from magma, under conditions discussed here for the upper part of a hypothesized magma chamber, calculations (following Shinohara, 1994; with data from Bodnar et al., 1985; Chou, 1987; Shinohara et al., 1989; Silver et al., 1990) indicate ~95 percent of the volatiles would have been vapor.

The quantity of magma necessary to supply the H_2O and Cl for the quantities of brine and/or vapor estimated (Table 5) depends in part on the initial amounts of these components dissolved in the melt. Little is yet known about initial H_2O and Cl content of Alumbrera magma, but for a variety of other magmas of similar composition and setting, estimates based on melt inclusions and/or erupted volatiles (Johnston, 1980; Lowenstern, 1995; Gerlach et al., 1996) are typically 3 to 6 percent H_2O and 0.1 to 0.5 percent Cl . These figures and results of the calculations (Table 5) suggest that Cl concentration in the magma would be the limiting factor determining the quantity of brine alone that can exsolve from a given quantity of magma. The calculations assume ~0.1 percent Cl exsolved for the brine-only case for P2-related fluids, an amount within the range of estimates of Cl loss related to eruptions (Johnston, 1980; Gerlach et al., 1996). A higher proportion of Cl, H_2O, and Cu would have exsolved from the magma by the time of later porphyries and their mineralization.

The H_2O concentration in the magma would be the factor limiting the quantity of brine plus vapor that could exsolve, due to the large proportion of low-salinity vapor. Two factors which can cause H_2O to exsolve are magma crystallization and pressure decrease. Crystallization of 25 percent feldspars and quartz by the time of emplacement of P2 (Table 1) would have released ~1 percent H_2O from a melt that originally was saturated at ~4 percent H_2O. The average pressure decrease for magma convecting from the bottom to the top of a ~5-km-deep magma chamber would be ~0.7 to 1 kbar and would lower H_2O solubility ~1.5 to 2 percent (Silver et al., 1990; Moore et al., 1998), although this may have been incomplete at the time of emplacement of P2. The calculations assume ~1.5 percent H_2O exsolved for the brine-vapor case for P2-related fluids and ~3 percent for all Cu-bearing fluids.

For comparison to magma volumes estimated in Table 5, a cone-shaped magma chamber, 6 km in diameter and 5 km deep, would have a volume of ~47 km^3.

Because a significant proportion of the Cu appears to have been part of K2 assemblage, probably deposited by brine, the volatiles likely consisted of a brine-vapor mix, between the brine-only and the vapor-brine calculations. Whether Cu was carried in brine, vapor, or both, the amount of required volatiles is greater than the amounts of porphyry magma

TABLE 5. Calculated Quantities of Magma and Volatile Fluids Required to Supply and Transport Cu in Alumbrera Orebody

	Required brine[1] (t)	Required vapor[2] (t)	Required H_2O[3] (t)	Required Cl[3] (t)	Required magma[4] (km^3)	H_2O required from magma	Cu required from magma (ppm)	Cl required from magma
1.3×10^6 t of Cu associated w/ P2 all carried in brine	$\sim 325 \times 10^6$	–	$\sim 150 \times 10^6$	$\sim 100 \times 10^6$	~40	~0.14%	~12	(calculation assumes 0.1%)
4×10^6 t of Cu associated w/all porphyries all carried in brine	$\sim 1000 \times 10^6$	–	$\sim 450 \times 10^6$	$\sim 300 \times 10^6$	~73	~0.23%	~20	(calculation assumes 0.15%)
1.3×10^6 t of Cu associated w/ P2 carried in brine and vapor exsolving simultaneously	$\sim 50 \times 10^6$	$\sim 920 \times 10^6$	$\sim 917 \times 10^6$	$\sim 32 \times 10^6$	~22	(calculation assumes 1.5%)	~22	~0.06%
4×10^6 t of Cu associated w/all porphyries carried in brine and vapor exsolving simultaneously	$\sim 150 \times 10^6$	$\sim 2{,}800 \times 10^6$	$\sim 2790 \times 10^6$	$\sim 98 \times 10^6$	~33	(calculation assumes 3%)	~44	~0.11%

[1] Assumes ~0.4 percent Cu in brine
[2] Assumes ~0.1 percent Cu in vapor
[3] Assumes 50-70 wt percent NaCl equiv in brine, ~2-2.5 wt percent NaCl equiv in vapor
[4] For brine-only cases, assumes ~0.1 percent Cl exsolved from melt to make brine associated with P2 and a total of ~0.15 percent Cl exsolved to make total brine associated with all porphyries; for simultaneous brine-vapor cases, assumes ~1.5 percent H_2O exsolved from melt to make P2-associated brine and vapor, and ~3 percent H_2O exsolved to make total brine and vapor associated with all porphyries

emplaced, which provides additional permissive evidence for a magma chamber below.

Volatiles released from porphyry matrix, due to pressure release during emplacement and due to solidification, would have been small in volume because of the relatively small volumes of the porphyries. Due to lower partition coefficient for Cl into the volatile phase at lower P (Williams et al., 1995), and possible slower diffusion of Cl into the volatile phase relative to H_2O (Gerlach et al., 1996), these volatiles may have been H_2O rich. They probably did not contribute significantly to overall transport of ore minerals but may have contributed to the complex variety of early veins at Alumbrera.

Original sulfide assemblages and late sulfidation: Observations described above on relationships between sulfides assemblages and alteration lead to the conclusion that much of the Cu and Au was originally deposited in low-sulfidation assemblages with potassic alteration during emplacement of earlier porphyries and that the more common chalcopyrite-pyrite assemblage is the result of sulfidation during later alteration overprint. Sulfide minerals and their distribution and ratios, as seen in the deposit now, did not form as part of original Cu sulfide deposition but are a combination of original deposition and late overprint. Au appears to have originally been deposited with Cu, and Au/Cu ratios appear to have been little affected by late overprint and sulfidation (except in a few narrow, isolated, very late veins).

Separation of Cu from S in early mineralization: If early, high-temperature, volatile fluids included both vapor and brine, sulfur, existing mainly as SO_2 and H_2S gas (Bondarenko and Gorbaty, 1997), would be expected to partition more strongly into the vapor (Burnham, 1997; Fournier, 1999). For Cu carried in brine, this could provide a mechanism to separate Cu from much of the sulfur and could help explain the relatively low sulfidation Cu-Fe-S-O mineral assemblage of nonoverprinted K2 mineralization.

Deposition of Cu sulfides: Volatile fluids, migrating upward through fractures in newly solidified porphyry, would have been hottest immediately after emplacement, probably initially near the ~750°C temperature of the magma chamber. They would have begun to cool and to deposit K1 assemblage and A veins but may have been too hot initially to deposit Cu sulfides (Fig. 15B). Fluids escaping into andesite would have encountered lower temperatures, and deposition of Cu with K2, K3, and/or B may have begun there (Fig. 15B).

The progression of assemblages in P2 from K1 to K2 to K3 (Table 2) suggests changing conditions. Cooling of porphyry and of rising, expanding volatile fluids may have allowed Cu sulfide-bearing assemblages to become stable (Holland, 1967; Meyer and Hemley, 1967). Anhydrite deposition, due to Ca released from alteration of hornblende to biotite and anorthite to K-feldspar, may also have promoted Cu sulfide deposition by consuming SO_4^{2-} and thereby promoting hydrolysis of SO_2 to H_2S and H_2SO_4 (Burnham, 1979; Hemley and Hunt, 1992). Alternatively some veins or assemblages may have been deposited by brine and others by vapor. Also, volatiles that exsolved in the magma chamber may have differed from those that exsolved from magma that had been emplaced as porphyry (see above), and further, new fluids could have evolved from upward-moving fluids through boiling or condensation. It appears that a complex variety of magmatic

volatile fluids would have been possible, even associated with a single porphyry stage. This is consistent with the great variety of veinlets and alteration assemblages and with the complex crosscutting relationships found in early mineralization.

Silica: The ratio of vein quartz to Cu associated with P2 is about eight (Table 3), so if silica was carried mostly by the same volatile fluids that carried the Cu, silica solubility about an order of magnitude greater than the amount of dissolved Cu is suggested (assuming efficient deposition of Cu and SiO_2). For brine with a few 1,000 ppm Cu, silica solubility of tens of thousands of ppm would be required. However based on equations of Fournier (1985, pers. commun., 2000) and density data of Anderko and Pitzer (1993), at 1 kbar and ±750°C only ~3,400 ppm SiO_2 in equilibrium with quartz would be soluble in a 63 wt percent NaCl brine (density ~1.09). For a coexisting 2.5 wt percent NaCl vapor at these conditions (density ~0.27), which may have carried ~1,000 ppm Cu, the equations indicate SiO_2 solubility of only ~4,000 ppm. The discrepancy is greater for later porphyries, which have higher ratios of vein quartz to Cu (Table 3).

Possible explanations for the discrepancies include the following:

1. More volatile fluid may have been involved than that necessary to move the Cu (e.g., if most of the deposited Cu was carried by brines and part of the silica by vapor or if quartz was deposited much more efficiently than Cu). This would imply a much larger magma chamber source and/or higher magma volatile concentrations than discussed above and additional difficulties with volatile fluid emplacement mechanisms, as discussed above. The close time-space association of quartz veins and Cu and their upward dying out in Early P3 (Figs. 6, 10) suggest that the efficiency of deposition of quartz and Cu was not very different.
2. SiO_2 solubility may actually be higher than calculated, as suggested by Rimstidt (1997, fig. 10.7). In fact, there are no actual experimental data available at the T, P, and salinities discussed above. However, even the somewhat higher solubilities suggested by equations of Shibue (1996) are insufficient to resolve the discrepancy.
3. Amorphous silica, rather than quartz, may have temporarily controlled solubility, due to contact of volatile fluids with melt or glass not in equilibrium with quartz (quartz eyes in porphyries are rounded, resorbed), so that volatile fluids carried higher concentrations of silica (Fournier, 1999, pers. commun., 2000). The equigranular, anhedral texture of quartz in many A veins has been suggested as evidence for crystallization from amorphous silica (Fournier, 1985).
4. Silica for some veins may have been carried by high-silica fluids that might originate if Na and/or K were to exceed Al in parts of the melt-volatile system, as noted in experimental work (Tuttle and Bowen, 1958, p. 84–88; Luth and Tuttle, 1968, p. 539–542).

Biotite zone: Age relationships show that the large zone of secondary biotite with low Cu and Au grades surrounding Cu-Au ore formed during the same general time period as porphyry emplacement and higher grade mineralization. Although this could have formed from volatile fluids migrating outward from the porphyries, such fluids would have had to move at a large angle from vertical. An alternative is that low-grade outer parts of the biotite zone formed from a weaker flux of fluid rising from deeper, outer parts of the magma chamber (Fig. 15C-F). The limits of the biotite zone (Proffett, 2003, Map 3), which indicate the outer limit of significant encroachment of magmatic fluids, reached a maximum during or after emplacement of Early P3 but had begun to retreat inward by the time Late P3 was emplaced.

Sulfide zoning pattern: In the outer edge of the Cu zone, pyritic veinlets are not truncated by Late P3, which truncates Cu ore in the central part. Yet in Late P3 and older rocks in the outer zone, in places where late overprinting alteration is lacking, the small amount of Cu present occurs as chalcopyrite with secondary biotite and with little or no pyrite. In many places this fringe Cu extends outward beyond the zone of strong, late sericite-pyrite (Proffett, 2003, Map 3). These observations suggest that when Cu sulfides were originally deposited, they were not zoned outward to a pyritic fringe, and that the pyritic fringe was established during late overprint. No evidence has been observed for early pyrite that was part of the original Cu sulfide assemblages, even in the outer fringe.

Low-grade core: Low-grade core mineralization, with abundant quartz veins, magnetite, and secondary K-feldspar, but low sulfides (K1), is developed mostly in Early P3. Therefore it is younger than Cu-Au associated with P2, not older than Cu ore as suggested in some porphyry models (Beane and Titley, 1981). Its asymmetrical distribution, in the northeast part of Early P3, where the wall rocks were preheated by P2 and cooling of Early P3 was likely slower, suggests that high temperature was a factor in localizing the low-grade core. The large size of Early P3 compared to P2 may also have contributed to slower cooling and higher temperatures at the time of maximum volatile flux. High temperatures may have prevented Cu sulfide saturation, resulting in the deposition of mainly barren K1 (Fig. 15D-F). If Early P3-related fluids were not yet at Cu sulfide saturation when they encountered previously deposited Cu sulfides in P2, they may have dissolved and remobilized some of the Cu (Fig. 15E). This may explain patches of P2 in the low-grade core that are low-grade, but higher in grade than adjacent Early P3, such as in holes 48.4-54 and 49-52 (Fig. 6). Farther from the thermal axis, higher Cu-Au grades occur in Early P3 with K2 and K3 assemblages (Fig. 15F).

An additional factor contributing to the formation of the low-grade core in Early P3 may have been that the magma was partly depleted in Cu and Au relative to other volatiles by Early P3 time, compared to P2 time, as suggested by the higher ratio of vein quartz to Cu in Early P3 (Table 3).

Late K1: At upper levels in the deposit late barren veinlets of K1 assemblage overprint secondary biotite alteration with low to moderate Cu and Au grades. This suggests a late volatile flux at high f_{O2} and temperature and depleted Cu and Au concentrations (Fig. 15G-H). This could have originated by exsolution from a depleted magma source or could have evolved from a Cu-Au–bearing volatile fluid through earlier deposition of the Cu and Au.

Epidote-chlorite alteration

Epidote-chlorite alteration overprints Northwest porphyries but is truncated by Postmineral porphyries, indicating

that it was contemporaneous with at least the latter part of potassic alteration and Cu-Au mineralization but older than feldspar destructive alteration.

Lack of sulfides with epidote-chlorite alteration suggests that the altering fluids either carried little sulfur or were in the process of being heated (Hemley et al., 1992), or both. Because fluids moving out from the porphyries would be likely to have carried sulfur and would have been cooling, it is unlikely that epidote-chlorite alteration was caused by such fluids. The epidote-chlorite zone lacks significant quartz veins, also consistent with fluids being heated (Fournier, 1985).

The above observations and peripheral location of epidote-chlorite alteration are consistent with an origin related to meteoric water moving in toward the cooling porphyry (Fig. 15D-G).

Feldspar destructive alteration

The age relationships described above show that two to five porphyries were emplaced between the time of Cu-Au deposition and the time of feldspar destructive alteration, so fluids responsible for feldspar destructive alteration at exposed levels could not have evolved from the Cu-Au–bearing potassic fluids. Age relationships also show that at least part of feldspar destructive alteration is younger than epidote-chlorite alteration.

Although the strongest feldspar destructive alteration occurs in a shell around ore, it cannot be considered an intermediate zone between the potassic and epidote-chlorite zones. The shell of strongest feldspar destructive alteration mainly overprints the outer part of the potassic zone and locally the inner parts of the epidote-chlorite zone, but in some places the outer fringe of potassic alteration extends outside the shell of strongest feldspar destruction, where potassic alteration is in direct contact with epidote-chlorite alteration (Proffett, 2003, Map 3). Because potassic alteration appears to be directly related to a magmatic source, this distribution of feldspar destructive alteration suggests that magmatic input was essential to its origin also. The lack of sulfur implied for nonmagmatic fluids thought to have formed epidote-chlorite also suggests that the high sulfur content of feldspar destructive alteration was due to a magmatic component.

Where ore is overprinted by pervasive or partial feldspar destructive alteration, sulfides are chalcopyrite and pyrite, without bornite, and magnetite is partly destroyed. Early, low-sulfidation Cu-Au–bearing assemblages, with chalcopyrite, bornite, and magnetite, were apparently sulfidized by the later, feldspar destructive fluids.

Although the zone of strongest feldspar destructive alteration surrounds Cu-Au ore, in detail these two features are not closely related spatially (Figs. 6, 8, 13; Proffett, 2003, Map 3) or in time (Fig. 14, Tables 2, 4). Feldspar destructive fluids did not introduce significant Cu or Au, and remobilization of Cu and Au by these fluids was on a local scale. Alumbrera, at exposed levels, does not fit models in which Cu ore is related to an interface between sericitic and potassic zones or in which potassic alteration grades into sericitic alteration (e.g., Lowell and Guilbert, 1970).

The radial and conical-concentric pattern of most D veins (Proffett, 2003, Map 4), and some B veins, centered near the center of intrusion of many later porphyries (cf. Gustafson and Hunt, 1975) suggests that an upward-directed force focused in the area, possibly from the centroid of a magma chamber below. This indicates that activity in that chamber continued during feldspar destructive alteration, even though practically all porphyry intrusion had ceased.

Acknowledgments

Field work and much data compilation were funded by Minera Alumbrera Ltd., who provided logistic support and kindly gave permission to publish this paper. Pete Forrestal and Steve Brown of Mount Isa Mines were closely involved in the project and made many significant contributions. Field visits and discussions with John Hunt, Rick Valenta, Vic Wall, Dave Keough, Nino Salgado, Maria Carrizo, Juan Angera, Luis Rivera, Anthony Harris, Nicolás Montenegro, the late Dante Indri, and a number of other geologists who have been involved with Alumbrera geology have also been helpful. Hilde Proffett provided able assistance in the field. Personnel of Yacimientos Mineros Agua de Dionisio (YMAD) were helpful with many aspects of the project and Mario Alderete provided geologic information and historic insight about many aspects of the Farallón Negro district. Discussions with Julian Hemley, Bob Fournier, John Dilles, Marco Einaudi, Lew Gustafson, and John Hunt about various aspects of porphyry copper geology and geochemistry provided much helpful insight. Part of the computer drafting was done by Helen Richmond of Mount Isa Mines. Reviews by John Hunt, Bob Fournier, Lew Gustafson, Marta Godeas, Alan Clark, Jeremy Richards, Marco Einaudi, and Mark Hannington helped improve the manuscript and are much appreciated. Funds for the color illustrations, including maps in the accompanying supplement, were contributed by Minera Alumbrera Ltd.

February 5, 2001; February 13, 2003

REFERENCES

Allmendinger, R.W., 1986, Tectonic development, southeast border of the Puna plateau, northwest Argentine Andes: Geological Society of America Bulletin, v. 97, p. 1070–1082.

Anderko, A., and Pitzer, K.S., 1993, Equation-of-state representation of phase equilibria and volumetric properties of the system NaCl-H_2O above 575°K: Geochimica et Cosmochimica Acta, v. 57, p. 1657–1680.

Barazangi, M., and Isacks, B.L., 1976, Spatial distribution of earthquakes and subduction of the Nazca plate beneath South America: Geology, v. 4, p. 686–692.

Bassi, H.G.L., and Rochefort, G., 1980, Estudio geológico del yacimiento cuproaur'fero de la Alumbrera: Buenos Aires, Argentina, Ministerio Economica, Servicio Minera Nacional, 78 p.

Beane, R.E., and Titley, S.R., 1981, Porphyry copper deposits, Part II. Hydrothermal alteration and mineralization: Economic Geology 75th Anniversary Volume, p. 235–269.

Bevis, M., and Isacks, B.L., 1984, Hypocentral trend surface analysis: Probing the geometry of Benioff zones: Journal of Geophysical Research, v. 89, p. 6153–6170.

Bodnar, R.J., Burnham, C.W., and Sterner, S.M., 1985, Synthetic fluid inclusions in natural quartz: III. Determination of phase equilibrium properties in the system NaCl-H_2O to 1000°C and 1500 bars: Geochimica et Cosmochimica Acta, v. 49, p. 1861–1873.

Bondarenko, G.V., and Gorbaty, Y.E., 1997, In situ Raman spectroscopic study of sulfur saturated water at 1000 bars between 200 and 500°C: Geochimica et Cosmochimica Acta, v. 61, p. 1413–1420.

Burnham, C.W., 1979, Magmas and hydrothermal fluids, *in* Barnes, H.L., ed., Geochemistry of hydrothermal ore deposits, 2nd ed.: New York, John Wiley and Sons, p. 71–136.

——1997, Magmas and hydrothermal fluids, *in* Barnes, H.L., ed., Geochemistry of hydrothermal ore deposits, 3rd ed.: New York, John Wiley and Sons, p. 63–123.

Caelles, J.C., Clark, A.H., Farrar, E., McBride, S.L., and Quirt, S., 1971, Potassium-argon ages of porphyry copper deposits and associated rocks in the Farallón Negro-Capillitas district, Catamarca, Argentina: ECONOMIC GEOLOGY, v. 66, p. 961–964.

Cahill, T., and Isacks, B.L., 1985, Shape of the subducted Nazca plate [abs.]: EOS, v. 66, p. 299.

——1992, Seismicity and shape of the subducted Nazca plate: Journal of Geophysical Research, v. 97, p. 17503–17529.

Carmichael, I.E.S., Turner, F.J., and Verhoogen, J., 1974, Igneous petrology: New York, McGraw-Hill, 739 p.

Carten, R.B., 1986, Sodium-calcium metasomatism: Chemical, temporal, and spatial relationships at the Yerington, Nevada, porphyry copper deposit: ECONOMIC GEOLOGY, v. 81, p. 1495–1519.

Cashman, K.V., and Mangan, M.T., 1994, Physical aspects of magmatic degassing II. Constraints on vesiculation processes from textural studies of eruptive products: Reviews in Mineralogy, v. 30, p. 447–478.

Chou, I-M., 1987, Phase relations in the system NaCl-KCl-H_2O. III: Solubilities of halite in vapor-saturated liquids above 445°C and redetermination of phase equilibrium properties in the system NaCl-H_2O to 1000°C and 1500 bars: Geochimica et Cosmochimica Acta, v. 51, p. 1965–1975.

Clode, C., Proffett, J., Mitchell, P., and Munajat, I., 1999, Relationships of intrusion, wall-rock alteration and mineralization in the Batu Hijau copper-gold porphyry deposit: Australasian Institute of Mining and Metallurgy Publication Series 4/99, p. 485–498.

Commission for the Geologic Map of the World, 1981, Geologic World Atlas, Map 5 (southern South America), 1:10,000,000: Paris, UNESCO.

Cross, T.A., and Pilger, R.H., 1982, Controls of subduction geometry, location of magmatic arcs, and tectonics of arc and back-arc regions: Geological Society of America Bulletin, v. 93, p. 545–562.

Davidson, P., and Kamenetsky, V.S., 2001, Immiscibility and continuous felsic melt-fluid evolution within the Rio Blanco porphyry system, Chile: Evidence from inclusions in magmatic quartz: ECONOMIC GEOLOGY, v. 96, p. 1921–1929.

Dilles, J.H., and Proffett, J.M., 1995, Metallogenesis of the Yerington batholith, Nevada: Arizona Geological Society Digest 20, p. 306–315.

Engebretson, D.C., Cox, A., and Gordon, R.G., 1985, Relative motions between oceanic and continental plates in the Pacific Basin: Geological Society of America Special Paper 206, 59 p.

Fournier, R.O., 1985, The behavior of silica in hydrothermal solutions: Reviews in Economic Geology, v. 2, p. 45–61.

——1999, Hydrothermal processes related to movement of fluid from plastic into brittle rock in the magmatic-epithermal environment: ECONOMIC GEOLOGY, v. 94, p. 1193–1212.

Frank, M.R., Candela, P.A., and Piccoli, P.M., 1998, Estimated copper concentrations in magmatic vapor and brine in a sulfur-bearing brine-vapor-haplogranite melt-intermediate solid solution-pyrrhotite system at 800° and 100 MPa [abs.]: Geological Society of America Abstracts with Programs, v. 30, p. A-371.

Gammons, C.H., and Williams-Jones, A.E., 1997, Chemical mobility of gold in the porphyry-epithermal environment: ECONOMIC GEOLOGY, v. 92, p. 45–59.

Gerlach, T.M., Westrich, H.R., and Symonds, R.B., 1996, Preeruption vapor in magma of the climactic Mount Pinatubo eruption: Source of the giant stratospheric sulfur dioxide cloud, *in* Newhall, C.G., and Punongbayan, R.S., eds., Fire and mud, eruptions and lahars of Mount Pinatubo, Philippines: Seattle, University of Washington Press, p. 415–433.

González Bonorino, F., 1947, Carta Geológico-Econ—mica de la Repœblica Argentina, Hoja 12d, Capillitas, 1:200000: Dirección General de Minas y Geolog'a de Argentina.

Guilbert, J.M., 1995, Geology, alteration, mineralization and genesis of the Bajo de la Alumbrera porphyry copper-gold deposit, Catamarca Province, Argentina: Arizona Geological Society Digest 20, p. 646–656.

Gustafson, L.B., and Hunt, J.P., 1975, The porphyry copper deposit at El Salvador, Chile: ECONOMIC GEOLOGY, v. 70, p. 857–912.

Haq, B.U., and Van Eysinga, F.W.B., 1998, Geologic time scale, 5th ed.: Netherlands, Elsevier, 1 sheet.

Heinrich, C.A., Gunther, D., Autétat, A., Ulrich, T., and Frischknecht, R., 1999, Metal fractionation between magmatic brine and vapor, determined by microanalysis of fluid inclusions: Geology, v. 27, p. 755–758.

Hemley, J.J., and Hunt, J.P., 1992, Hydrothermal ore-forming processes in the light of studies in rock-buffered systems: II. Some general geologic applications: ECONOMIC GEOLOGY, v. 87, p. 23–43.

Hemley, J.J., Cygan, G.L., Fein, J.B., Robinson, G.R., and D'Angelo, W.M., 1992, Hydrothermal ore-forming processes in the light of studies in rock-buffered systems: I. Iron-copper-zinc-lead sulfide solubility relations: ECONOMIC GEOLOGY, v. 87, p. 1–22.

Holland, H.D., 1967, Gangue minerals in hydrothermal deposits, *in* Barnes, H.L., ed., Geochemistry of hydrothermal ore deposits, 1st ed.: New York, Holt, Rinehart and Winston, p. 382–436.

Johnston, D.A., 1980, Volcanic contribution of chlorine to the stratosphere: More significant to ozone than previously estimated?: Science, v. 209, p. 491–493.

Jordan, T.E., Isacks, B.L., Allmendinger, R.W., Brewer, J.A., Ramos, V.A., and Ando, C.J., 1983, Andean tectonics related to geometry of subducted Nazca plate: Geological Society of America Bulletin, v. 94, p. 341–361.

Kay, S.M., Maksaev, V., Moscoso, R., Mpodozis, C., Nasi, C., and Gordillo, C.E., 1988, Tertiary Andean magmatism in Chile and Argentina between 28°S and 33°S: Correlation of magmatic chemistry with a changing Benioff zone: Journal of South American Earth Sciences, v. 1, p. 21–38.

Llambías, E.J., 1970, Geologia de yacimientos mineros de Agua de Dionisio, Departamento de Belen, Provincia de Catamarca: Unpublished map for Yacimientos Mineros Agua de Dionisio (YMAD), scale 1:20000.

——1972, Estructura del grupo volcanico Farallón Negro, Catamarca, Republica Argentina: Revista de la Asociación Geológica Argentina, v. 27, p. 161–169.

Lowell, J.D., and Guilbert, J.M., 1970, Lateral and vertical alteration zoning in porphyry copper ore deposits: ECONOMIC GEOLOGY, v. 55, p. 373–408.

Lowenstern, J.B., 1995, Applications of silicate-melt inclusions to the study of magmatic volatiles: Mineralogical Association of Canada Short Course, v. 23, p. 71–99.

Luth, W.C., and Tuttle, O.F., 1968, The hydrous vapor phase in equilibrium with granite and granitic magmas: Geological Society of America Memoir 115, p. 513–548.

Mavrogenes, J.A., Williamson, M.A., and Bodnar, R.J., 1992, Cu, Fe and S concentrations in magmatic/hydrothermal fluids: Evidence from natural and synthetic fluid inclusions [abs.]: Geological Society of America Abstracts with Programs, v. 24, no. 7, p. A144.

McBride, S.L., Caelles, J.C., Clark, A.R., and Farrar, E., 1976, Paleozoic radiometric age provinces in the Andean basement, latitudes 25°-30°S: Earth and Planetary Science Letters, v. 29, p. 373–383.

Meyer, C., and Hemley, J.J., 1967, Wall rock alteration, *in* Barnes, H.L., ed., Geochemistry of hydrothermal ore deposits, 1st ed.: New York, Holt, Rinehart and Winston, p. 166–235.

Moore, G., Vennemann, T., and Carmichael, I.S.E., 1998, An empirical model for the solubility of H_2O in magmas to 3 kilobars: American Mineralogist, v. 83, p. 36–42.

Naney, M.T., 1983, Phase equilibria of rock-forming ferromagnesian silicates in granitic systems: American Journal of Science, v. 283, p. 993–1033.

Pilger, R.H., Jr., 1981, Plate reconstructions, aseismic ridges, and low angle subduction beneath the Andes: Geological Society of America Bulletin, v. 92, p. 448–456.

Proffett, J.M., 1979, Ore deposits of the western United States: A summary: Nevada Bureau of Mines and Geological Report 33, p. 13–32.

——1999, The Alumbrera porphyry copper-gold deposit, NW Argentina [abs.]: Geological Society of America Abstracts with Programs, v. 31, no. 6, p. A-86.

——2003, Maps to accompany geology of the Bajo de la Alumbrera porphyry copper-gold deposit, Argentina: Supplement to ECONOMIC GEOLOGY, v. 98, no. 8, 4 maps.

Proffett, J.M., and Dilles, J. H., 1984, Geologic map of the Yerington district, Nevada: Nevada Bureau of Mines and Geology Map 77.

Proffett, J.M., Keough, D.C., and Forrestal, P.J., 1998, The geology of the Bajo de la Alumbrera porphyry copper-gold deposit, Argentina [abs.]: Geological Society of Australia Abstracts, no. 49, p. 365.

Rimstidt, J.D., 1997, Gangue mineral transport and deposition, *in* Barnes, H.L., ed., Geochemistry of hydrothermal ore deposits, 3rd ed.: New York, John Wiley and Sons, p. 487–515.

Roedder, E., 1971, Fluid inclusion studies on the porphyry-type ore deposits at Bingham, Utah, Butte, Montana, and Climax, Colorado: ECONOMIC GEOLOGY, v. 66, p. 98–120.

——1981, Origin of fluid inclusions and changes that occur after trapping: Mineralogical Association of Canada Short Course Handbook, v. 6, p. 101–137.

Sasso, A.M., 1997, Geological evolution and metallogenetic relationships of the Farallón Negro volcanic complex, NW Argentina: Unpublished Ph.D. thesis, Kingston, ON, Canada, Queens University, 842 p.

Sasso, A.M., and Clark, A.H., 1998, The Farallón Negro group, northwest Argentina: Magmatic, hydrothermal and tectonic evolution and implications for Cu-Au metallogeny in the Andean back-arc: Society of Economic Geologists Newsletter 34, p. 1, 8–18.

Shibue, Y., 1996, Empirical expressions of quartz solubility in H_2O, H_2O + CO_2, and H_2O + NaCl fluids: Geochemical Journal, v. 30, p. 339–354.

Shinohara, H., 1994, Exsolution of immiscible vapor and liquid phases from a crystallizing silicate melt: Implications for chlorine and metal transport: Geochimica et Cosmochimica Acta, v. 58, p. 5215–5221.

Shinohara, H., Ilyama, J.T., and Matsuo, S., 1989, Partition of chloride compounds between silicate melt and hydrothermal solutions: I. Partition of NaCl-KCl: Geochimica et Cosmochimica Acta, v. 53, p. 2617–2630.

Sillitoe, R.H., 1973, The tops and bottoms of porphyry copper deposits: Economic Geology, v. 68, p. 799–815.

Silver, L.A., Ihinger, P.D., and Stolper, E., 1990, The influence of bulk composition on the speciation of water in silicate glasses: Contributions to Mineralogy and Petrology, v. 104, p. 142–162.

Simon, G., Kesler, S.E., Essene, E.J., and Chryssoulis, S.L., 2000, Gold in porphyry copper deposits: Experimental determination of the distribution of gold in the Cu-Fe-S system at 400° to 700°C: Economic Geology, v. 95, p. 259–270.

Skewes, M.A., and Stern, C.R., 1994, Tectonic trigger for the formation of late Miocene Cu-rich breccia pipes in the Andes of central Chile: Geology, v. 22, p. 551–554.

Sourirajan, S., and Kennedy, G.C., 1962, The system H_2O-NaCl at elevated temperatures and pressures: American Journal of Science, v. 260, p. 114–141.

Stults, A.H., 1985, Geology of the Bajo la Alumbrera copper and gold deposit, Catamarca Province, Argentina: Unpublished M.Sc. thesis, Tucson, University of Arizona, 72 p.

Tuttle, O.F., and Bowen, N.L., 1958, Origin of granite in the light of experimental studies in the system $NaAlSi_3O_8$-$KAlSi_3O_8$-SiO_2-H_2O: Geological Society of America Memoir 74, 153 p.

Ulrich, T., 1999, Genesis of the Bajo de la Alumbrera porphyry Cu-Au deposit, Argentina: Geological, fluid geochemical, and isotopic implications: Unpublished Ph.D. thesis, Zürich, Switzerland, ETH, 207 p.

Ulrich, T., Gunther, D., and Heinrich, C.A., 1999, Gold concentrations of magmatic brines and the metal budget of porphyry copper deposits: Nature, v. 399, p. 676–679.

Williams, H., and McBirney, A.R., 1979, Volcanology: San Francisco, Freeman, 397 p.

Williams, T.J., Candela, P.A., and Piccoli, P.M., 1995, The partitioning of copper between silicate melts and two-phase aqueous fluids: An experimental investigation at 1 kbar, 800°C and 0.5 kbar, 850°C: Contributions to Mineralogy and Petrology, v. 121, p. 388–399.

Whitney, J.A., Hemley, J.J., and Simon, F.O., 1985, The concentration of iron in chloride solutions equilibrated with synthetic granitic compositions: The sulfur-free system: Economic Geology, v. 80, p. 444–460.

Wones, D.R., 1989, Significance of the assemblage titanite + magnetite + quartz in granitic rocks: American Mineralogist, v. 74, p. 744–749.

Wones, D.R., and Eugster, H.P., 1965, Stability of biotite: Experiment, theory, and application: American Mineralogist, v. 50, p. 1228–1272.